THE OPTIMISATION OF CREST LEVEL DESIGN OF SLOPING COASTAL STRUCTURES THROUGH PROTOTYPE MONITORING AND MODELLING

Contract number: MAS3-CT97-0116

FINAL REPORT

Detailed scientific and technical report

MAS03/1031

<u>Coordinating institution:</u> Ghent University, Belgium

<u>Partner institutions:</u>   Flanders Community – Coastal Division
Flanders Community – Flanders Hydraulics
Aalborg University
Leichtweiβ Institut für Wasserbau
University College Cork
Delft Hydraulics
Rijkswaterstaat
Universidad Politécnica de Valencia
Instituto Hidrográfico

<u>Authors:</u> Prof. Dr. Ir. J. DE ROUCK
Ir. C. BOONE
Ir. B. VAN DE WALLE

MAST III

THE OPTIMISATION OF CREST LEVEL DESIGN OF SLOPING COASTAL STRUCTURES THROUGH PROTOTYPE MONITORING AND MODELLING

OPTICREST

contract: MAS3-CT97-0116

Detailed scientific and technical report

Julien DE ROUCK, Cathy BOONE and Björn VAN DE WALLE
Ghent University, Department of Civil Engineering
Technologiepark 9
B – 9052 ZWIJNAARDE

Partner	Abbreviation
Universiteit Gent	UG
Flanders Community – Coastal Division	FCCD
Flanders Community – Flanders Hydraulics	FCFH
Aalborg University	AAU
Leichtweiβ Institut für Wasserbau	LWI
University College Cork	UCC
Delft Hydraulics	DH
Rijkswaterstaat	RIKZ
Universidad Politécnica de Valencia	UPV
Instituto Hidrográfico	IH

Index

List of figures

List of tables

INTRODUCTORY TEXT

This text introduces the 'Detailed scientific and technical report' of the MAST III project MAS03-CT97-0116 'The optimisation of crest level design of sloping coastal structures through prototype monitoring and modelling' (acronym: OPTICREST). This report gives an account of the detailed scientific and technical outcome of the project referring to the whole project period 1/3/'98-28/2/'01. For each task or subtask as described in the Technical Annex, this report describes the work carried out and summarises the most important results and conclusions.

More detailed information on the scientific results and a description of the methodologies are provided in the annexes enclosed with this report.

For tasks which have been finished before T_0+12, reference has been made to the final reports on these tasks attached to the first annual report: *'Annual Report (12 months)'* (ref. no. MAS03/797) and for tasks which have been finished between T_0+12 and T_0+24, reference has been made to the final reports on these tasks attached to the second annual report: *'Annual Report (T_0+12 till T_0+24)'* (ref. no. MAS03/999). These reports are no longer included in the annexes of this report.

TASK 1: REVIEW OF AVAILABLE INFORMATION

In order to organise an exchange of information and knowledge from the very beginning of the project, all partners provided publications and available reports related to wave run-up, overtopping and spray. These publications, together with the existing literature, have been reviewed and a literature review, which constitutes the first part of the report on this task, has been written by UG. The second part of this report is a text, summarising design formulae of run-up and overtopping. This text was written by prof. Burcharth and will be published in the forthcoming Coastal Engineering Manual of the US Corps of Engineers.

This report, *'Task 1 - Review of available data'*, is attached as the first Annex to the *'Annual Report (12 months)'* and is therefor not reproduced here. This report serves as a source of information for each partner. It summarises the knowledge from all partners on wave run-up, overtopping and spray and makes it available for everybody in the OPTICREST group.

TASK 2: PROTOTYPE MEASUREMENTS

Subtask 2.1: Methodology and analysis of available data

The collection of full scale data has been the most crucial and demanding aspect of this project. Placing and maintaining sensitive instrumentation in the marine environment requires specialist knowledge and experience, and (continuous) maintenance testing and calibrating in order to obtain reliable results.

Based on different meetings and visits to both Zeebrugge and Petten prototype measurement sites, agreements have been made between UG, FCCD and RIKZ about the data acquisition, data collection, data presentation, data management and data analysis. The methods used have been described already in the report *'Description of field sites for the measurement of wave run-up'*, prepared by RIKZ. This report was given in the second Annex of the *'Annual Report (12 months)'*.

The **rubble mound breakwater at Zeebrugge** is instrumented for the measurement of the attacking wave climate and for wave run-up and wave overtopping measurements. All channels are low-pass filtered and are sampled at a sample rate of 10 Hz. Using a modem connection, all instruments are checked on a regular basis from Ghent. The data are stored on a hard disk in fifteen minutes duration files. The data are transferred to Ghent University using a portable hard disk. The interesting measurement sessions are then archived on CD-ROM. A data catalogue giving an overview of all measurements is made to have a quick view of interesting measurements and to see if an instrument is working or not.

The **Petten sea-dike** is instrumented for the measurement of the attacking wave climate and for wave run-up measurement. The measurements of different instruments are sampled with different sample rates and treated by different systems. Interesting storm sessions are stored on CD-ROM.

Subtask 2.2: Prototype measurements in Zeebrugge (Belgium)

a) Instrumentation

At the Northern Westdam of the outer Zeebrugge harbour, prototype measurements are carried out on a conventional rubble mound breakwater. The armour layer consists of 25 ton grooved cubes. A jetty is constructed above the breakwater. Figure 1 shows the cross section of the breakwater and the jetty.

The instrumentation at the Zeebrugge rubble mound breakwater consists of:

- two **wave rider buoys** which measure the wave climate in front of the breakwater and which are located at a distance of approximately 150 m and 215 m respectively from the breakwater.
- an **infrared meter** is placed on the measuring jetty near the pile supporting this jetty and measures the wave climate at the toe of the structure. The infrared meter data is used to calculate the mean water level.
- a 'spiderweb system' (SP) consisting of 7 step gauges placed vertically between the armour units and the measuring jetty. At the lower end these are attached to an armour unit and at the upper end to the jetty by means of a heavy spring. Wave run-up levels are computed from the step gauge measurements.
- a **run-up gauge** (RU) consisting of 5 gauges placed along the slope of the breakwater on top of the armour units. These gauges detect wave run-up in a straight forward way.
- an **anemometer** is placed on the jetty to measure wind speed and wind blowing direction.
- a **video camera**, suspended on the jetty and directed towards the breakwater yields video images of wave run-up on the breakwater.
- behind the crest of the breakwater an **overtopping tank** of 28 m³ is constructed in order to collect the overtopping discharges in a section of 7.30 m. A compound weir controls the outflow of the water catched by the overtopping tank. The mean overtopping discharge and the volumes of the individual overtopping waves are calculated by measuring the water height in the tank and the calibration formula of the compound weir.
- four **wave detectors** are placed on the crest of the breakwater. These allow the detection of the number, the extent and the location of the overtopping wave(s) in the instrumented section.
- six **rain gauges** with datalogger, placed on a pedestal at distinct distances (0, 30, 70, 110, 220 and 1000 m) behind the crest of the breakwater detect spray.

Table 1 overviews all the measuring devices available at the Zeebrugge site.

b) Database with storms

Thirteen storms (with significant wave height H_{mo} varying between 2.40 m and 3.13 m, mean wave period $T_{0.1}$ on average 6.24 s, peak wave period T_p around 7.93 s and wind ($\geq$ 7 Beaufort) direction almost perpendicular to the breakwater) have been observed at the Belgian coast during the period from 1995 to 2000 and have been analysed. Periods of time of two hours symmetric around the

moment of high water t_{HW} are called 'storm sessions'. The data catalogue includes the storm sessions listed in table 2.

<u>Table 1:</u> Measurement devices installed at the Zeebrugge rubble mound breakwater.

Channel N°	Sensor	Z [m]	X [m]	Variables measured
1	Pressure sensor 3498	3.1	-6.88	hydrodynamic pressure
2	Pressure sensor 3499	0.83	-12.66	hydrodynamic pressure
3	Pressure sensor 3502	3.06	-7.26	hydrodynamic pressure
4	Pressure sensor 3504	0.74	-2.48	hydrodynamic pressure
5	Pressure sensor 3505	0.74	-8.96	hydrodynamic pressure
6	Pressure sensor 3507	0.77	-6.88	hydrodynamic pressure
7	Pressure sensor 3511	3	-2.48	hydrodynamic pressure
8	Pressure sensor 381	2.44	-2.48	hydrodynamic pressure
9	Pressure sensor 382	2.51	-6.88	hydrodynamic pressure
10	Pressure sensor 383	-0.35	-37.6	hydrodynamic pressure
11	Pressure sensor 384	2.32	8.97	hydrodynamic pressure
12	Pressure sensor 385	2.43	-10.06	hydrodynamic pressure
13	Pressure sensor 386	2.36	-7.78	hydrodynamic pressure
14	Pressure sensor 388	2.43	3.97	hydrodynamic pressure
15	Pressure sensor 137	1.09	-37.6	hydrodynamic pressure
16	Pressure sensor 138	2.9	-18.46	hydrodynamic pressure
17	Run-up gauge 1	11.96	-15.31	wave run-up
18	Run-up gauge 2	11.26	-13.51	wave run-up
19	Run-up gauge 3	10.64	-11	wave run-up
20	Run-up gauge 4	9.58	-9.12	wave run-up
21	Run-up gauge 5	7.45	-6.93	wave run-up
22	IR-Laser Waveheight meter	17.11	-30	surface elevation
23	Waverider I buoy (close)	0	-150	surface elevation
24	Waverider II buoy (far)	0	-215	surface elevation
25	Stepgauge Spiderweb 1	2.75	-18.45	wave run-up & surface elevation
26	Stepgauge Spiderweb 2	4.03	-17.84	wave run-up & surface elevation
27	Stepgauge Spiderweb 3	6.39	-14.82	wave run-up & surface elevation
28	Stepgauge Spiderweb 4	7.3	-13.34	wave run-up & surface elevation
29	Stepgauge Spiderweb 5	9.5	-11.4	wave run-up & surface elevation
30	Stepgauge Spiderweb 6	10.14	-9.44	wave run-up & surface elevation
31	Stepgauge Spiderweb 7	11.12	-7.26	wave run-up & surface elevation
32	Pressure sensor 1123960	overtopping		hydrodynamic pressure
33	Pressure sensor 1123962	overtopping		hydrodynamic pressure
34	Digital wavedetector 1	overtopping		presence of seawater
35	Digital wavedetector 2	overtopping		presence of seawater
36	Digital wavedetector 3	overtopping		presence of seawater
37	Digital wavedetector 4	overtopping		presence of seawater
38	Wind speed	17.5	-32	wind speed
39	Wind direction	17.5	-32	wind direction
40	Videocamera	14	-30	video images of the run-up
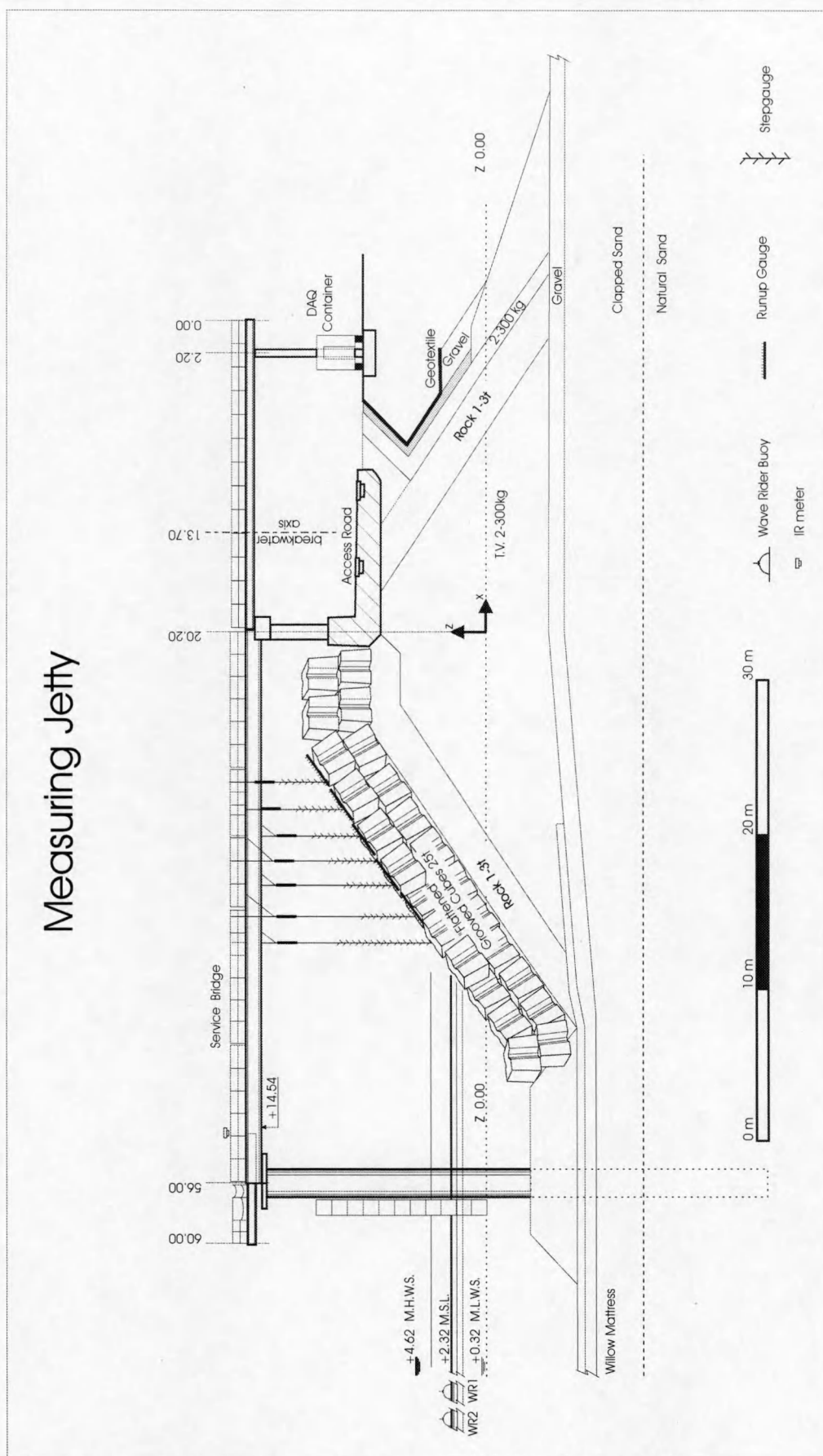
Figure 1: Cross section of the Zeebrugge rubble mound breakwater with the measuring devices.

Table 2: Storm sessions

Datum	Hour
August 28, 1995	02h45 - 04h45
August 28, 1995	15h00 - 17h00
January 19, 1998	16h00 - 18h00
January 20, 1998	04h15 - 06h15
February 7, 1999	16h00 - 18h00
February 17, 1999	12h45 - 14h45
February 22, 1999	15h45 - 17h45
November 6, 1999	11h30 - 13h30
November 6-7, 1999	23h45 - 01h45
December 3, 1999	21h00 - 23h00
December 4, 1999	22h00 - 0h00
January 22, 2000	12h30 - 14h30
January 23, 2000	00h45 - 02h45

c) Analysis of prototype measurements

Wave run-up data is collected by means of the spiderweb system (SP) and the run-up gauge (RU). The 2% exceedence level of the expected wave run-up Ru is used for comparison. Also other exceedence probabilities x are considered. t_{HW} is the moment of high water and the ith hour before or after this moment of high water are noted down as $t_{HW}-i$ and $t_{HW}+1$ respectively.

The average value of the dimensionless wave run-up values $Ru_{x\%}/H_{mo}$ (9 values for RU data and 13 values for the SP data) are listed in table 3. Time series of a period of time of two hours at high tide (from $t_{HW}-1$ to $t_{HW}+1$) have been used in the analysis of the measurement data.

Table 3: Mean $Ru_{x\%}/H_{mo}$ values, using SP data collected during 13 storms and using RU data collected during 9 storms, from $t_{HW}-1$ to $t_{HW}+1$ and using 2 hours time series in the analysis.

	RU	SP
Ru_{max}/H_{mo}	2.35	2.25
$Ru_{1\%}/H_{mo}$	1.94	1.87
$Ru_{2\%}/H_{mo}$	**1.76**	1.75
$Ru_{5\%}/H_{mo}$	1.55	1.66
$Ru_{10\%}/H_{mo}$	1.34	-
Ru_{s}/H_{mo}	1.23	-
$Ru_{25\%}/H_{mo}$	0.97	-
$Ru_{50\%}/H_{mo}$	0.68	-

Wave run-down, characterised by the 2% exceedence probability, has been measured in prototype as $Rd_{2\%}/H_{mo}$ = **-0.86** when a two hours time series at high water is analysed. Only the spiderweb system yielded data for the determination of wave run-down.

When half a tide cycle is investigated, subsequent time series of a period of time of 30 minutes are used. The results are plotted in figure 2. One can see that $Ru_{x\%}/H_{mo}$ values decrease with increasing water level and $Ru_{x\%}/H_{mo}$ values are smaller during receding tide than during rising tide. The lower the exceedence probability x, the more dependency of the water level on the dimensionless wave run-up value is seen.

More analysis results are written down in the final report '*Prototype measurements at the Zeebrugge site*' (see Annex 2.2 of this report).
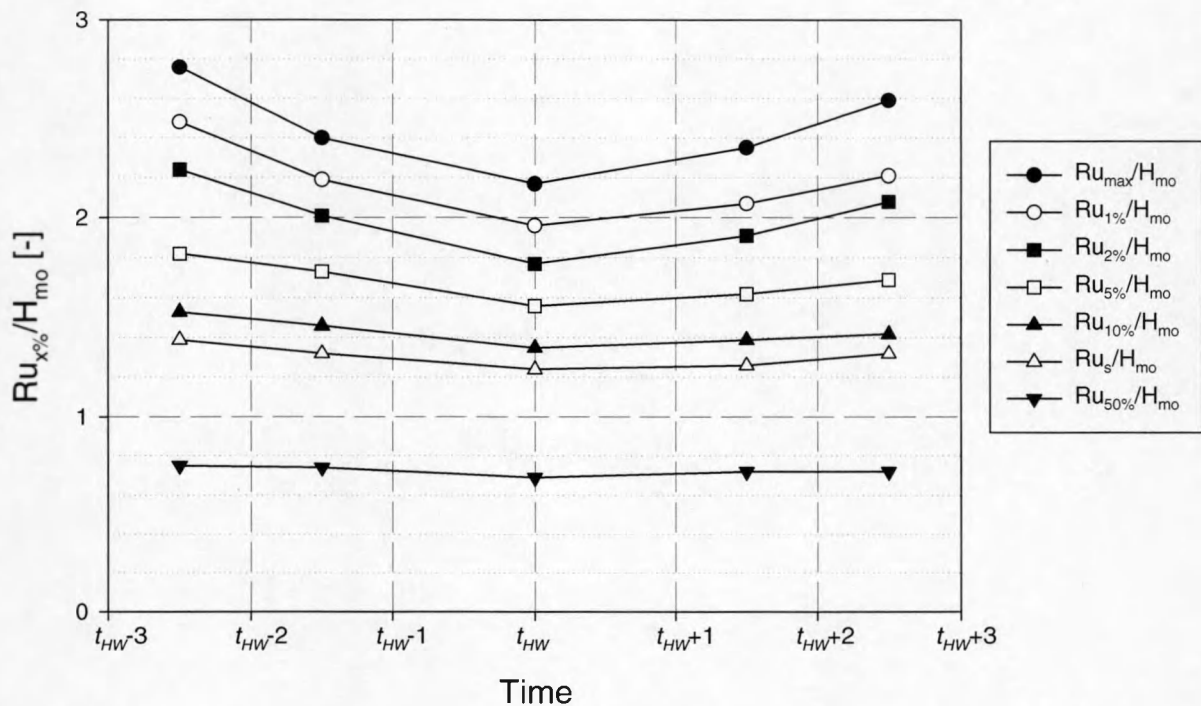
Figure 2: Dimensionless prototype wave run-up $Ru_{x\%}/H_{mo}$ vs. time, using RU data collected during 9 storms and 30 minutes time series, from t_{HW}-3 to t_{HW}+3.

d) **Conclusions**

The main **conclusions** which are drawn from the prototype measurements are:

(1) The mean value of the dimensionless 2% wave run-up value $Ru_{2\%}/H_{mo}$ equals **1.76** when the RU data collected during 9 storms and during the period from t_{HW}-1 to t_{HW}+1 is analysed in its full entirety (i.e. a time series of 2 hours)).

The mean value of the dimensionless 2% wave run-up value $Ru_{2\%}/H_{mo}$ equals 1.75 when the SP data collected during 13 storms and during the period from t_{HW}-1 to t_{HW}+1 is analysed in its full entirety (i.e. a time series of 2 hours)).

When 30 minutes time series are used in the analysis of the RU data collected during 9 storms and during half a tide cycle (from t_{HW}-3 to t_{HW}+3), the mean dimensionless wave run-up values given in table 4 are obtained.

When 30 minutes time series are used in the analysis of the SP data collected during 13 storms and during half a tide cycle (from t_{HW}-3 to t_{HW}+3), the mean dimensionless wave run-up values given in table 5 are obtained.

Table 4: Mean $Ru_{2\%}/H_{mo}$ values using 30 minutes
time series and RU data collected during 9 storms

Time series	$Ru_{2\%}/H_{mo}$
from t_{HW}-3 to t_{HW}-2	2.24
from t_{HW}-2 to t_{HW}-1	2.01
from t_{HW}-1 to t_{HW}+1	**1.77**
from t_{HW}+1 to t_{HW}+2	1.91
from t_{HW}+2 to t_{HW}+3	2.08

Table 5: Mean $Ru_{2\%}/H_{mo}$ values using 30 minutes
time series and SP data collected during 13 storms

Time series	$Ru_{2\%}/H_{mo}$
from t_{HW}-3 to t_{HW}-2	2.40
from t_{HW}-2 to t_{HW}-1	2.03
from t_{HW}-1 to t_{HW}+1	**1.78**
from t_{HW}+1 to t_{HW}+2	1.99
from t_{HW}+2 to t_{HW}+3	2.22

One can conclude that in fact the length of the used time series does not affect the results (when the water level is constant).

(2)   The mean value of the dimensionless 2% wave run-down value $Rd_{2\%}/H_{mo}$ equals **-0.86** when the SP data collected during 13 storms and during the period from t_{HW}-1 to t_{HW}+1 is analysed in its full entirety (i.e. a time series of 2 hours)).

(3)   The dimensionless 2% wave run-up value $Ru_{2\%}/H_{mo}$ is dependent on the water level: this value increases when the water level decreases. The wave run-up value Ru is less dependent on the water level than the $Ru_{2\%}/H_{mo}$ values, but wave run-up also increases when the water

level decreases. This may be caused by the water depth and/or the fact that at lower water level the wave run-up occurs on a lower part of the armour layer. The lower the exceedance probability, the more dimensionless wave run-up values vary with changing water levels.

(4) The dimensionless wave run-up values are larger during rising tide than during receding tide by which an influence of currents and/or the asymmetric tide is suspected.

(5) Two different wave run-up measuring devices (spiderweb system and run-up gauge), placed in different cross sections of the breakwater yield comparable results for low exceedance probabilities.

(6) Wave run-up is Rayleigh distributed.

The Zeebrugge site has proven to be capable of collecting data on wave characteristics and wave run-up at prototype scale.

Subtask 2.3: Prototype measurements in Petten (The Netherlands)

The Petten sea-dike is smooth and impermeable and protected with basalt blocks. Figure 3 and table 6 show the instruments used during the 1998-2000 measurements.

During the storm seasons (from October 15th till April 15th) 1998-1999, 1999-2000, 2000-2001, measurements have been executed at the Petten field site. Various wave buoys, instrumented poles, frames and other equipment were deployed offshore, in the surf zone and on the sea dike in a cross-shore line with a length of nearly 8000 meters. Wind, water levels, waves and wave run-up have been measured up to six times during each storm season.
Both the set-up and the acquisition systems were several times improved and elaborated during the OPTICREST project.

The measurements at the Petten site have resulted in a large database with hydraulic data which is used for the analysis of hydraulic phenomena (National Institute for Coastal and Marine Management/RIKZ, 1999). Unfortunately no periods with substantial wave run-up occurred. Therefore data measured in 1995 at the Petten field site was used for the comparison between the prototype measurements and the laboratory models.

The measurement site of Petten has shown to be successful in collecting full scale measurements of hydraulic processes in front of and on the Petten sea dike.
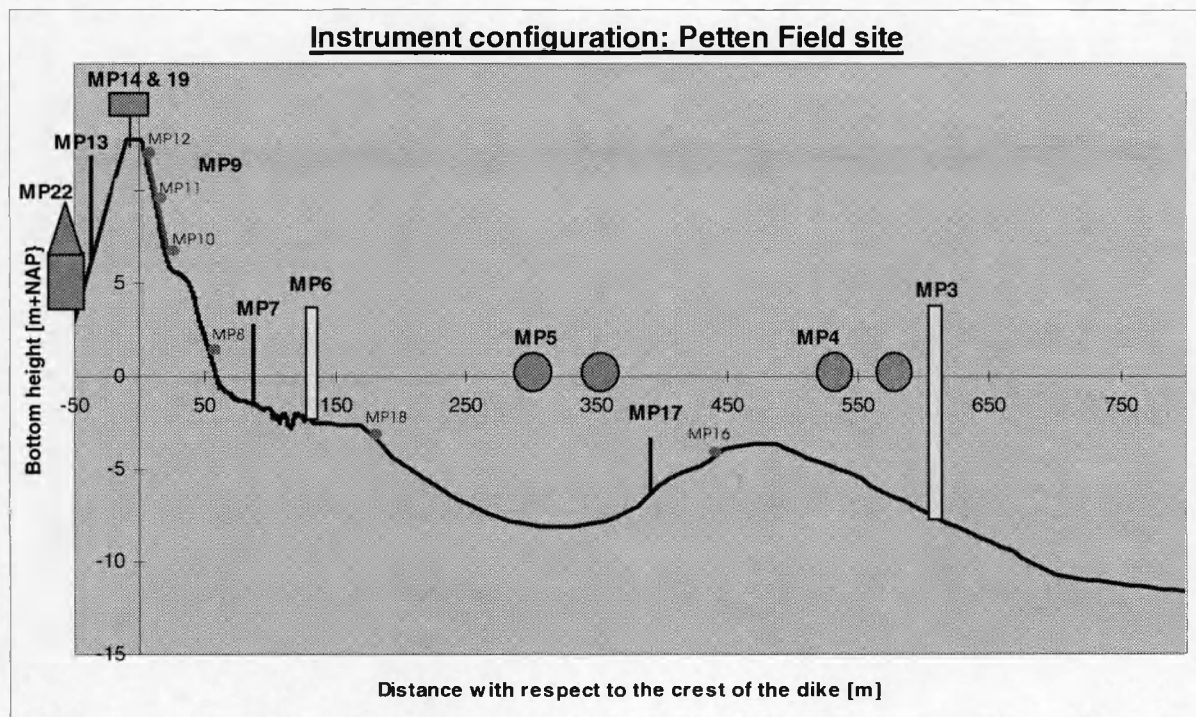
Figure 3: Position of measuring locations at the Petten field site.

RIKZ has delivered a CD-ROM with all data during the period 1995-2000 ('*Stormdata of the Petten Field Site: 1995-2000*') which can be obtained at RIKZ. A description of the data on the CD-ROM is given in a report '*Stormdata of the Petten Field Site: 1995-2000*', attached in Annex 2.3.

Table 6: Measurement devices at the measurement site in Petten

Location (Code)	Measuring period	Sensor	Distance to dike crest [m]	Local depth to datum [m NAP]	Elevation sensor to datum [m NAP]	Variables measured	Sampling frequency [Hz]
MP1	1994-2000	Directional Waverider	7972	-20	-	surface elevation wave direction	1.28 1.28
MP2	1994-2000	Waverider	3497	-10	-	surface elevation	4
MP3.1 MP3.2	1994-2000 1994-2000	Stepgauge Water Level Meter	610	-8.0	-3.0 -	surface elevation surface elevation	10 1/10
MP4 MP4	1994-1997 1997-2000	Waverider Waverider	604 527	-8.0 -8.0	- -	surface elevation surface elevation	4 4
MP5A MP5	1996-1997 1994-2000	Directional Waverider	302	-8.5	-	surface elevation wave direction	1.28 1.28
MP6.1 MP6.2 MP6.3	1994-2000 1994-2000 1999-2000	Capacitance Wire Pressure sensor Radar-levelmeter	122.9 122.7	-2.0	-0.47 -0.69	surface elevation hydrodynamic pressure	4 4 2.56
MP7.1 MP7.2	1997-2000 1997-2000	Pressure sensor (upper) Pressure sensor (lower)	75.2		+0.199 -0.271	hydrodynamic pressure hydrodynamic pressure	4 4
MP8	1997-2000	Pressure sensor	55.7	+0.5	+0.53	hydrodynamic pressure	4
MP9 called MP7 '94-'97	1994-2000	Run-up gauge	19.4	+5.7 .. +9.0	5.7..8.92	wave run-up	4
MP10 called MP7A '96-'97	1996-2000	Pressure sensor	25.6	+5.67	+5.60	hydrodynamic pressure	4
MP11 called MP7B '96-'97	1996-2000	Pressure sensor	18.2	+7.24	+7.16	hydrodynamic pressure	4
MP12 called MP7C '96-'97	1996-2000	Pressure sensor	12.7	+9.39	+9.28	hydrodynamic pressure	4
MP13	1997-2000	Anemometer Windvane	-35		± 12 ± 12	wind speed wind direction	4 4
MP14	1997-2000	Videocamera 1	-0.2		17.3	-	-
MP16	1999-2000	Pressure sensor	439			hydrodynamic pressure	4
MP17.1 MP17.2	1999-2000 1999-2000	Pressure sensor Flow velocity meter	392 391			hydrodynamic pressure flow velocity	4 ± 0.13
MP18	1999-2000	Pressure sensor	174			hydrodynamic pressure	4
MP19.1 MP19.2	1999-2000 1999-2000	Videocamera 2 Videocamera 3	1.1	+12.8 +12.8	+16.6	- -	- -
MP22 called MP8 '94-'95 called MP9 '96-'97 called MP15 '97-'99	1994-2000	Barometer	-35				

Subtask 2.4: Synthesis of prototype measurements

Task 4 ('Link between prototype and laboratory results) makes a clear distinction between the two different types of structures: a smooth sea dike (task 4a) and a rubble mound breakwater (task 4b).

During the project, the two sites (a smooth sea dike (Petten) on the one hand and a conventional rubble mound breakwater (Zeebrugge) on the other hand) have shown to be completely different to each other with regard to wave run-up. Prototype and laboratory measurements on the same type of structure have to be considered together.

Therefore, tasks 2.4 and 3.6 which were originally planned to synthesise the prototype measurements and the laboratory testing results respectively, have been reassigned. As the comparison of prototype and laboratory investigation results are part of linking the prototype measurements to the laboratory results, task 2.4 and task 3.6 have become part of task 4 'Link between prototype and laboratory results'.

TASK 3: LABORATORY INVESTIGATIONS

Subtask 3.1: Methodology including wave generation

In the project a focused and well directed set of model tests had to be carried out in order to compare prototype measurements with model test results. Uniform data instrumentation, acquisition and analysis methods have been essential for both the prototype measurements and the model test results. Six different laboratories and the two prototype sites have all followed a prescribed methodology, developed by AAU at the very beginning of the project.

The used methodology includes a description of:
- the position of measurement devices,
- the foreshore topography,
- the structure,
- the wave generation,
- the data acquisition,
- the software routines for analysis,

and the definition of :
- the wave parameters,
- the plotting routines.

The report on this Subtask *'Task 3.1 – Laboratory investigations – Methodology'* has been prepared by AAU and is given in Annex II of the *'Annual Report (To+12 till To+24)'*. It gives detailed guidelines for the laboratory investigation. An example is the placing of the blocks on the Zeebrugge breakwater models. All individual blocks have been placed according to drawings/photos from the site. An other example is a very precise and detailed description of how to filter acquired data.

In order to ensure the quality of the laboratory investigations software and model drawings have been cross examined.

During workshops measurements from different laboratories have been analysed and double-checked with software from other laboratories.

Furthermore laboratory models have been inspected by researchers from other laboratories. Several visits during model testing and some longer duration stays (each more than a week) of visiting researchers have guaranteed that the same methodology has been applied everywhere in order to obtain comparable model test results.

Subtask 3.2: Run-up measurement optimisation and analysis of existing data

a) Background and objectives

In the MAST II project 'Full Scale Dynamic Load Monitoring of Rubble Mound Breakwaters' (MAS2-CT92-0023) extensive 2D testing was carried out on the Zeebrugge breakwater and run-up values obtained did not compare well with prototype. Also, there were significant differences between the results of the different laboratories (Kingston and Murphy, 1994) which could not be totally explained by differences in model scales or test set-up. It was concluded that although the extreme point for wave run-up may be difficult to record exactly due to the foamy nature of run-up after wave breaking and the very thin run-up edge, the manner of placement of the wave probes was also a contributory factor. This can result in inconsistencies between otherwise similar sets of experiments and thus create uncertainty as to the reliability of results. Ultimately inaccurate wave run-up prediction can lead to the under design of coastal structures. Therefore the importance of consistency between experimental studies, as will be carried out in this project, cannot be over emphasised and resulted in Subtask 3.2 being included in the OPTICREST work programme.

The objectives are defined in the Technical Annex as follows,
- Optimise existing run-up measurement techniques (vertical step gauges, wave staff along the slope, ...) based on experience both on site and in the laboratory.
- Investigate new techniques e.g. added value of video recording
- Collect and analyse existing wave run-up data

In the study existing methods of run-up measurement were examined and evaluated, and recommendations were made regarding techniques to be employed within the OPTICREST project. Also possible sources of errors associated with using existing instrumentation was detailed. The magnitudes of these errors are then quantified through a series of 2D physical model tests. Finally the results of the experiments are applied to sample sets of existing data. The report on this Subtask also contains an annex which includes information obtained from the other laboratories within the project group regarding their wave run-up measurement techniques. Each of the tasks will now be briefly described.

For more detailed information on the work of this study the final report 'Wave Run-up Measurement Techniques' should be consulted. This report was included in Annex IV of the 'Annual Report (12 months)'.

b) Review of measurement methods

A number of different methods of measuring wave run-up were reviewed with their relative advantages and limitations discussed. The following is a list of the instruments that were reviewed,

1. Wave Probes
   - Conductivity/Resistance Probes
   - Capacitance Probes
   - Digital Run-up Probe
2. Video Recording
3. Camera Measurements
4. Visual Recording
5. Acoustic/Infra-red Methods
6. Surface Point Follower

c) Experimental study

A physical model study was carried out to help quantify the magnitude of the errors associated with different run-up probe placements. A test series was designed such that run-up was measured using five conductivity probes placed parallel to the slope at different distances from the surface for a variety of wave conditions. Four different types of armouring was used along with two different slope gradients. Although the models were not intended to represent any particular structure, the chosen scale of 1:30 helps ensure that the results will be applicable to future modelling within the project. The following model slopes were constructed:

1. SHED units at slope of 1:1.5
2. DIAHITIS* units at slope of 1:2.5
3. Antifer Cubes at slope of 1:1.5
4. Smooth impermeable slope of 1:2.5

This study provided some quantification of the differences in measured run-up as a result of varying the slope/probe separation. It also highlighted some of the problems associated with using multiple sloping probe arrays and difficulties in trying to extrapolate the results.

d) Re-analysis of existing data

A re-analysis of run-up data obtained in the MAST II project was carried out based on the findings of the previous study. The data as obtained from model studies in the Aalborg University, Flanders Hydraulics (HRLB) and the University College of Cork were adjusted to account for possible errors arising from the run-up probe placement. The adjusted values were obtained by multiplying the original data set by a factor dependent on the Iribarren number. The biggest adjustment was made to the data as obtained from HRLB as the probe in this case was placed 3.5 cm from the slope. If the prototype values, for irregular waves, are considered to be correct, due to the nature by which they were obtained, then it can be seen that the adjusted values are much more in agreement (with the

---

* *the DIAHITIS is a hollow block unit designed to be placed in a single layer and regular pattern on a breakwater slope. The design is such that very high porosities can be achieved through correct placement. This unit has been developed by the HMRC.*

prototype) than the original data set. This analysis seems to indicate that the order of magnitude of the adjustment is correct.

The regular data was also adjusted upwards in the same manner and shows that the fitted curve should be closer to the Losada et al. (1982) predicted values for rip-rap.

e) Conclusions and recommendations of subtask 3.2 (formulated at To+12)

The following conclusions and recommendations were made regarding wave run-up measurement techniques.

- Run-up probes (conductivity, capacitance or electrode) can accurately trace the water movement, however due to the manner in which they are placed can give errors in run-up magnitudes.

- A number of alternative methods (other than probes) can be used to measure run-up but very often these are not easy to apply.

- Single probe measurements of wave run-up can considerably underestimate the magnitude of wave run-up depending on the separation between slope and probe. The magnitude of the error seems to be dependent on the Iribarren Number.

- The use of multiple probes requires very careful test set-up, probe calibration and zero water level checks to ensure that results will be consistent.

- Linear extrapolation of multiple probe results can give an accurate representation of wave run-up for ξ values greater than 4. The accuracy of other extrapolation methods should be investigated for low ξ values.

- Given the fact that run-up is underestimated by existing probe measurement methods it is critical that techniques used in this project enable accurate results to be obtained. Therefore for experiments where the ξ values are less than 4 it is essential that multiple probes, at least three, are used and a non-linear extrapolation technique is used to obtain maximum levels. It may be desirable that one of the partners within the project group takes on the task of software development and so prevent the unnecessary duplication of work.

- The measurement techniques to be used for the OPTICREST tests should take account of the structure type. Wire probes and digital step gauges are the primary techniques that will be used. Laboratories are encouraged to take the opportunity of trying secondary methods such as visual recording to examine their effectiveness.

- For the Zeebrugge models multiple sloping probes should be used (minimum of three) with the two laboratories agreeing on the number of probes and their relative spacings. It is recommended that one probe is placed as close to the structure as is physically possible. Placement of vertical

probes in a similar manner to the prototype would be a useful exercise but may be difficult to undertake at model scale. Each laboratory should examine the feasibility of vertical probe measurements to determine its practicality. The analysis methodology should also be consistent particularly in the extrapolation techniques that will be used to determine the maximum run-up levels.

- The Petten models are more amenable to the use of vertical step gauges as they have smooth slopes. These gauges are comparable to the prototype measurement technique and are generally easier and simpler to use than wire probes. For the tests the gauge should be flush with the structure and both laboratories should have similar pin arrangements. Supplementary measurements should be taken using a wire probe for validation and comparison purposes.

f) More recent experience

While running laboratory tests (prototype storms) and comparing results with prototype results it was found that laboratory run-up was much smaller, in fact even not comparable to, than prototype wave run-up. Further research at Ghent University has led to the design and construction of a novel digital step gauge. The mechanical measuring device consists of a so-called comb of which the needles can be adjusted one by one. So the irregular surface of the armour layer can be followed very accurately. The necessary electronics is designed and constructed at Ghent University. This digital step gauge has been used in AAU, FH and UP and yielded very reliable results.

Subtask 3.3: 2D testing

a) Petten

a.1) Description of the model

Prototype measurements were performed and analysed by Rijkswaterstaat-RIKZ. For the 2D model test the most relevant equipment concerns wave buoys/capacitance wires at locations MP3, MP5 and MP6, at respectively 635 m, 300 m and 130 m seaward of the crest of the dike. The dike itself consists of a 1:4.5 slope below the berm with a slope of 1:20 (between NAP+5 m and NAP+5.7 m) and a 1:3 slope above the berm. On this upper slope a wave run-up gauge is placed.

Two-dimensional physical model tests were performed and analysed by WL | Delft Hydraulics. Results of the 2D physical model tests on the Petten Sea-defence are described in the report *'Physical model investigations on coastal structures with shallow foreshores – 2D model tests on the Petten Sea-defence'* and is given in Annex III of the *'Annual Report (To+12 till To+24)'*. Figure 4 shows the last kilometre of the foreshore as it was modelled in the flume (scale 1:40), while figure 5 shows the structure with the step gauge to measure wave run-up at the slope above the berm.
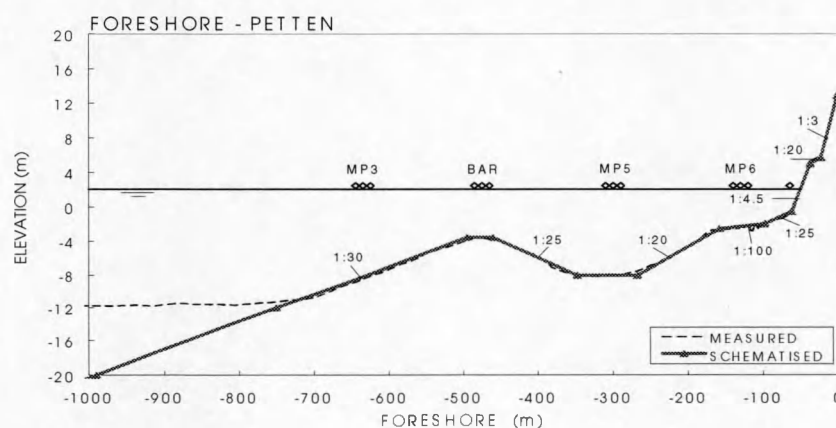
Figure 4: Foreshore as schematised for the model tests.

Since only the most landward bar could be modelled in the tests, the spectral shapes at the corresponding position of the wave board in the prototype situation were affected by wave breaking on the offshore bar. Therefore, for the tests where measured storms were modelled also the measured wave energy spectra were used, instead of standard spectral shapes such as Pierson-Moskowitz spectra or Jonswap-spectra. The waves, approximately 1000 waves per wave condition, were generated such that at the location MP3 the wave energy spectra were similar to those measured in prototype.
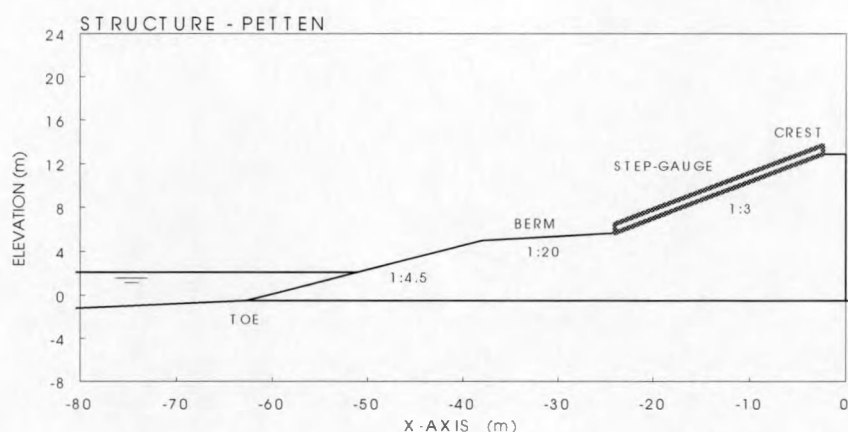
Figure 5: Structure as schematised for the model tests.

a.2) Results

At several positions on the foreshore wave conditions were measured in the model tests; at deep water, at the crest of the bar, at the toe of the structure and at three positions where wave conditions have been measured in the prototype situation: MP3, MP5 and MP6. Figure 6 shows an example of the evolution of wave heights over the foreshore while figure 7 shows an example of the evolution of wave energy spectra over the foreshore.
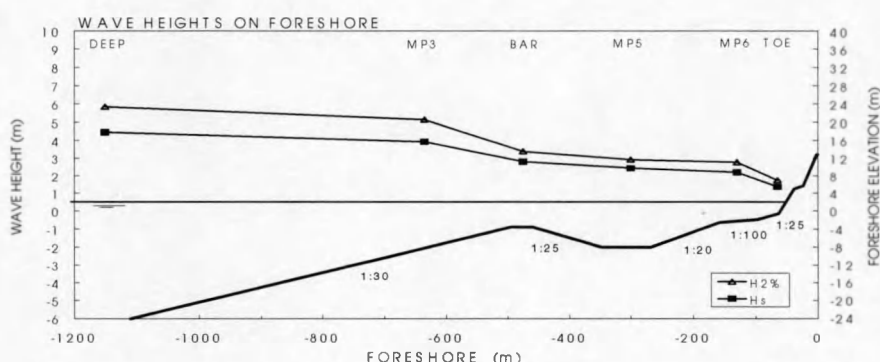
Figure 6: Example of evolution of wave heights over the foreshore.

Table 7 shows the comparison of the measured wave heights at three locations (MP3, MP5 and MP6). The average difference between the measured significant wave heights (H_s=$H_{1/3}$) in prototype and in the model tests is at MP3 (1.5 %), at MP5 (3.4%) and at MP6 (8.8%). These differences can be caused by many factors such as a slightly different foreshore during the actual storms than used in the model tests, 3D effects, effects of wind, schematisation-effects, slightly different data acquisition and data analysis procedures and scale effects. Nevertheless, the observed differences are considered acceptable to further investigate wave run-up.

Figure 7: Example of evolution of wave energy spectra over the foreshore.

Table 7: Comparison between prototype measurements and 2D model tests.

Measured storms and wave run-up levels in prototype and physical model tests.													
	MWL (MP3)		$H_{s\text{-}T}$(MP3)		$H_{s\text{-}T}$(MP5)		$H_{s\text{-}T}$(MP6)		$z_{2\%}$ (NAP)			$z_{2\%}/H_{s\text{-}T\text{-}MP6}$ differences		
Test	P	M	P	M	P	M	P	M	P	M1	M2	P	M2	%
1.01	2.10	2.14	4.24	4.29	2.61	2.69	2.94	2.62	8.3	6.8	7.5	2.12	2.05	-3.3
1.02	2.01	2.01	4.24	4.13	2.65	2.68	2.81	2.56	7.6	6.9	7.4	1.99	2.09	5.1
1.03	2.18	2.21	3.84	3.83	2.61	2.77	2.99	2.69	8.7	7.5	8.4	2.17	2.30	6.0
1.04	1.64	1.62	4.24	4.38	2.39	2.58	2.64	2.53	6.9	6.9	7.1	1.99	2.15	7.9
1.05	1.60	1.59	3.08	3.08	2.37	2.39	2.60	2.30	6.4	5.8	5.8	1.86	1.81	-3.0
1.06	2.00	2.02	3.70	3.76	2.66	2.70	2.78	2.58	7.7	6.8	7.3	2.04	2.04	0.0
P = 'Prototype'; M = 'Model tests'; M1= 'step-gauge result'; M2= 'extrapolated to zero water layer'.														

In prototype thin water layers (between 0.02 m and 0.1 m) were also recorded as wave run-up while in the model tests the step gauge could not record water layers thinner than 0.1 m (prototype scale). Therefore, comparison between the wave run-up levels measured in prototype (indicated by 'P' in Table 7, including thin water layers, and the step gauge in the model tests (indicated by 'M1' in Table 7), not including thin water layers, is not straightforward. However, linear extrapolations based on the measured wave run-up levels with a minimum water layer of 0.1 m (step gauge) and the measured wave run-up levels with a minimum water layer of 0.2 m (wave gauge along the slope), yields estimates of wave run-up levels including thin water layers. These levels are indicated by 'M2' in Table 7. These 'M2'-levels are used for comparison with prototype measurements. The comparison is also made for the non-dimensional wave run-up level, where the wave run-up level is the height above the *mean* water level (MWL) and the wave heights are the total significant wave heights ($H_s=H_{1/3}$) measured at MP6. Although wave run-up levels are normally defined as the height above the *still* water level (SWL), the *mean* water level has been used for this comparison because for the prototype circumstances the *mean* water level is available, unlike the *still* water level. The differences in percentage are listed in the last column of Table 6. The average of the differences (absolute values) is 3.9 %. Figure 8 shows the comparison between these wave run-up levels measured in prototype and in the model tests. Although these differences can also be caused

by many factors such as schematisation and scale effects, related to for instance the roughness of the slope and the effects of wind on wave run-up, the differences are considered small.
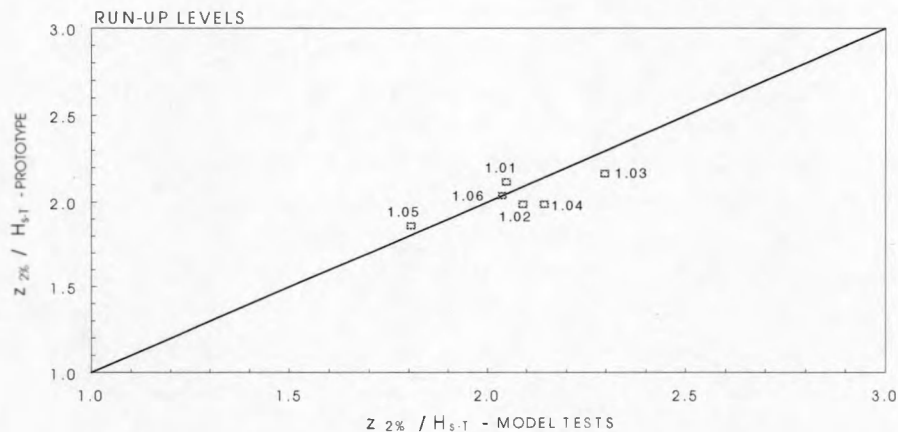
Figure 8: Comparison between wave run-up levels measured in 6 storms in prototype and those obtained from 2D model tests.

In addition to the comparison with prototype storms a parameter analysis was performed where wave heights, wave periods, water levels and wave energy spectra were varied. For these results reference is made to Annex III of the *'Annual Report (To+12 till To+24)'*.

a.3) Conclusions

Combining results from the comparison between the prototype measurements, the 2D model tests on the Petten Sea defence, other 2D model tests, and numerical model computations led to the following conclusions (Van Gent, 2000):

- Comparisons between storms measured in prototype and storms modelled in the 2D physical model tests show good agreement. The non-dimensional wave run-up levels differ only 4% on average (absolute values of the differences); considering the observed differences between prototype measurements and physical model tests it can be concluded that the schematisation and scale effects in the physical model tests are small.

- Numerical model computations support the use of the wave period $T_{-1,0}$ at the toe of coastal structures to account for the effects of wave energy spectra on wave run-up. This is in conformance with the characteristic wave period by Battjes (1969) for wave energy transport.

- Physical model tests also support the use of the wave period $T_{-1,0}$ at the toe of coastal structures to account for the effects of wave energy spectra on wave run-up. In Van Gent (1999) it was shown that these conclusions are also valid for wave overtopping.

- Using the peak wave period in predictions on wave run-up may lead to large inaccuracies for situations with shallow foreshores.

- A smooth and simple formula for wave run-up on coastal structures was proposed with a gradual curve towards an upper limit of the non-dimensional wave run-up:

$$z_{2\%} / (\gamma \, H_s) = c_0 \, \xi_{s,-1} \qquad \text{for } \xi_{s,-1} \leq p$$

$$z_{2\%} / (\gamma \, H_s) = c_1 - c_2 / \xi_{s,-1} \qquad \text{for } \xi_{s,-1} \geq p \qquad (1)$$

where H_s is the significant wave height of the incident waves at the toe of the structure ($H_s = H_{1/3}$), the reduction factor γ ($\gamma = \gamma_f \, \gamma_\beta$) takes the effects of angular wave attack (γ_β) and friction (γ_f) into account, the surf-similarity parameter is defined as $\xi_{s,-1} = tan\varphi / \sqrt{2\pi H_s / g T_{-1.0}^2}$, and continuity between both sections and their derivatives determine $c_2 = 0.25 \, c_1^2/c_0$ and $p = 0.5 \, c_1/c_0$. Equation 1 was calibrated based on physical model tests: $c_0 = 1.35$ and $c_1 = 4.7$ (with a standard deviation of 0.37). If for the significant wave height the spectral wave height $H_s = H_{m0}$ is used the coefficients become $c_0 = 1.45$ and $c_1 = 3.8$ (with a standard deviation of 0.24). Most data concerned situations in the range $1 < \xi_{s,-1} < 10$, in which $2.5 \leq tan \, \varphi \leq 6$. To which extent application of Equation 1 outside these ranges is appropriate still needs to be investigated. This formula is rather generic because it can be used for situations with relatively deep water at the toe of coastal structures and also for situations with shallow foreshores. Important is that the influence of wave energy spectra on wave run-up is accounted for by using the spectral wave period $T_{-1.0}$ of the incident waves at the toe of coastal structures.

b) Zeebrugge

b.1) 2D-testing at Flemish Community - Flanders Hydraulics

Introduction

This summary describes two-dimensional model tests of the Zeebrugge breakwater performed by Flemish Community - Flanders Hydraulics (FCFH) in the project MAS03-CT97-0116 "The optimisation of crest level design of sloping coastal structures through prototype monitoring and modelling" (OPTICREST) within the Mast III framework of EU.

The objectives of these two-dimensional model tests were to study wave run-up and overtopping and to model measured prototype storms. The report on this Subtask, titled *'Laboratory investigations: 2D testing – the Zeebrugge breakwater'* is given in Annex 3.3a.

Description of the model

The Zeebrugge breakwater (except the core) has been scaled 1:30 using the Froude criterion. In order to model the flow in the core properly, a scale of 1:20 for the core material (Burcharth et al., 1999) has been chosen.

Figure 9: Layout of the Zeebrugge model.
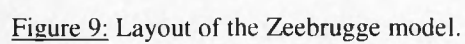
The layout of the model (see Annex II, *'Annual Report (T_0+12 till T_0+24)'*) is shown in figure 9. An important adaptation in the cross-section is the slope of the breakwater. Design drawings mention 1/1.5 but measurements (Versluys (1999)) proved that the slope in prototype is somewhat steeper. The model has been built with a slope of 1/1.3 in order to simulate wave run-up in prototype as close as possible.

The foreshore has been modelled up to 600 m in front of the breakwater to include the bar at approximately 550 m. The foreshore is shown in figure 10.
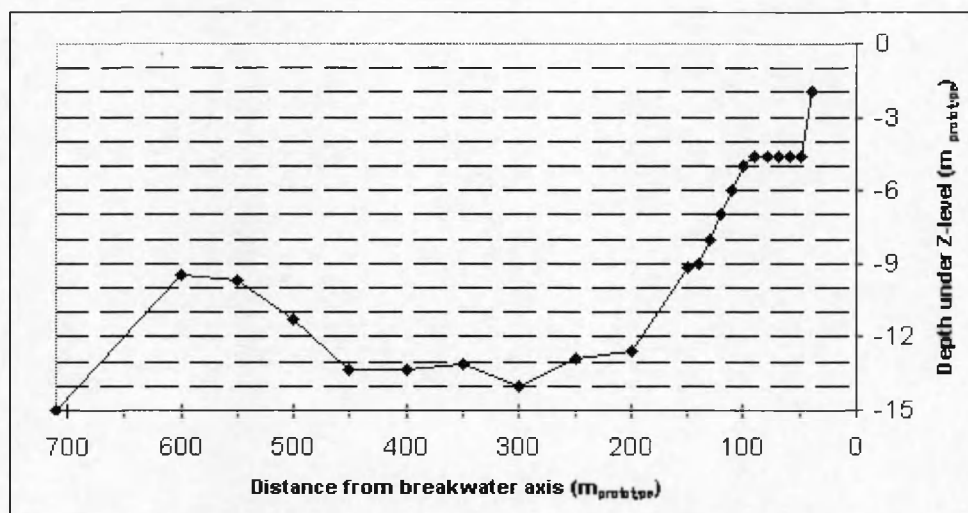
Figure 10: The foreshore in front of the Zeebrugge breakwater.

In the case of the Zeebrugge breakwater, the permeability of the breakwater plays a prominent part in the wave run-up. Therefore it was important to place the Antifer cubes in the top layer according to a record of the actual position in prototype. Also the sand levels measured in the breakwater core were modelled. During the tests, it was ascertained that this sand infiltration in the model was partly washed out.

Wave measurements were done at locations corresponding to wave measurements in prototype.

Run-up measurements have been carried out with 2 different instruments (see Annex IV, *'Annual Report (12 months)'*).
Three sloping gauges parallel to the breakwater surface (see figure 11a) resulted in 2 run-up signals. The first one is the signal measured by the lowest run-up gauge, the second one is an extrapolation of all 3 run-up measurements towards the breakwater surface. These run-up signals were not reliable due to the different distances between the gauges and every single cube.
An improved accuracy has been obtained with a digital step gauge (see figure 11b) that was able to follow the pattern of the cubes.
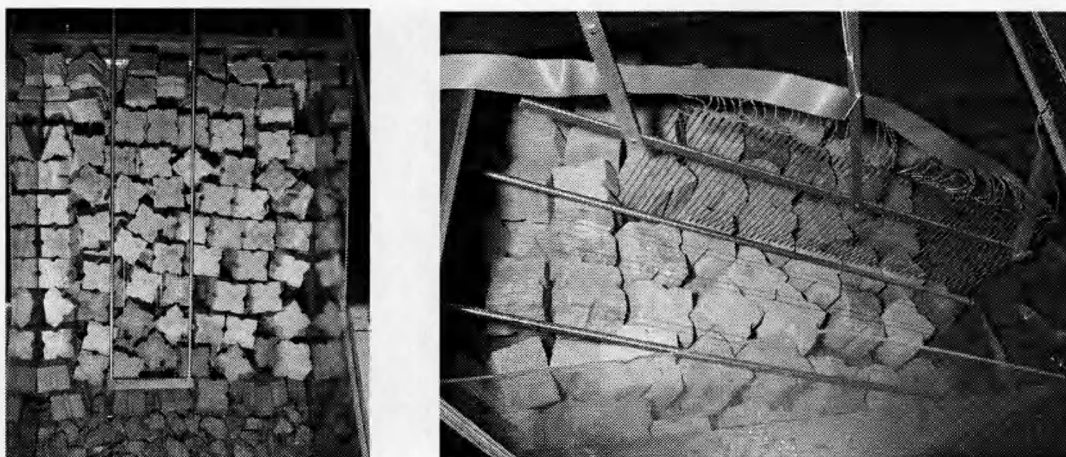
Figure 11: Run-up gauges: (a) sloping gauges, (b) step gauge.

The amount of overtopping water was measured as a total volume after each test. Only very few overtopping events occurred.

Results

Fifteen storm periods were modelled to compare results of model tests with prototype measurements in Zeebrugge. It concerns 5 tests reproducing 5 different storm periods at high water level, and 10 tests reproducing 2 different storms each divided into 5 storm periods around high water.

To reproduce the storms an iterative procedure has been applied to obtain similar shapes of the wave energy spectra in model and in prototype offshore. The agreement of all reproduced spectra is considered acceptable for the present investigation.
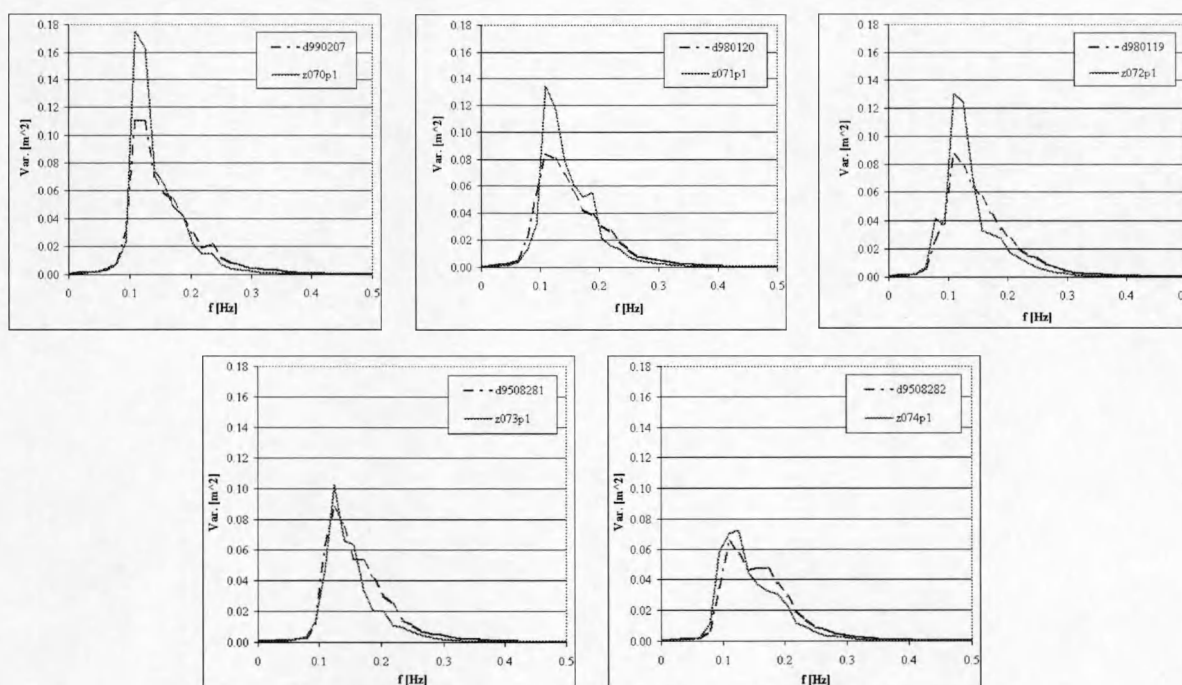
Figure 12: Comparison wave energy spectra in model and in prototype (storms z070-z074).

For example figure 12 shows the comparison of the wave energy spectra in model and in prototype for 5 storms at high water level. The peak period is close to the target, the difference in $T_{0.1}$ is somewhat larger due to more energy at f_p, and slightly less energy at higher frequencies. The average difference in $T_{0.1}$ is 8.5%, in H_{m0} 5.2%.

Table 8 summarises the measurements of the 7 storm periods at high water.

The difference between model and prototype is between 0.6% and 11.6% for H_{m0}, between 10.2% and 20.3% for $Ru_{2\%}$ and between 0.6% and 22.0% for $Ru_{2\%}/H_{m0}$. In the model the average of $Ru_{2\%}/H_{m0}$ is approximately 1.46 whereas this value equals 1.73 in prototype. Important conclusion is the fact that run-up is smaller in model than in prototype for comparable wave conditions.

Table 8: Summary of the storm periods at high water.

Test	z070p1	z071p1	z072p1	z073p1	z074p1	z101c1	z102c1
Prototype							
H_{m0} [m]	3.13	3.01	2.95	2.87	2.68	3.01	2.58
$Ru_{2\%}$ [m]	5.42	5.37	5.09	4.27	4.43	5.55	4.76
$Ru_{2\%}$ / H_{m0} [-]	1.73	1.79	1.73	1.49	1.66	1.85	1.84
Model							
H_{m0} [m]	3.34	3.17	2.98	2.54	2.64	3.08	2.56
$Ru_{2\%}$ [m]	4.63	4.46	4.57	3.76	3.76	4.42	4.02
$Ru_{2\%}$ / H_{m0} [-]	1.39	1.40	1.53	1.48	1.42	1.44	1.57
Difference							
H_{m0} [m]	6.7%	5.4%	1.1%	-11.6%	- 1.4%	2.2%	-0.6%
$Ru_{2\%}$ [m]	-14.6%	-17.0%	-10.2%	-12.0%	-15.1%	-20.3%	-15.5%
$Ru_{2\%}$ / H_{m0} [-]	-19.9%	-21.5%	-11.4%	- 0.6%	-14.2%	-22.0%	-15.0%

Table 9: Summary of storm z101 around high water.

	HW-3 - HW-2	HW-2 - HW-1	HW-1 - HW+1	HW+1 - HW+2	HW+2 - HW+3
Test	z101a1	z101b1	z101c1	z101d1	z101e1
Prototype					
H_{m0} [m]	2.34	2.74	3.01	2.89	2.48
$Ru_{2\%}$ [m]	5.92	6.01	5.55	5.49	5.77
$Ru_{2\%}$ / H_{m0} [-]	2.53	2.19	1.85	1.90	2.33
Model					
H_{m0} [m]	2.74	3.00	3.08	2.98	2.62
$Ru_{2\%}$ [m]	3.46	4.39	4.42	4.39	4.12
$Ru_{2\%}$ / H_{m0} [-]	1.26	1.46	1.44	1.47	1.57
Difference					
H_{m0} [m]	17.1%	9.5%	2.2%	3.1%	5.8%
$Ru_{2\%}$ [m]	-41.6%	-27.0%	-20.3%	-20.1%	-28.5%
$Ru_{2\%}$ / H_{m0} [-]	-50.1%	-33.3%	-22.0%	-22.5%	-32.4%

Table 10: Summary of storm z102 around high water.

	HW-3 - HW-2	HW-2 - HW-1	HW-1 - HW+1	HW+1 - HW+2	HW+2 - HW+3
Test	**z102a1**	**z102b1**	**z102c1**	**z102d1**	**z102e1**
Prototype					
H_{m0} [m]	2.52	2.62	2.58	2.52	2.16
$Ru_{2\%}$ [m]	5.86	5.81	4.76	5.41	4.83
$Ru_{2\%} / H_{m0}$ [-]	2.33	2.22	1.84	2.15	2.24
Model					
H_{m0} [m]	2.80	3.01	2.56	2.80	2.49
$Ru_{2\%}$ [m]	3.84	4.51	4.02	4.11	3.34
$Ru_{2\%} / H_{m0}$ [-]	1.37	1.50	1.57	1.46	1.34
Difference					
H_{m0} [m]	11.3%	15.0%	-0.6%	11.3%	15.4%
$Ru_{2\%}$ [m]	-34.4%	-22.4%	-15.5%	-24.1%	-30.8%
$Ru_{2\%} / H_{m0}$ [-]	-41.1%	-32.5%	-15.0%	-31.8%	-40.1%

Table 9 and table 10 summarise the measurements of the 2 storms divided into 5 storm periods around high water.

The differences between model and prototype become larger at lower water level. This can clearly be seen in figure 13. As opposed to prototype, no larger dimensionless run-up $Ru_{2\%}/H_{m0}$ was measured at lower water level in the model.

These differences can be caused by many factors such as differences in permeability, the pattern of the 2 Antifer layers, different sand infiltration levels, slightly different measurement systems, imperfect modelling of target spectra, effects of wind and current, model effects and scale effects (viscous effect).
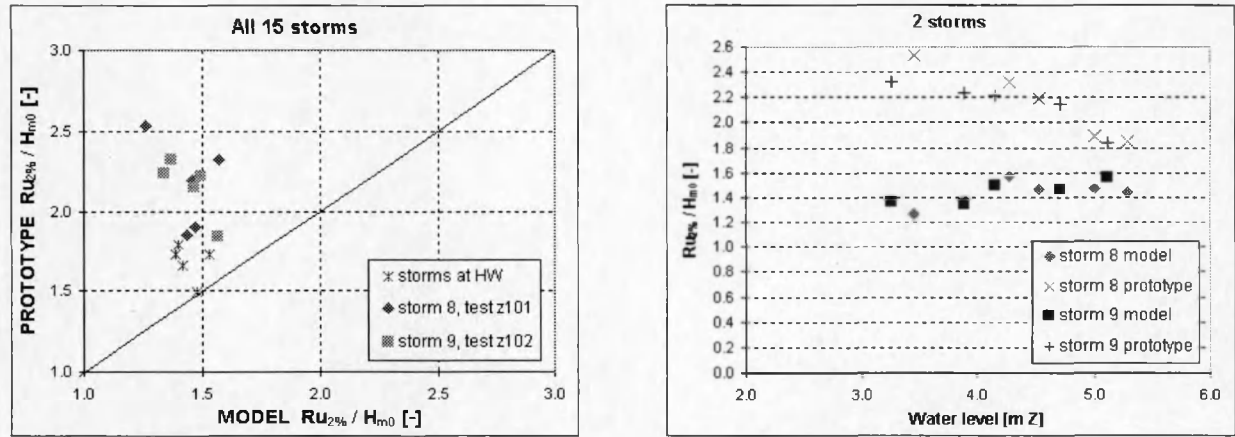
Figure 13: Comparison of the dimensionless run-up for all storms.

The influence of the pattern of the cubes beneath the electrodes of the step gauge has been examined. The upper 10 electrodes were located on top of a hole between the cubes. To examine its influence on run-up measurements this hole was partly filled to prevent water going down in stead of being registered by the step gauge (see figure 14).

(a)   (b)
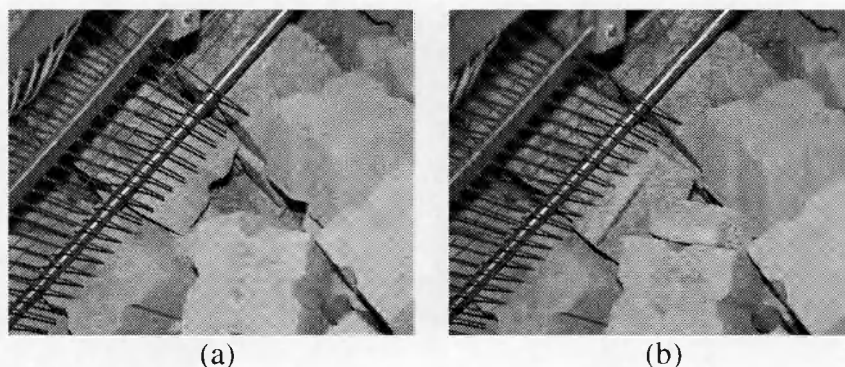
Figure 14: Hole between cubes: (a) original pattern, (b) hole partly filled.

The results showed a clearly larger run-up measured by the step gauge; the dimensionless run-up $Ru_{2\%}/H_{m0}$ was approximately 25% larger in this specific set-up. It can be concluded that the pattern of the cubes has a large impact on run-up measurements. This is due to the fact that wave height, run-up level and its variation are of the same order of the dimensions of the Antifer cubes.

A limited range of all wave parameters was investigated by simulating the prototype storms. Within these ranges it is shown that the dimensionless run-up $Ru_{2\%}/H_{m0}$ gives a very consistent estimate of the run-up. In these two-dimensional model tests the overall $Ru_{2\%}/H_{m0}$ value equals approximately 1.45, whereas this values is approximately 1.7 in prototype.

Conclusions

The reproduction of 7 prototype storms at high water level showed that the dimensionless run-up $Ru_{2\%}/H_{m0}$ is underestimated 10%-20% when comparing with prototype measurements.
The model results differed even more at lower water levels.

A number of factors are thought to be responsible for the smaller wave run-up in the model:
- differences in permeability,
- the pattern of the 2 Antifer layers,
- different sand infiltration levels,
- slightly different measurement systems,
- imperfect modelling of target spectra,
- effects of wind and current,
- scale effects (viscous effect)
- model effects ...

The research within this project made it not possible to quantify the influence of these factors.

Extra tests carried out with a slightly different pattern of the cubes beneath the electrodes of the step gauge, showed clearly a large impact of the pattern of the cubes on run-up measurements. It is supposed that this is due to the fact that wave height, run-up level and its variation are of the same order as the dimensions of the Antifer cubes.

<u>b.2) 2D-testing at Universidad Politécnica de Valencia (UPV)</u>

Introduction

This summary describes the results from the experiments on the 2D model test of Zeebrugge breakwater conducted at the UPV wind and wave flume. The principal objectives of these tests were: (1) to reproduce as best as possible the 2-D model and experiments conducted at the FCFH and (2) to study the influence of wind on wave run-up and wave overtopping.

Although several preliminary tests were conducted at the UPV wind and wave test facility in 1998 and 1999 (several interferences and discrepancies among different sensors were detected during the preliminary tests), this summary focuses the results of the last series of 2D experiments conducted in October to November of 2000 as the UPV experimental input to the II Bremen Workshop (12-13 December 2000) and the additional experiments carried out after the II Bremen workshop during January 2001.

The 1:30 Zeebrugge breakwater model was constructed following the instructions of FCFH during January to March 2000. The UPV wind and wave test facility is similar to the FH wave flume so similar results were expected to be obtained when using null windspeed. The wave run-up measurements systems used in this final experiments were: (1) the OPTICREST-standard UG wave run-up step gauge with external comb for experiments without wind, (2) a modified wave run-up step gauge with the UPV internal comb for experiments with wind and (3) overtopping measurement system.

Model set-up

The UPV wind and wave test facility has a piston type hydraulic controlled wavemaker able to generate regular and irregular waves without active absorption (maximum piston displacement: 80 cm). The power of the blower is controlled manually to fix a specific wind speed for each test. The model was constructed following as close as possible the instructions given by FCFH in order to construct the same model in the UPV flume (without the bar located 550 meters from the structure). Because UPV flume is wider (120 cm instead 70 cm) additional information was required from the topographic description of the prototype to complete the model. Scale and gradation were similar to that used in the FCFH model.

Figure 15 shows the layout of the 2D model tested in the UPV wind and wave facility. The sand contamination of the core detected in prototype and considered in FCFH were also considered in the

UPV model although the test proved in both laboratories that sand is unstable in the core near the armour layer (it was washed away).
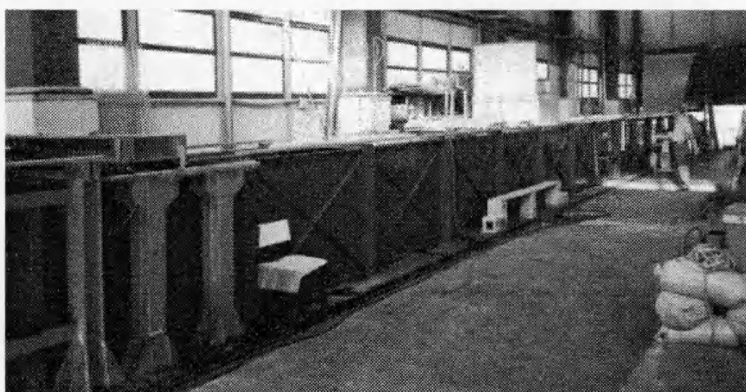
Figure 15: General view of the UPV wind and wave test facility.

The 1:30 model was constructed with the topographic information of the prototype and the FCFH construction details. The agreement with FCFH model was considered excellent (without foreshore bar and having a wider section and coloured blocks). Waves, water levels and rundown were measured using capacitance wave gauges. For tests without wind, wave run-up was measured using the Step-Gauge Run-up Measurement System (S-GRMS) constructed by University of Ghent following similar design guidelines than the S-GRMS used by FCFH and AAU; a modified UPV version of internal comb was used for test with wind Overtopping was measured using a cannel and weighting box placed in the centre of the section.

The windspeed was measured using pitot tubes at different positions in the wind tunnel. The general flux or air in the wind tunnel was related to a reference point in which the windspeed was stable and measured during the tests with waves and wind.

Test programme and experimental results

The UPV tests correspond to regular and irregular tests described in the test matrix defined in the Methodology with additional cases using windspeeds of 3, 5 and 7 m/sec.

The wave parameters were calculated "cleaning" high and low frequency waves from records. It is interesting to point out the difference between the spectrum offshore and the spectrum measured at the toe of the structure. The high and low frequency components are analysed during the experiments. In addition to the major difference between waves measured offshore and at the toe of the structure, the other very important difference in measuring wave run-up is that related to the wave gauge. Capacitance wave gauges currently used to measure wave run-up systematically underestimate wave run-up. Therefore, step gauge is used to measure wave run-up.

(i)   Wave run-up measurements

Regular waves

The wave amplitudes recorded at the toe of the structure showed a significant reduction for the test matrix. The cases similar to storms 8 and 9 showed amplification and no breaking. Figure 16 shows the relationship between mean wave amplitude recorded at the toe of the structure and in $Ze1$ as function of $Ir(Ze1)$ and $H(Ze1)/h$.
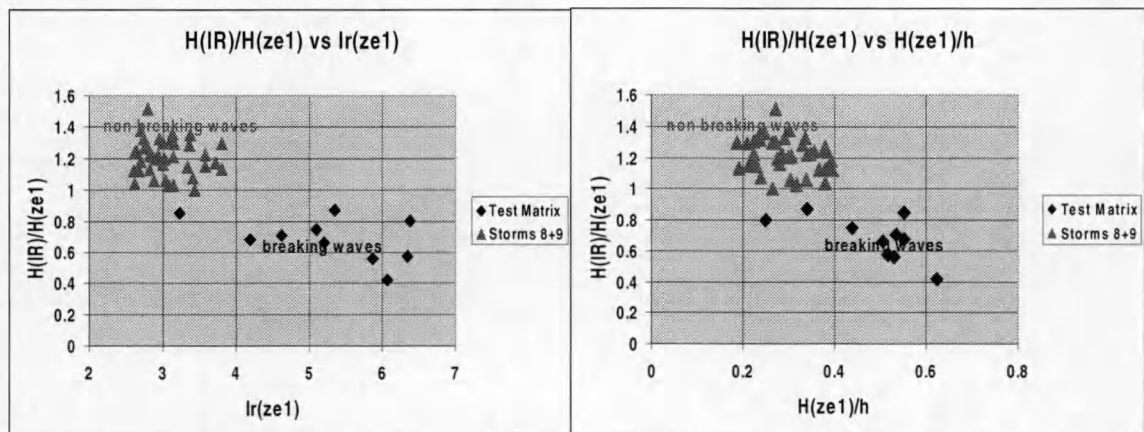
Figure 16: $H(IR)/H(Ze1)$ as function of $Ir(Ze1)$ and $H(Ze1)/h$.

The ratio Ru/H is given in figure 17 (Ru was corrected using MWL at IR). Most waves were breaking at the toe of the structure for the test matrix case but the ratio $Ru/H(Ze1)$ is similar to the regular cases of storms 8 and 9.
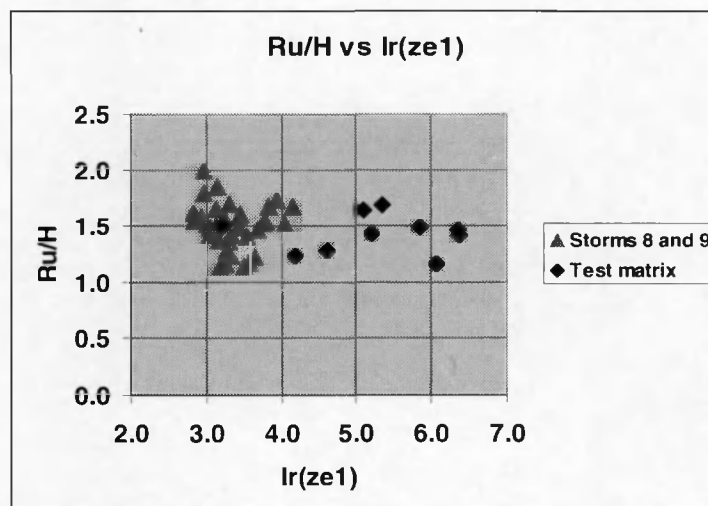
Figure 17: Ru/H as function of $Ir(Ze1)$.

Irregular waves

Wave breaking plays a very important role defining the waves really attacking the structure; the reduction of H_{mo} depends on the MWL. Figure 18 shows the ratio $H_{mo}(IR)/H_{mo}(Ze1)$ as function of $H_{mo}(Ze1)/h$. Irregular waves show a similar pattern than regular waves. The irregular cases corresponding to the test matrix show a reduction of magnitudes due to breaking while the cases similar to the prototype storms show less reduction of H_{mo}.
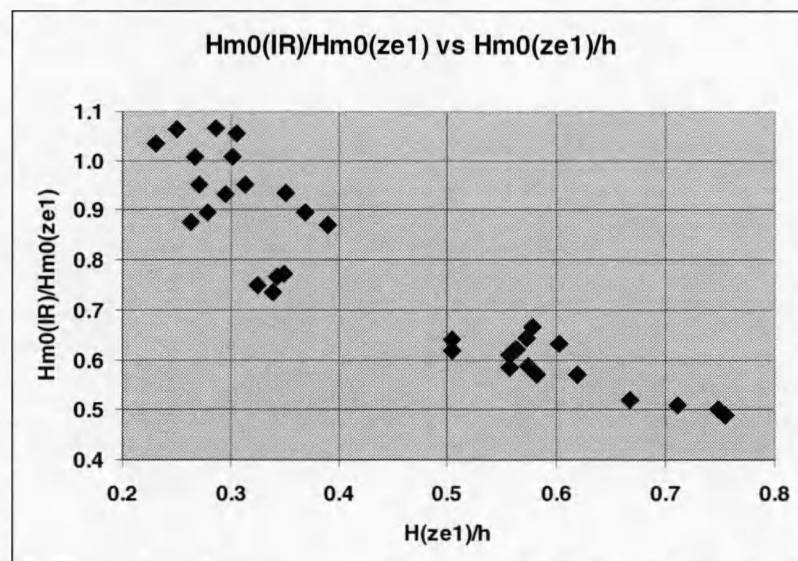
Figure 18: $H_{mo}(IR)/H_{mo}(Ze1)$ as function of $H_{mo}(Ze1)/h$.

Prototype observations of ratio $Ru_{2\%}/H_{mo}$ in the range 1.2 to 1.8 (significantly higher than 1 for $Ir = 3.0$ were the starting point of OPTICREST. If H_{mo} is computed in $Ze1$ (incident + reflected waves), the ratio $Ru_{2\%}/H_{mo}$ measured in the UPV overtopping experiments (test matrix cases which overtopping rate were expected to be significant) ranged 1.3 to 1.7 for $MWL = +3$ and ranged 1.1 to 1.3 for $MWL = +4$ or $MWL = +5$. However, it is obvious that $Ru_{2\%}$ observations were "distorted" by the overtopping event; the "distortion" is higher for higher water levels and can be measured by the ratio $Ru_{2\%}/Ru_{25\%}$ (1.67 for Rayleigh distribution). The explanation of this apparently discrepancy between observations of $Ru_{2\%}$ and $Ru_{25\%}$ is simple: the highest wave run-up events produce overtopping and are recorded as wave run-up lower than it should be if the crest elevation was high.

Figure 19 shows the Rayleigh-equivalent $Ru_{2\%}/H_{mo}(Ze1)$ corresponding to the tests with irregular waves depending on MWL, compared to the 80% confidence band of the Rayleigh-equivalent $Ru_{2\%}/H_{mo}(Ze1)$ measured in prototype (storms 8 and 9). The wave run-up measurements corresponding to cases with significant overtopping were removed from the analysis. The ratio R-E $Ru_{2\%}/H_{mo}(Ze1)$ is not very sensitive to MWL; on the contrary, figure 20 shows that R-E $Ru_{2\%}/H_{mo}(Ze1)$ increases with $Ir(Ze1)$. The $Ru_{2\%}/H_{mo}$ dependency on $Ir(Ze1)$ could not be checked with the prototype storms because measured $Ir(Ze1)$ in prototype were in the very narrow range: $3.1 < Ir(Ze1) < 3.9$.
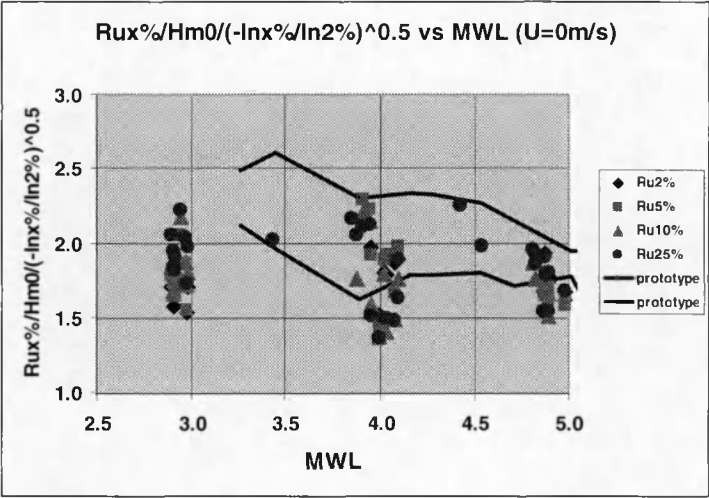
Figure 19: Rayleigh equivalent $Ru_{2\%}/H_{mo}$ versus MWL vs. to 80% confidence band of prototype storms 8 and 9.
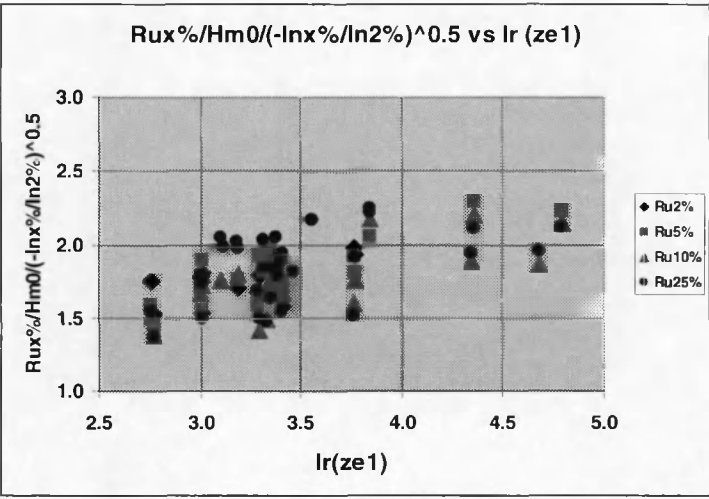
Figure 20: Rayleigh equivalent $Ru_{2\%}/H_{mo}$(ze1) versus Ir(ze1).

Storms 8 and 9

Prototype observations of storms 8 and 9 were compared during the II Bremen workshop (12-13 Dec 2000). Prototype, AAU, FCFH and AAU observations were available. Distributions of $Ru_{x\%}$ were analysed ($x\% = 2\%$, 5%, 10%, 25% and 50%) as well as spectral shapes and distributions of wave heights. Figure 21 shows the Rayleigh equivalent-$Ru_{2\%}$ corresponding to prototype for different water levels.

Rux%/Hm0/(-lnx%/ln2%)^0.5 vs MWL (prototype)
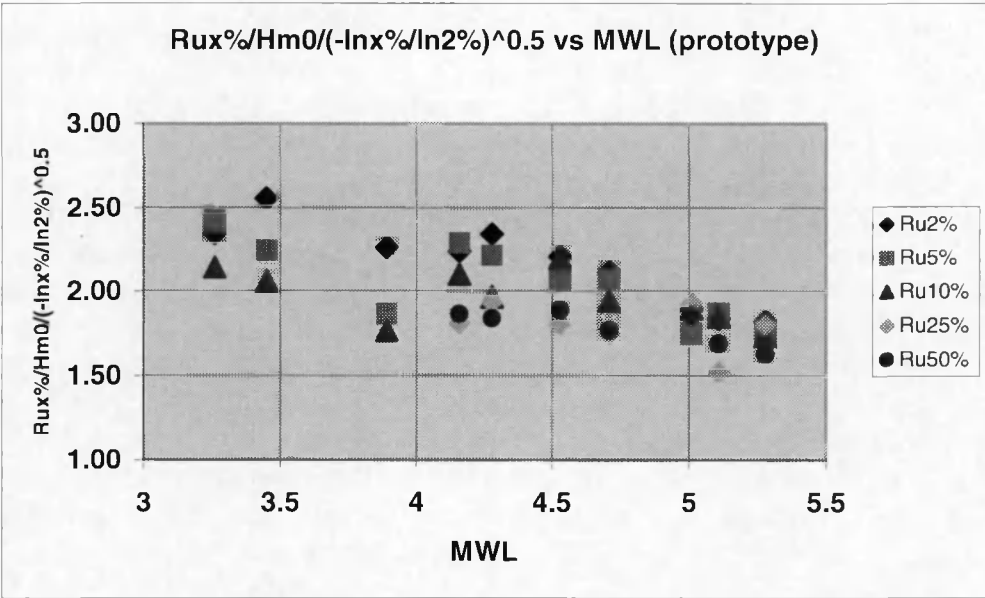
Figure 21: Rayleigh equivalent-$Ru_{2\%}$ (prototype) for different water levels.

If wave run-up events were Rayleigh distributed, the points in figure 21 were not disperse and the order of $Ru_{x\%}$ points would be independent of x%. The prototype $Ru_{x\%}$ observations are dependent of the *MWL* showing higher $Ru_{x\%}/H_{mo}$ for lower *MWL*. Rayleigh distribution of *Ru* seems to be a good approximation for higher water levels (*MWL* > +5) but not for lower water levels (*MWL* < +4.5).

Rux%/Hm0/(-lnx%/ln2%)^0.5 vs MWL (UPV)
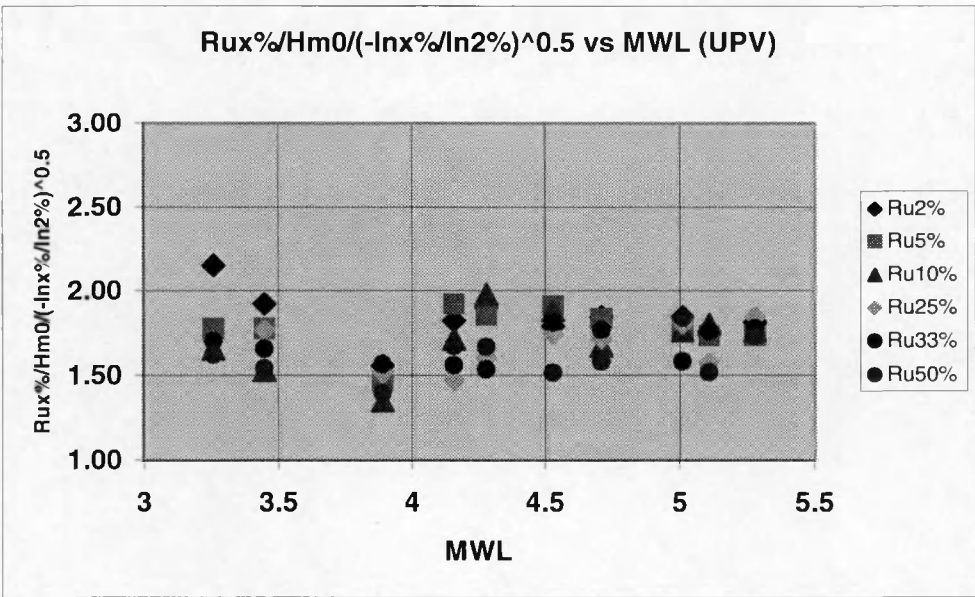
Figure 22: Rayleigh equivalent-$Ru_{2\%}$ (UPV) for different water levels.

Figure 22 shows the Rayleigh equivalent-$Ru_{2\%}/H_{mo}$ corresponding to UPV modelling of storms 8 and 9 for different water levels. Wave run-up events seems to be Rayleigh distributed for higher water levels and a departure from Rayleigh is observed for lower water levels similar to prototype. Figure 23 shows the 80% confidence band of the Rayleigh equivalent $Ru_{2\%}/H_{mo}$ corresponding to prototype, FCFH and UPV (storms 8 and 9) and the $Ru_{2\%}/H_{mo}$ measured by AAU.
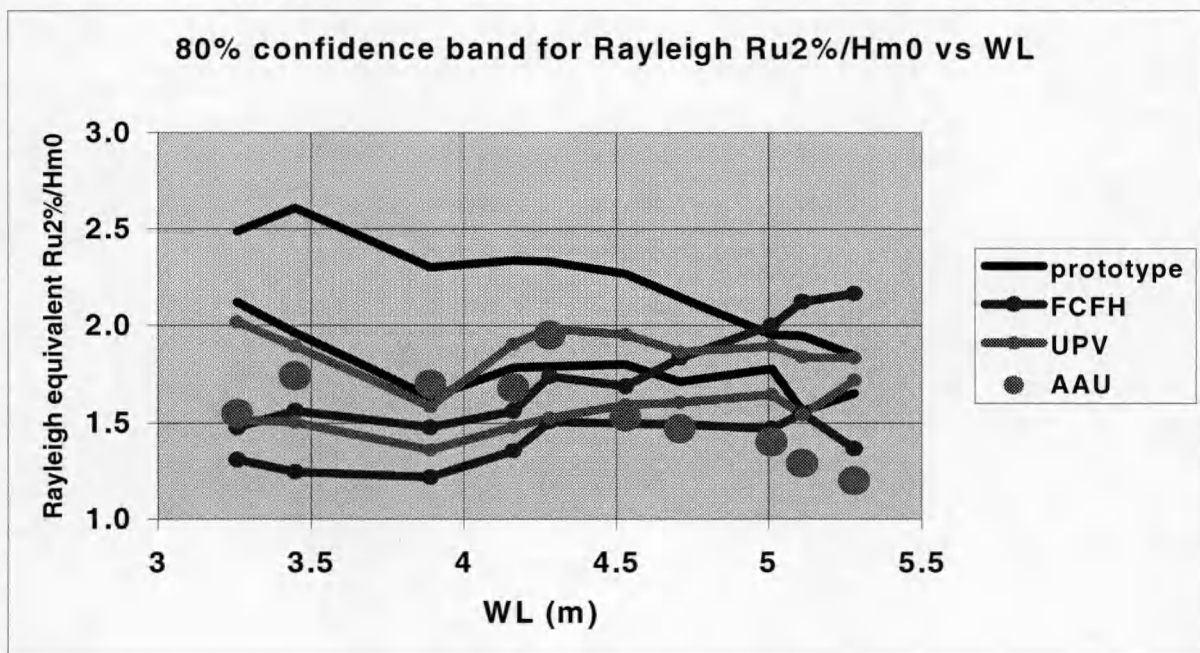
Figure 23: 80% confidence bands of Rayleigh equivalent-$Ru_{2\%}$ *for different water levels and laboratories.*

(ii) Rundown measurements

Regular waves

The rundown measured with the capacitance wave gauges produced the ratios *Rd/H* shown in figure 24.
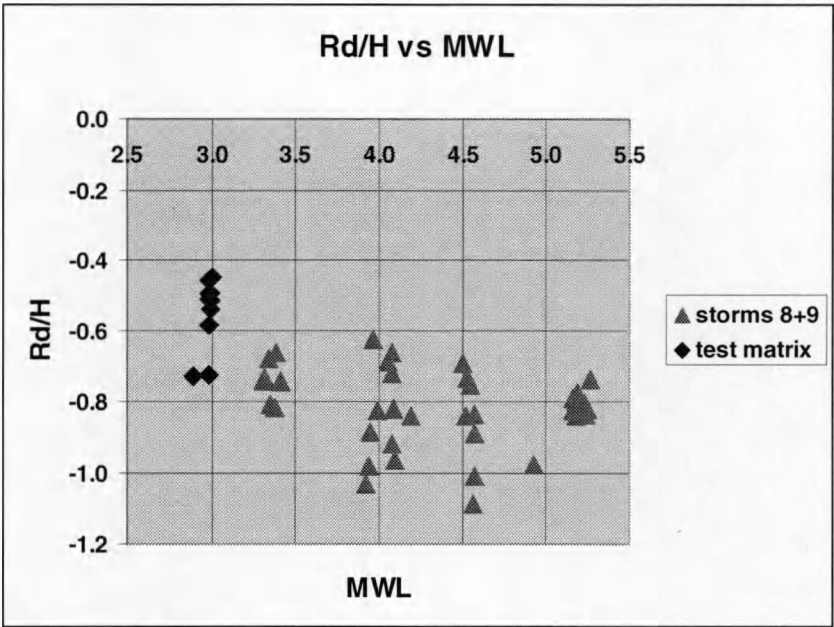
Figure 24: Rd/H as function of MWL.

Irregular waves

The observed $Rd_{2\%}$ using the capacitance wave gauges presented in Figure 25 show a similar pattern than regular waves. $Rd_{2\%}$ depends on MWL.
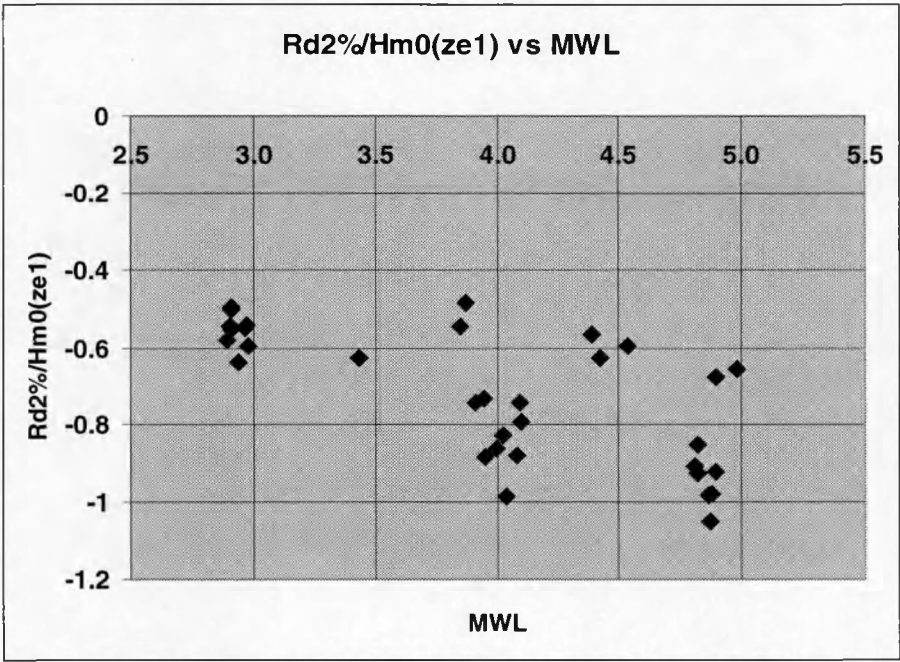
Figure 25: $Rd_{2\%}/H_{mo}$ as function of MWL.

(iii) Overtopping measurements

Regular waves

No significant overtopping was observed to any combination of wave heights and periods for water levels +3 and +4. Wave breaking process were limiting the waves really attacking the structure. Irregular waves with much less intensity were able to produce overtopping because specific combinations of wave heights and periods generate large wave run-up and wave overtopping events.

Irregular waves

The overtopping rates depend on many factors (H_{mo}, Rc, Ir, etc.). Figure 26 represents the normalized overtopping rate (test matrix $H_{mo} > 4.0m$) as function of

$$Ru = Ru - Rc$$

$$Ru = Ru - Rc = 1.7 * Ru_{25\%} - Rc$$

$Ru = 1.7 * Ru_{25\%}$ is the Rayleigh equivalent $Ru_{2\%}$ based on the $Ru_{25\%}$ and Rc is the crest freeboard. The dependency of the overtopping rate on $Ru - Rc$ is very strong.
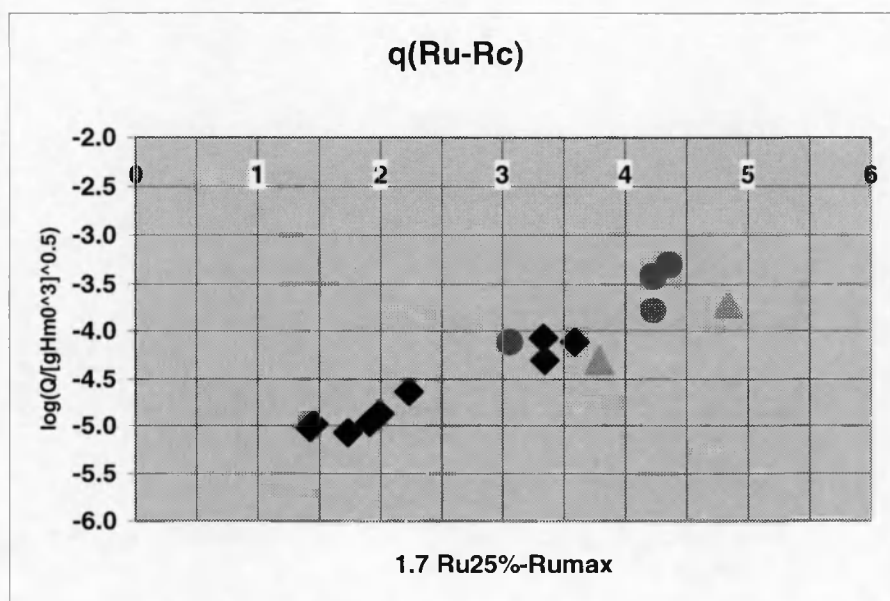
Figure 26: $\log(Q/H_{mo}{}^{\wedge}1.5)$ as function of $(Ru-Rc)$

Taking into consideration that UPV observations of Rayleigh equivalent Ru2% is almost independent of water levels with values in the range 1.6 to 2.0, and approximate estimation of theoretical Ru2% based on Hm0 is RuH=1.8 Hm0. Figure 27 shows the influence of wind on wave overtopping.
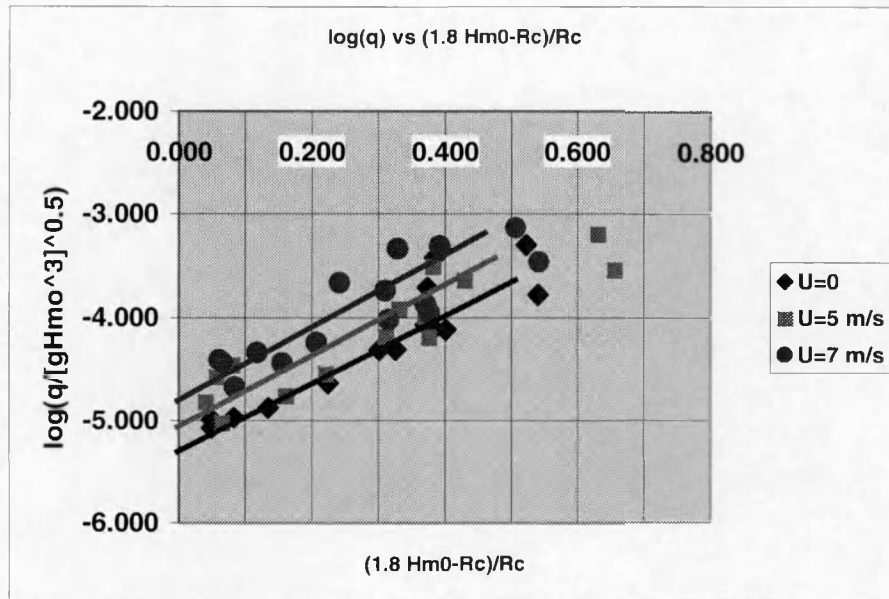
Figure 27: $\log(Q/H_{mo}{}^{\wedge}1.5)$ as function of $\{(RuH\text{-}Rc)/Rc\}$ and windspeed.

The corresponding wave overtopping formula for low and moderate wave overtopping and no wind corresponding to figure 27 ($RuH=1.8\ H_{mo} > Rc$) is:

$$\frac{q}{\sqrt{gH_{m0}^3}} \approx \exp\left[7.5\left(\frac{1.8H_{m0} - Rc}{Rc}\right) - 12\right]$$

b.3) 2D-testing at Aalborg University

A three dimensional small scale model (1:40) has been built in the wave tank at AAU. For the reproduction of the prototype storms, perpendicular ($\theta = 0°$) incident waves (2D longcrested waves) have been applied. Therefore, these are reported in this paragraph about 2D testing.

The model set-up and extensive description of the instrumentation have beend escribed in Annex VIII of 'Annual Report (To+12 till To+24)'. The most important results are summarised here. Wave run-up has been measured with two different measuring devices: a traditional resistance gauge and the novel UG step gauge.

Figure 28 shows the spectra of the five reproduced storm sessions. The method of reproducing the waves in the laboratory does not ensure the wave spectra to be completely the same as in prototype. The agreement between the measured wave height H_{mo} in prototype and the wave height obtained in the laboratory is satisfactory. However, the T_{01} in laboratory is systematically higher than in prototype. This means, that the reproduced storms contain more low frequent energy. This can be seen in table 11.
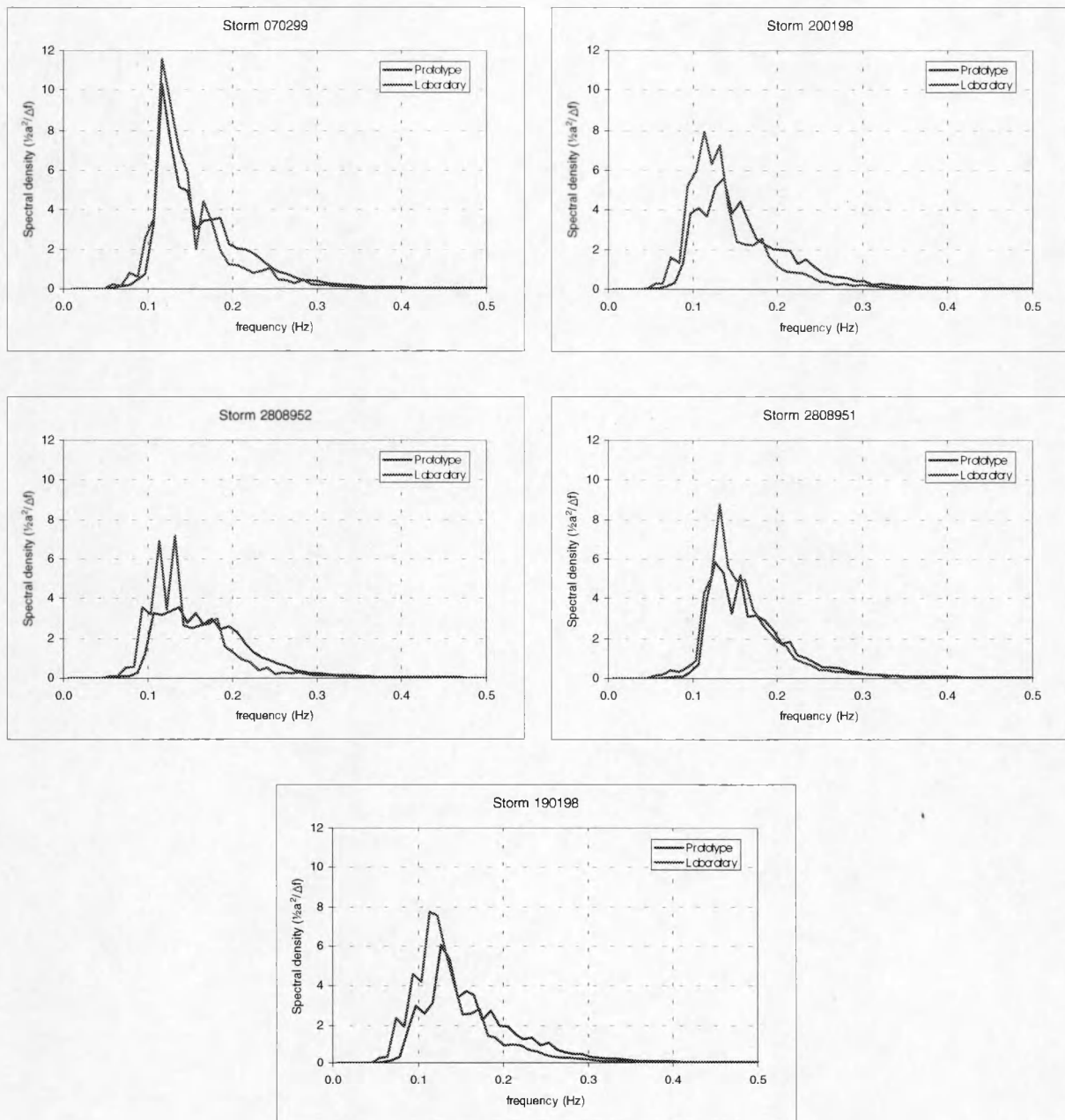
Figure 28: Comparison of wave energy spectra in model and in prototype.

Table 11: Comparison of wave conditions.

Storm	Prototype			Laboratory		
	H_{mo} [m]	T_p [s]	T_{01} [s]	H_{mo} [m]	T_p [s]	T_{01} [s]
070299	3.14	8.53	6.53	3.12	8.98	6.94
190198	2.99	8.53	6.61	2.96	8.26	7.21
200198	3.08	8.53	6.58	3.00	9.14	7.23
280895(1)	2.86	7.31	6.18	2.90	7.42	6.26
280895(2)	2.69	9.31	6.40	2.69	8.98	6.86

Table 12 shows the $Ru_{2\%}/H_{mo}$ values of both prototype and AAU laboratory measurements. A good agreement is seen when wave run-up is measured by the novel step gauge. The resistance gauge clearly underestimates wave run-up.

Table 12: Comparison of $Ru_{2\%}/H_{mo}$ value, obtained by prototype measurements and laboratory testing.

Storm	Prototype	Laboratory	
	$Ru_{2\%}/H_{mo}$ [-]	$Ru_{2\%}/H_{mo}^{(1)}$ [-]	$Ru_{2\%}/H_{mo}^{(2)}$ [-]
070299	1.73	1.35	1.71
190198	1.73	1.38	1.76
200198	1.79	1.45	1.89
280895(1)	1.49	1.05	1.52
280895(2)	1.66	1.38	1.91

[1]: resistance gauge; [2] UG step gauge

Additional information on the reproduction of these storms can be found in Annex 3.4c.1.

In any case these test demonstrate that the UG step gauge should be used instead of the resistance gauge. On the other hand the value of $Ru_{2\%}/H_{mo}$ found in laboratory may be too high due to the shifting of the spectrum to the low frequencies.

Additional storm simulations have been carried out: 10 tests reproducing 2 consecutive storms (i.e. the storm which occurred on November 6, 1999 (storm 8) and November 6-7, 1999 (storm 9)) each containing five storm sessions covering half a tide cycle have been carried out to investigate the influence of the water level on wave run-up. The spectra have been reproduced extremely accurately: at least 8 iteration steps were made to obtain an acceptable spectrum. The comparison between the measured wave characteristics in prototype and those in the laboratory is given in table 13.

Table 13: Comparison between prototype and laboratory wave characteristics (storms 8 & 9).

Storm n° / time	Prototype			Laboratory		
	H_{mo} [m]	T_p [s]	T_{01} [s]	H_{mo} [m]	T_p [s]	T_{01} [s]
8 / 09h30 - 10h30	2.31	6.83	5.23	2.43	6.83	5.66
8 / 10h30 - 11h30	2.75	6.83	5.58	2.76	6.29	5.75
8 / 11h30 - 13h30	2.99	6.83	5.88	3.12	7.63	6.22
8 / 13h30 - 14h30	2.90	6.83	5.86	2.88	6.83	6.34
8 / 14h30 - 15h30	2.49	6.83	5.73	2.38	6.83	6.06
9 / 21h45 - 22h45	2.49	8.53	5.66	2.42	6.83	5.82
9 / 22h45 - 23h45	2.60	6.83	5.69	2.52	6.83	6.00
9 / 23h45 - 01h45	2.59	6.83	5.70	2.61	8.63	5.99
9 / 01h45 - 02h45	2.54	8.53	5.73	2.40	8.63	6.02
9 / 02h45 - 03h45	2.14	8.53	5.35	2.08	7.63	5.57

The results of the reproduction of storms 8 & 9 are given in table 14.

The first tests (table 12) indicated laboratory wave run-up values very close to the run-up results of the prototype measurements. This conclusion could not be confirmed by the tests in which the

storms 8 & 9 were reproduced. Slight differences were expected due to small changes in the breakwater geometry and/or change of placement of the armour units in the armour layer of the breakwater.

The influence of the porosity of the armour layer was investigated. An increase in wave run-up was observed when the porosity was decreased. This was done by placing smaller stones in spaces between the armour units.

Table 14: $Ru_{2\%}/H_{mo}$, $Ru_{5\%}/H_{mo}$, $Ru_{10\%}/H_{mo}$ and $Ru_{50\%}/H_{mo}$, values of storm 8 & 9.

Storm	$Ru_{2\%}/H_{mo}$ [-]	$Ru_{5\%}/H_{mo}$ [-]	$Ru_{10\%}/H_{mo}$ [-]	$Ru_{50\%}/H_{mo}$ [-]
8 / 09h30 - 10h30	1.79	1.62	1.59	0.69
8 / 10h30 - 11h30	1.51	1.36	1.28	0.92
8 / 11h30 - 13h30	**1.42**	1.26	1.13	0.84
8 / 13h30 - 14h30	1.43	1.30	1.21	0.72
8 / 14h30 - 15h30	1.58	1.48	1.21	0.82
9 / 21h45 - 22h45	1.65	1.57	1.42	0.59
9 / 22h45 - 23h45	1.63	1.52	1.26	0.85
9 / 23h45 - 01h45	**1.29**	1.22	1.15	0.72
9 / 01h45 - 02h45	1.39	1.31	1.20	0.83
9 / 02h45 - 03h45	1.63	1.57	1.52	0.88
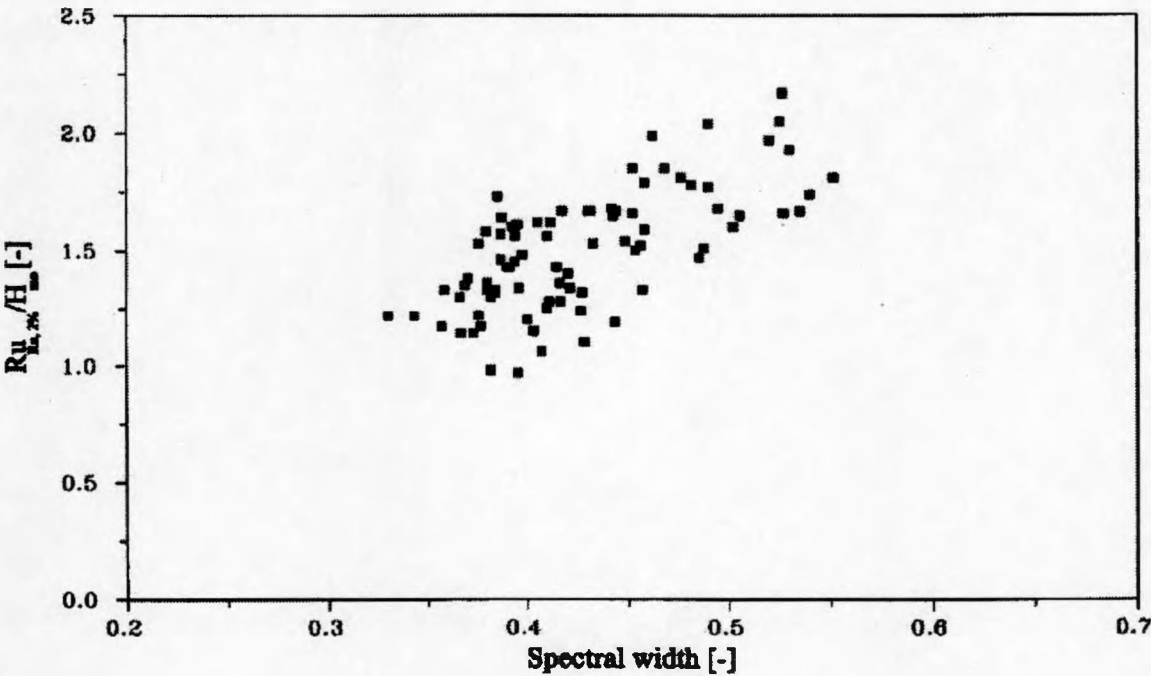
Figure 29: $Ru_{2\%}/H_{mo}$ vs. spectral width ε.

A clear influence of the spectral shape (characterised by the spectral width parameter ε) was noticed (figure 29) as well. This parameter is defined as $\varepsilon = \sqrt{\dfrac{m_0 m_2}{m_1^2} - 1}$. A small increase of this parameter

yields a clear increase in dimensionless 2% wave run-up value. Reference to Annex 3.4c.3 is made for further information.

Out of the measurements, following conclusions can be drawn:

- the wave run-up levels measured with the step gauge are more reliable than these measured with the resistance gauge.
- in the first series of tests the dimensionless wave run-up in laboratory is comparable to the prototype values. However, the spectra were slightly shifted to the low frequent energy. In the second series of tests with almost perfect reproduction of the prototype storms the laboratory $Ru_{2\%}/H_{mo}$ was lower than in prototype.
- an influence of the spectral width parameter ε and the permeability of the armour layer is seen: dimensionless wave run-up values increase with increasing value of ε and decreasing permeability.

Subtask 3.4: 3D testing

a) Petten (incl. low and high crested 1:6 dike)

a.1) Objectives of study

Subtask 3.4 of the Technical Annex of the OPTICREST project states that the specific objective of the 3D tests is to investigate three-dimensional effects in laboratory scale models. More specifically the following is stated, which is also applicable to the Aalborg University tests on the Zeebrugge breakwater:

"Again the two basic models are the prototype structures rough and permeable and smooth and impermeable. Full 3D tests are carried out at an approximate scale of 1:40, as close as possible to the 2D scale. These tests will first attempt to validate the prototype results and continue to investigate the influence of such parameters as wave height, wave period, water depth, angle of wave attack, directional spreading, currents, foreshore bathymetry and structure geometry on wave run-up, wave run-down and overtopping (average, probability distribution of the overtopping volume per wave)

Obviously the 3D tests will not be as wide ranging as the 2D due to difficulties in making changes. However, there is sufficient overlap of the test series such that necessary comparisons can be made."

The 3D tests undertaken at UCC involved the construction of three models, which can be described as follows,

- Petten dike including nearshore bar (scale 1:40)
- Low crested 1 in 6 dike (scale 1:2)
- High crested 1 in 6 dike

The need to undertake three sets of model tests, as opposed to the one set that was initially contracted arose from difficulties associated with generating high angle oblique waves for the testing of the 3D model of the Petten dike. The main problem with respect to this model was that it required the construction of a large section of the prototype foreshore and most importantly the inclusion of a nearshore bar such that the wave dissipation processes could be correctly modelled. This necessitated placement of the dike at the back of the basin, 25m from the paddle bank and so limited the amount of directionality that could be achieved. Although spread wave fronts can still be effectively generated, the range of angles for directional seas was severely curtailed. As a consequence it was decided that additional models (low crested and high crested 1 in 6 dike) would be constructed closer to the paddle array such that both the individual and combined effects of wave obliqueness and directional spreading on wave run-up and wave overtopping could be assessed. The wave overtopping tests were carried out at the specific request of the Leichtweiss Institut für Wasserbau (LWI).

For full details on all work carried out on this task the final report '*3D Physical Model Tests of Wave Run-up on Coastal Structures*' should be consulted. The report is given in Annex 3.4a.

<u>a.2) Petten Model</u>

The layout of the Petten model is shown in figure 30. This model extends laterally the full width of the basin and longitudinally beyond the deepwater pit and has a scale of 1:40. A major consideration in the design of the model was the construction of the Petten nearshore bathymetry. In this respect the approach adopted by Delft Hydraulics was repeated. For the 2D Delft tests the bathymetry was schematised into a number of well-defined slopes that corresponded closely to the prototype cross shore profile.
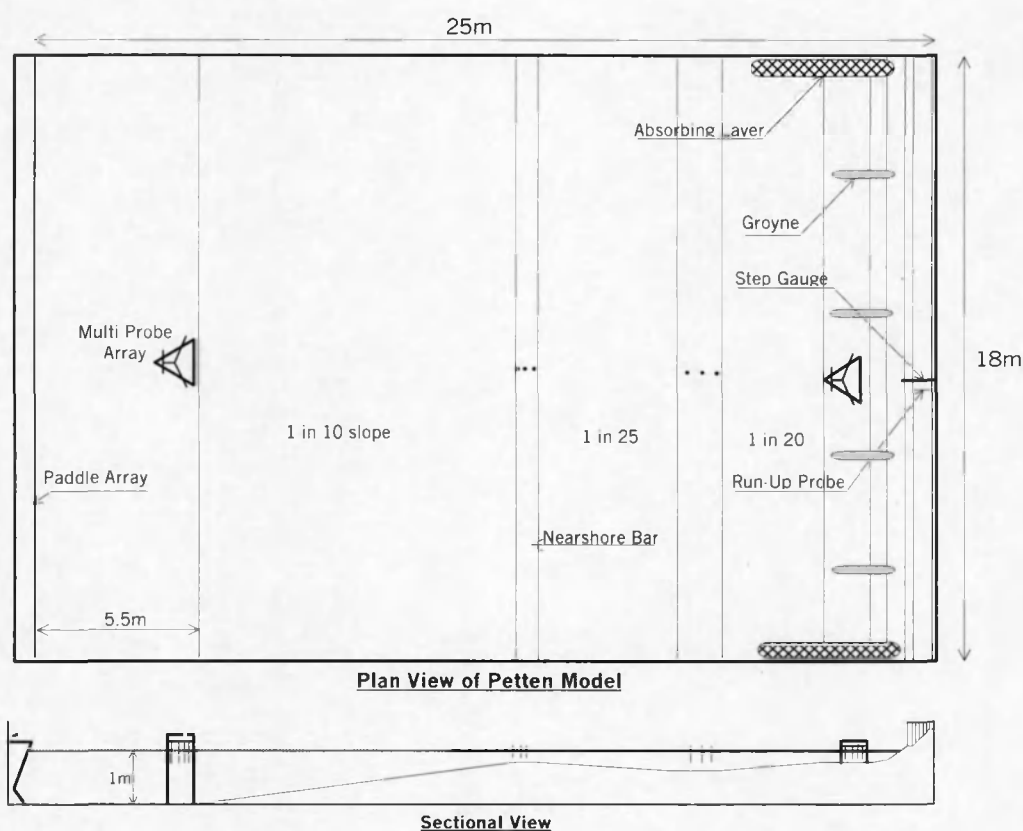
Figure 30: Petten model layout with instrumentation locations

Wave conditions, for the Petten tests, were measured at four locations of which three correspond to the prototype locations of MP6, MP5 and deepwater. The fourth location was at the nearshore bar. For this model it was expected that the shallow foreshore would have an influence on the wave spreading so it was important to have a wave directionality measurement close to the dike. Therefore, as well as placing a multi probe array in deepwater, a second array was placed at MP6 such that directional effects in the wave field could be determined close to the dike structure. Wave run-up was measured by means of a step gauge that was designed and fabricated in house at the Hydraulics and Maritime Research Centre (HMRC). It consists of 24 pairs of parallel conductivity

probes. All probes are co-linear and the minimum horizontal separation between two consecutive probes is 20mm. A sloping probe was also used in conjunction with the step gauge.

A variety of wave tests were carried out incorporating both measured and simulated wave conditions.

a.3) 1 in 6 dike model

A low crested dike with a slope of 1 in 6 was constructed after completion of the Petten model tests. This dike had a freeboard of 0.05m and was used for wave overtopping tests, which are described in a separate report *'3D model tests on wave overtopping for 1:6 dike'* attached in Annex 3.4b. This structure was subsequently extended such that it had a freeboard of 0.35m and a series of run-up tests were carried out. The layout of this structure is shown in figure 31. The toe of the structure was placed in 1m water depth at a distance of 5.5m from the paddles and it extended over the 1:10 slope of the Petten model. The width of the model at toe level was 13m and it reduced uniformly to 5m at 0.05m above the still water level and continued at this width to the crest. Tapering the model in this manner was considered necessary in order to ensure a smooth transformation of oblique waves as they propagated across the slope. Wave absorbing material was placed at either side of the model to reduce the effects of wave reflections.

Plan view of 1 in 6 Dike Run-up Test Layout

Sectional View
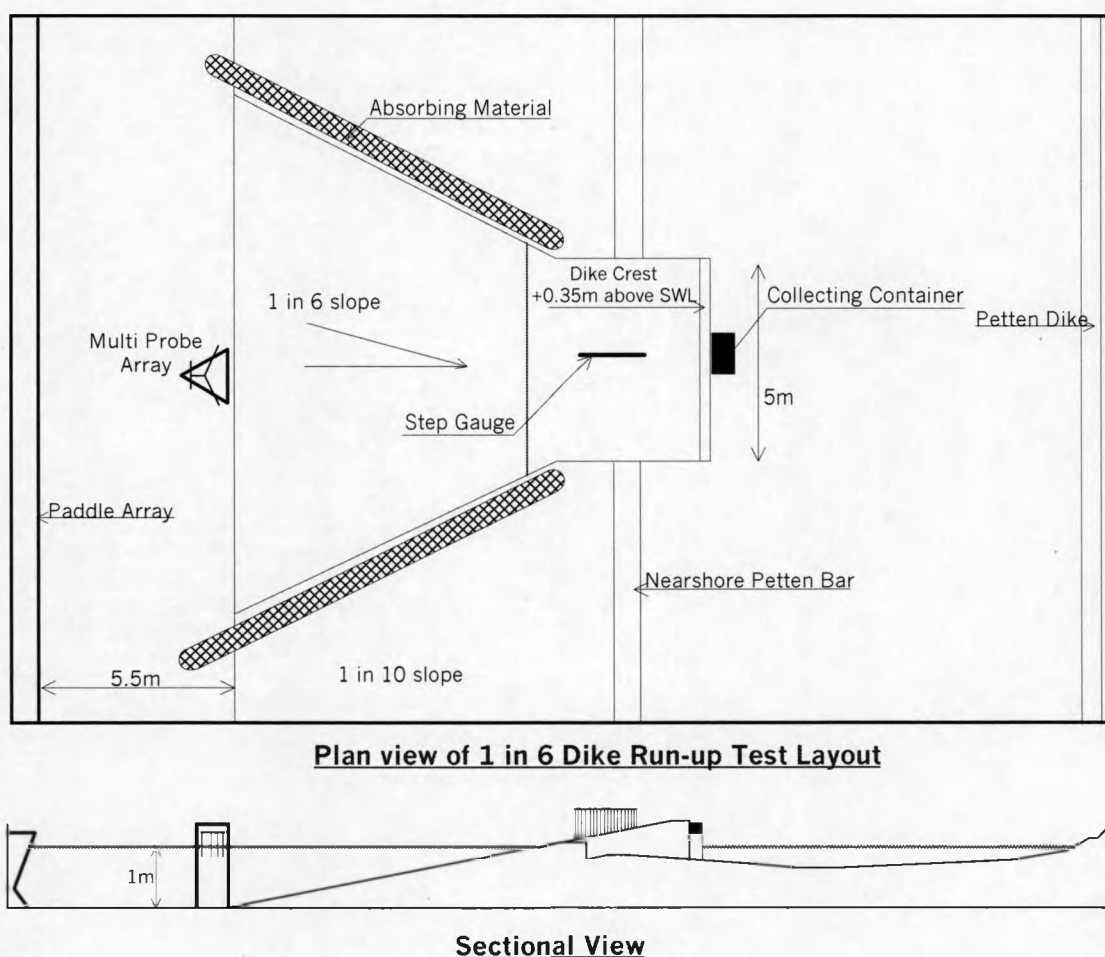
Figure 31: Dike (1 in 6) model layout with instrumentation locations

Wave conditions were measured using a multi probe array placed in front of the structure and run-up was measured using the same step gauge as was used for the Petten tests.

Since the main purpose of this model was to carry out an analysis of the factors that affect run-up a wide variety of tests were carried out in which the following parameters were varied: wave height, peak period, wave direction and directional spreading.

a.4) Results on the Petten dike

Sample results from the Petten study are shown in figures 32 and 33. They indicate that water depth has an influence on run-up magnitudes and that directional spreading only results in slight reductions in run-up magnitudes. There was good agreement between the model and prototype results.
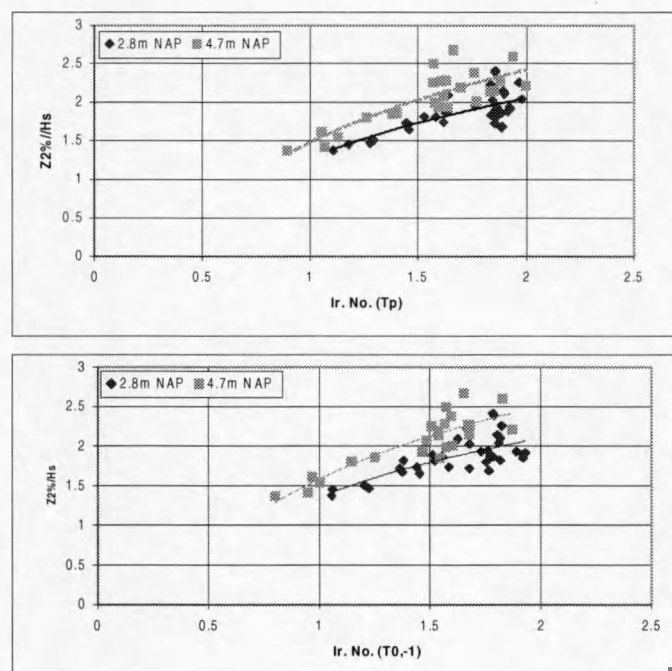
Figure 32: Measured 2% wave run-up levels for long crested waves using T_p (upper) and T_{0-1} (lower).
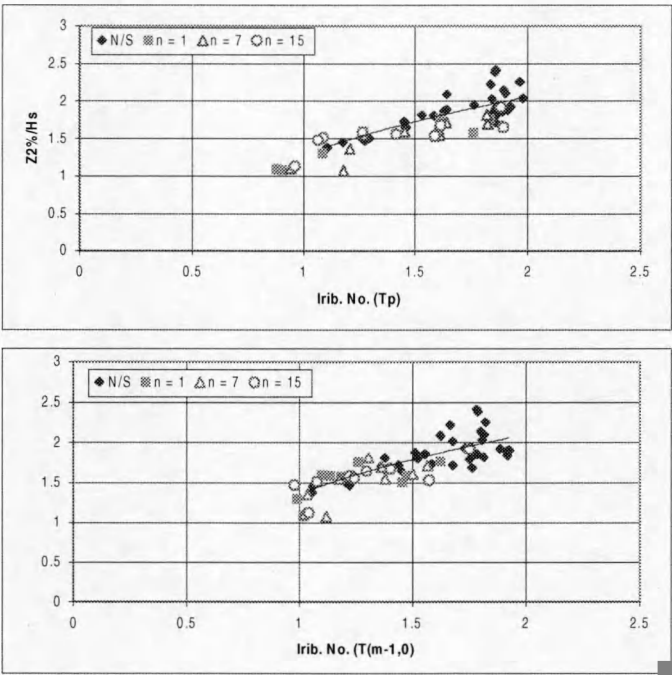
Figure 33: Measured 2% wave run-up levels for different
input spreading levels using T_p (upper) and $T_{0,-1}$ (lower).
(Water Level +2.8m NAP)

a.5) Results on the 1 in 6 dike

The tests showed that wave run-up was reduced as a result of oblique wave attack and by applying a directional spreading. The magnitudes of the reduction in comparison with the base condition (long crested waves approaching normally to the structure) were computed and are shown in table 15 for the three situations tested,

- Spreading only
- Wave direction only
- Combined spreading and direction

There is an additional column on this table which is called the 'Computed reduction factor' and it only applies to the combined tests. The values in this column are determined by multiplying the relevant factors as obtained when spreading and direction were examined individually. The values obtained can be compared with the corresponding values as contained in the 'Combined reduction factor' column. The purpose of this analysis was to determine whether the combined reduction factor could be calculated from knowledge of individual spreading and direction factors. The results seem to indicate that this is the case.

Table 15: Run-up reduction factors

Direction θ [deg]	Spreading factor	Spreading reduction factor a	Direction reduction factor b	Combined reduction factor c	Computed reduction factor a×b
0	0	1			
0	20	0.781			
0	10	0.769			
0	5	0.714			
0	1	0.694			
0	N/S		1		
5	N/S		0.91		
10	N/S		0.885		
15	N/S		0.87		
20	N/S		0.813		
25	N/S		0.77		
10	N/S			0.885	0.885
10	20			0.685	0.691
10	10			0.654	0.681
10	5			0.613	0.632
10	1			0.588	0.614
20	N/S			0.813	0.813
20	20			0.667	0.635
20	10			0.613	0.625
20	5			0.565	0.58
20	1			0.581	0.564

a.6) Conclusions

The following conclusions were made regarding the results of the Petten study.

1. Good reproduction of the measured storms was achieved in the UCC basin and the run-up results show relatively good agreement with prototype measurements. Maximum deviation from the prototype results was of the order of 10%. The prototype spectra when fitted with spreading factors tend to result in a reduction in run-up.

2. The water level tended to have an influence on the non-dimensional run-up magnitudes with higher levels giving greater relative run-up. The method of calculating slope angle for use in the ξ-parameter and the wave measurement location may be influential factors with respect to this result. It may be that the Iribarren number may not be the best parameter to use for relatively complicated coastal and structural configurations. Therefore it may be useful to consider the development of another parameter.

3. The shallow foreshore has the effect of reducing the level of directional spreading such the waves tend to become more long crested. Therefore, although the general trend in the results is for wave run-up to reduce as the n-value decreases it is not very pronounced, especially for lower Iribarren numbers, because of the shallow water effects.

4. Formulae have not been fitted to the data but all the results seem to fall below the line as given by the equation, $Ru_{2\%} / H_s = 1.6 \gamma \xi_p$ for the case of γ equal to 1 (i.e. neglecting the influence of the foreshore and the berm) which would be the correct trend. Of course care would be required in applying or proposing any formulae as the magnitudes of dimensionless run-up is very dependent on the location where the wave conditions are measured. In any case the results from this part of the study are applicable only to the Petten site and any formulae proposed from the results would not be totally relevant for any other location.

5. As a follow on from (4) above, the choice of wave parameters and the location on the foreshore where they are measured can have a significant influence on the results obtained. For instance H_s and T_p can change substantially between MP6 and the toe of the structure and so gives apparently different trends. Therefore, the $T_{0.-1}$ period does not seem to be as significant for the results of this study as it was for the 2D tests at Delft Hydraulics and the non-dimensional run-up value is lower as H_s at MP6 is larger than H_s at the toe.

6. Waves probes placed parallel to the slope, to measure wave run-up, can significantly underestimate wave run-up magnitudes and generally should not be used as the sole means of measurement for experimental studies.

7. More investigation into the measurement techniques for short crested waves should be carried out. Some inconsistencies were observed in the wave output.

The following conclusions were made from the run-up tests on the 1 in 6 dike,

1. Wave obliquity and directional spreading have the effect of reducing the magnitude of run-up from the equivalent long crested direct wave approach situation.

2. For tests with directional spreading the effect of changing the n-value is much clearer than for the Petten tests. This has been attributed to the absence of a shallow foreshore.

3. The magnitudes of run-up for tests with wave directionality seem to be less than what is commonly observed. Even small angles of wave obliquity seem to produce noticeable decreases in run-up. It is not clear whether the trends observed in this study are particular to the specific model and instrumentation set-up of this study. Indeed additional 3D model testing is required to further verify to results of this study.

4. For each wave direction and spreading factor a constant factor was found satisfactory for quantifying the difference to the base test condition (i.e. long crested direct wave approach).

However, this may not the case and the reduction factor may change according to the value of the Iribarren number. The range of values tested in this study precluded the examination of this effect.

5. The combined effect of wave obliqueness and directional spreading on wave run-up can be determined by considering the influence of each individually and multiplying the relevant reduction factors.

6. All run-up results can be fitted to the design formulae for smooth impermeable structures, $Ru_{2\%}/H_s = 1.6\gamma\xi_p$ through the use of various reduction factors as given in table 15.

b) Zeebrugge

In addition to the reproduction of the storm sessions, performed with long crested waves, parametric tests are carried out. A 1:40 scale model has been constructed in a wave basin at AAU in order to evaluate the following 3 dimensional effects:
- effect of wave obliquity,
- effect of spreading of waves (3 dimensionality of waves),
- effect of a longshore current,
- variations along the breakwater

Figure 34, showing $Ru_{2\%}/H_s$ of all the tests against mean wave incident angles, reveals that $Ru_{2\%}/H_s$ decreases with increasing wave incident angle.
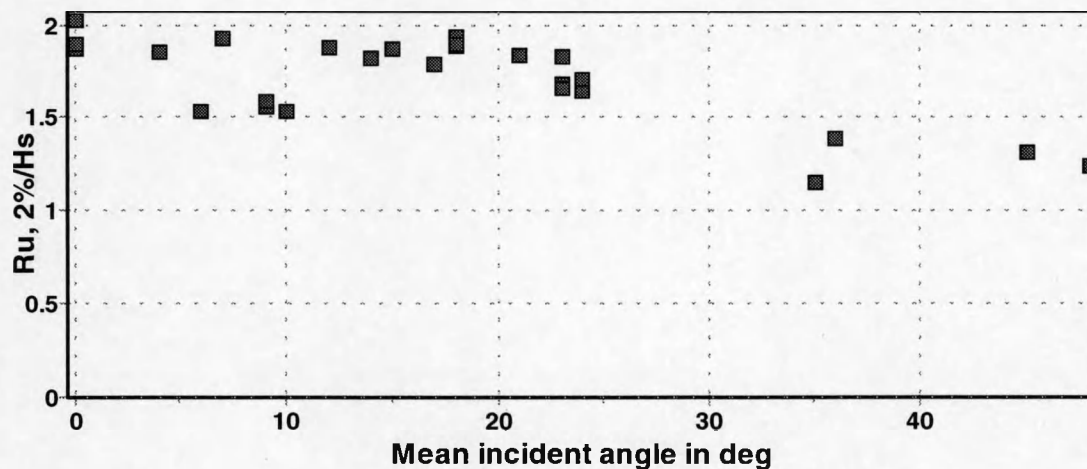
Figure 34: Wave run-up of all the tests.
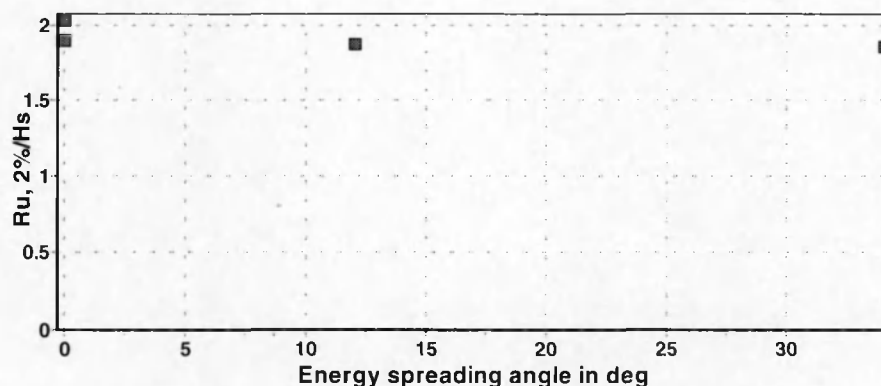
Figure 35: Run-up of head-on waves with various wave energy spreading angles.

Figure 35, showing $Ru_{2\%}/H_s$ of the head-on waves with various energy spreading angles, reveals that the energy spreading angle has insignificant influence on the wave run-up.

The conclusion is consistent with the previous research by De Waal and van der Meer (1992).

Tests with a longshore current (0.5-1.0 m/sec.) showed somewhat larger run-up levels compared to tests with no current.

Simultaneously measured run-up at different locations on the breakwater showed variations in the run-up levels up to 20% depending on the actual lay-out of the blocks on the breakwater.

Subtask 3.5: Crest stability

a) Introduction

Dikes protect the coastlines of Belgium, the Netherlands, Germany, Denmark and Poland on a length of several thousands of kilometres. Therefore, the design of these structures is very important to avoid high costs in the case of overdesign or underdesign. In general dikes are designed for a design storm surge level and a 2% exceedance wave run-up height today. Nevertheless, wave overtopping has to be taken into account due to the remaining uncertainties to predict the design storm surge level and the design waves. Present design formulas for wave overtopping are based on average overtopping rates which do not take into account the highly instationary flow field of wave overtopping. Therefore, formulas for the flow field of wave overtopping are required for the future. It was the objective of Task 3.5 to provide formulas for wave overtopping velocities and layer thicknesses on the crest and the landward slope of sea dikes.

b) Wave overtopping velocities and layer thicknesses

Schüttrumpf (2001) derived an analytical function for layer thicknesses and wave overtopping velocities on the crest and landward slope of a dike within the MAST-III-Opticrest – project. This work presents the major outcome of Task 3.5 and is summarised in the final report 'Prediction of wave overtopping flow parameters on the crest and landward slope of seadikes.' which is attached in Annex 3.5 of this report.

Schüttrumpf (2001) presents a closed solution for the description of layer thickness and velocities for the seaward slope, the dike crest and the landward slope. The flow parameters of the seaward slope were determined as an input for the wave overtopping flow. For the dike crest, a theoretical function for wave overtopping velocities was derived based on the momentum and continuity equations. This theoretical function assumes hydrostatic pressure conditions and depth integrated flow velocities.

$$v_K = v_0 \, exp\left(- \frac{x_K f}{2 h_K} \right)$$

with: v_K = overtopping velocity on the crest
       v_0 = overtopping velocity at the beginning of the crest
       x_K = position on the crest with $x_K = 0$ at the beginning of the crest
       f = friction coefficient
       h_K = layer thickness on the crest

All definitions are shown in figure 36. The evolution of layer thickness and wave overtopping velocities is examplarily given in figure 37.
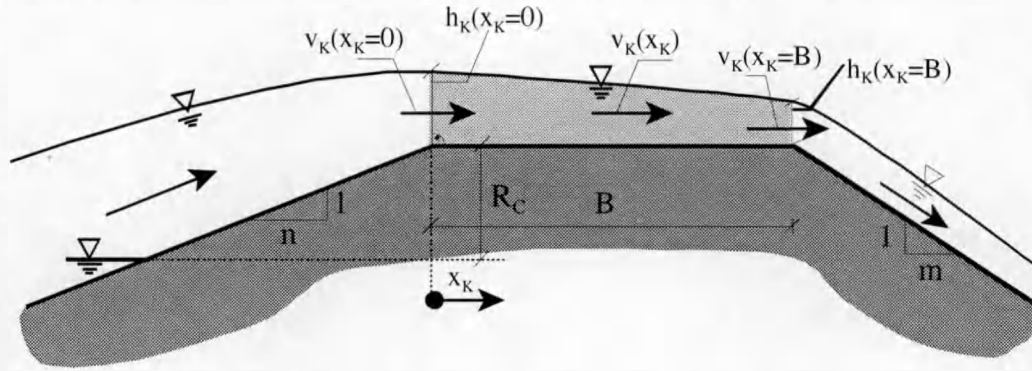
Figure 36: Definitions of wave overtopping parameters on the crest
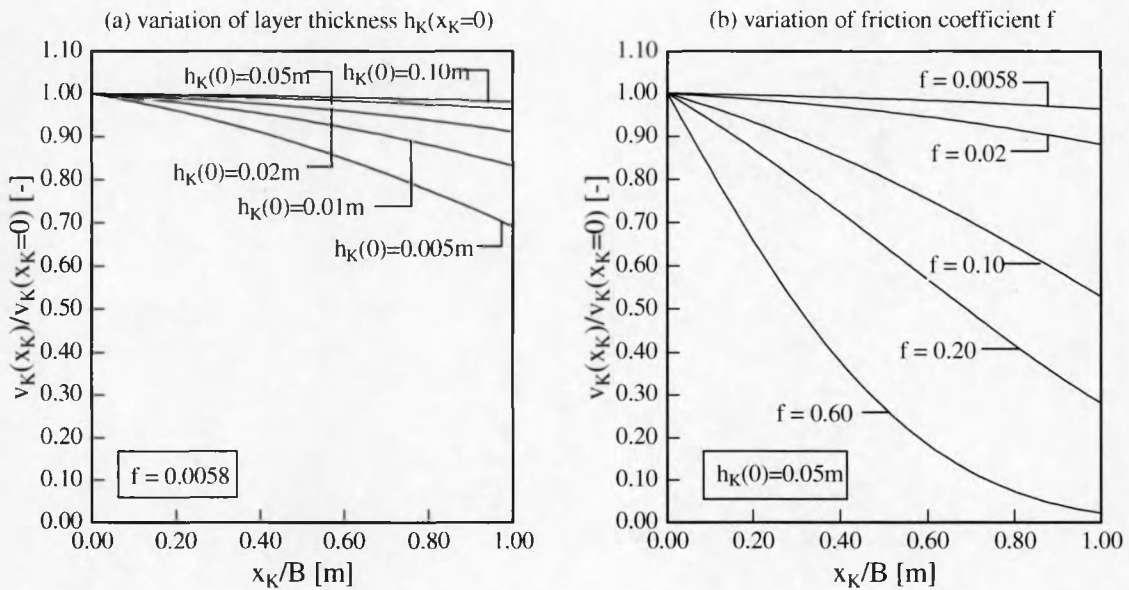
Figure 37: Evolution of layer thickness and wave overtopping velocities on the dike crest.

Another equation was derived for the landward slope from the general momentum and continuity equations assuming hydrostatic pressure conditions and depth integrated flow.

$$v_B = \frac{v_0 + \dfrac{k_l h_B}{f} \, tanh\!\left(\dfrac{k_l t}{2}\right)}{1 + \dfrac{f v_0}{h_B k_l} \, tanh\!\left(\dfrac{k_l t}{2}\right)}$$

with: v_B = overtopping velocity on the landward slope

v_0 = overtopping velocity at the beginning of the landward slope

t = time

f = friction coefficient

h_B = layer thickness on the landward slope

k_l = coefficient which includes position on the slope s_B and gradient of landward slope β

All relevant definitions are given in figure 38.
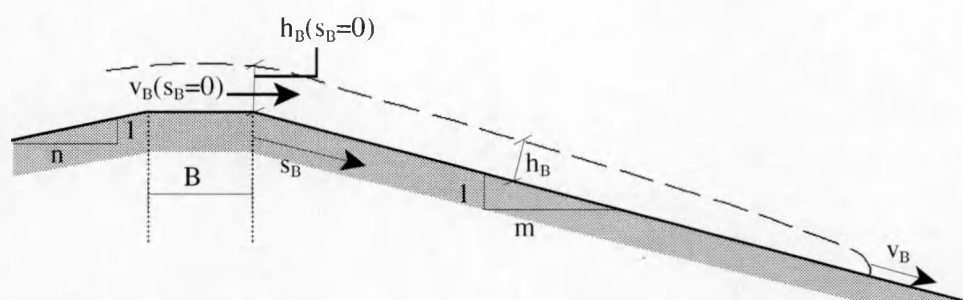
Figure 38: Definitions for the wave overtopping flow on the landward slope.

All equations were calibrated based on model tests with regular waves and verified by model tests with wave spectra. Calculated and observed data are in good agreement. An example for the wave overtopping flow is given in figure 39.
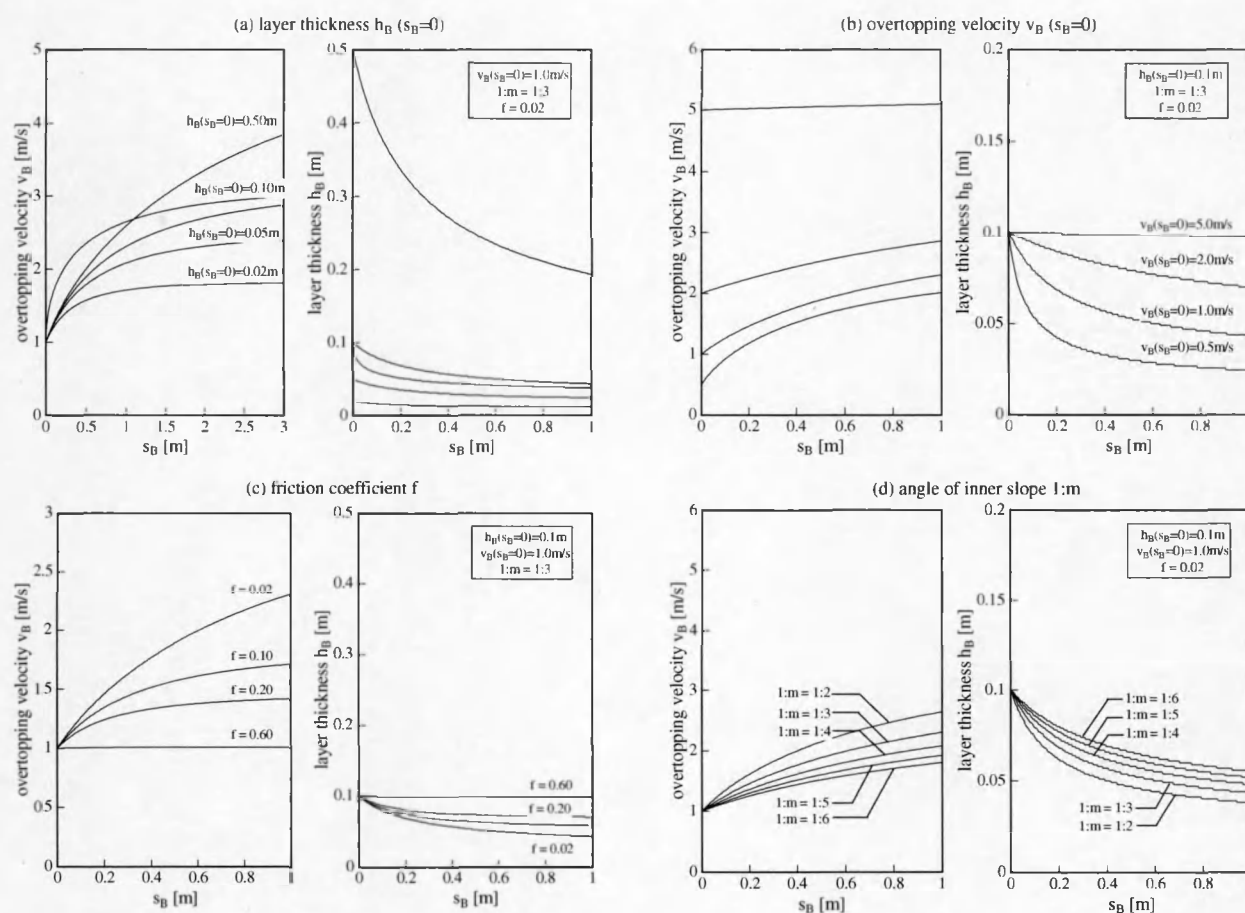
Figure 39: Sensitivity analysis for wave overtopping flow on the landward slope of seadikes

These formulas present the first approach worldwide for the calculation of wave overtopping velocities and layer thicknesses on the dike crest and landward slope of sea dikes. This is a first step towards a design of sea dikes which is based on the direct loading parameters and not on average overtopping rates. In a next step this model has to be validated for large scale model tests. At the moment, large scale model tests are performed for a final validation of the above mentioned theoretical formulas. Final results, which are not published yet, show a very good agreement. Finally, the wave overtopping velocities and layer thicknesses have to be considered in soil mechanics to provide tools for the stability of sea dikes.

Subtask 3.6: Synthesis of laboratory testing

For the same reason as mentioned in Subtask 2.4, Subtask 3.6 has been reassigned and relocated as it is partly included in Subtask 3.3, 3.4 and 3.5 (analysis) and partly in Task 4 (collection of data and comparison).

TASK 4: LINK BETWEEN PROTOTYPE AND LABORATORY RESULTS

The final results of OPTICREST (MAS3-CT97-0116) are described in two separated paragraphs corresponding to Petten en Zeebrugge respectively. The main goal of Task 4 was to link prototype and laboratory results, to know the reasons of the discrepancies of prototype and laboratory results and to discover the appropriate way to use them in providing adequate design guidelines for the crest level of coastal structures.

4.1 Link between the Petten prototype and laboratory results

a) Introduction

This section describes Task 4 corresponding to Petten case.

Reference is made to following Annexes:
- Annex II of the *'Annual Report (12 months)'*
- Annex III of the *'Annual Report (To+12 till To+24)'*
- Annex 3.4a *'3D physical model tests of wave run-up on coastal structures'*
- Annex 4a *'Link between prototype and laboratory results: Petten case'*

The link between prototype and laboratory results is described in three parts.
The first paragraph, called 'Methodology' describes the procedures defined in the OPTICREST original proposal for Task 4, the evolution of the methodology according to the results and the organisation of the final report of Task 4 in which all the relevant work is described.

The second part (*'Synthesis of Petten Measurements'*) describes the synthesis of measurements taken in prototype (RIKZ), 2D model tests (DH) and 3D model tests (UCC) and most important results of comparisons analysed during OPTICREST. The objective of this part is to provide an overview on the performed measurements corresponding to Petten in order to support the conclusions on impermeable dikes. It has been prepared by the partners involved in prototype, 2-D and 3-D experiments and gives a list of conclusions and recommendations interesting to reach the goal of OPTICREST. In relation to Task 4 (link between prototype and laboratory results), the principal conclusion of Task 4 is that 2D (DH) and 3D (UCC) model tests reproducing storms measured in Petten showed an excellent agreement.

The third part is the proper analysis of the link between prototype and laboratory results based on the methodology proposed for OPTICREST and the corresponding implementation during the project. This paragraph describes the summary of the results and comparison of variables with emphasis in the recommendations and conclusions on the use of model tests to design impermeably dykes. The description is focused on the main aspects of the link between prototype and laboratory results, also referring to an UPV report with the detailed description of the development of Task 4 in Petten.

Finally, the principal conclusions and recommendations corresponding to Task 4 in Petten (link between prototype and laboratory results) are given. The principal conclusion related to Task 4 is the excellent agreement of measurements of dimensionless run-up in prototype and 2D and 3D model tests (scale 1:40). The mean value of $Ru_{2\%}/H_{mo}$ was 2.03 and the differences found were 3.9% and 7.8% for 2D and 3D models respectively. The principal recommendation was to study the effects of surf beat phenomena, the propagation of wave groups and their associated wave motions, and their contribution to wave run-up. The foreshore wave breaking was relevant and also the low frequency component of the wave energy.

b) Methodology

Task 4 (link between prototype and laboratory results) was originally scheduled to start at To+24 and begin preliminary work at To+13. However, it was decided from the very beginning of the project that preliminary work should be done helping in the definition of the methodological aspects of OPTICREST (Subtask 3.1). Task 4 has been from the beginning of OPTICREST an assistant reflexive tool to improve the methodology applied both in prototype and laboratory observations of Petten. The continuous feedback process of ideas and concepts, experimental methods and analysis of results was the main streamline of Task 4. At the end of the project, the analysis of laboratory and prototype results and the comparisons made reflect the sedimentation of ideas and concepts.

Past experience in running experiments in different laboratories recommended that a careful description of experiments was a necessary condition to avoid large discrepancies of measurements taken in different laboratories. In Petten, the difficulties were higher because the facilities, conditions and limitations were different for different partners (prototype, 3D and 2D). It was considered reasonable to be ready from the beginning of OPTICREST to face significant discrepancies between results obtained from similar experiments in different facilities. The basic elements to be considered, which were continuously defined and redefined during the project were:

(1) anatomy of the sources of possible discrepancies between prototype and laboratory results;

(2) "a priori" subjective estimation of the impact of each source of discrepancy on the results;

(3) quantitative estimation of the effects of the resources of discrepancy;

(4) recommendations.

Several causes of the observed discrepancies between prototype and laboratory experiments were indicated in the proposal (foreshore changes, measuring systems, wind, roughness, randomness of sea conditions, etc). During OPTICREST, a complete anatomy of those possible sources of discrepancies was constructed and re-constructed on the basis of the opinions (subjective) of the different experts in the group of partners (see Annex 4a). Because different experts in the group had different points of view about the relative importance of some possible source of discrepancy, and because these views changed during the project, it was necessary to clarify what were the expectations (relative importance) of the different experts of the group on the discrepancies prototype-laboratory. Special attention was given to the most optimistic and pessimistic points of view in each aspect analysed.

The proposed first anatomy of sources of discrepancies corresponding to Petten was structured in four areas:

(1) SEA WAVES including the sources of discrepancies associated to the wave measurement, wave analysis and wave generation processes both in prototype and laboratory;

(2) LONG WAVES including the sources of discrepancies due to the generation of long waves in the field and laboratories and the corresponding resonance phenomena, as well as the different measurement techniques;

(3) WAVE RUN-UP AND WAVE OVERTOPPING including the sources of discrepancies related to the measurement system selected in prototype and laboratory, as well as calibration, reliability of equipment, and the ones involved with wind effects;

(4) WIND AND SPRAY including the measurement systems, calibration and influence of atmospheric variables. Although a complete list of trouble-makers variables were analysed and re-analysed during OPTICREST, the estimation of the impact on the results were decreasing during the project because of the evidence of a good agreement of both measurements of run-up on 2D and 3D model tests and prototype.

From the first discussions on the variables that could affect the Petten results, it became clear the low frequency waves could be very important and special attention was paid to that aspect of the models and prototype (new equipment and measurement procedures). The result is an excellent agreement between run-up measurements of storms in prototype and 2D and 3D models and the use of the wave parameter $T_{-1,0}$ to characterise wave action as a clear indicator of the importance of the low frequency components in Petten. This Task includes the synthesis of the prototype, 2D and 3D measurements of the Petten case as well as the description of the application of the methodology of the link between prototype and laboratory results to the Petten case.

The most important final results of Task 4 in Petten can be summarised as follows: 2D and 3D models (scale 1:40) can be used with step gauge run-up measurement systems to correctly model run-up phenomena on impermeable dikes. For a better analysis of wave run-up and wave overtopping events, special attention should be paid in Petten to foreshore changes in time, surfbeat phenomenon and low frequency wave component.

c) Synthesis of Petten measurements

c.1) Introduction

General

Within the framework of the European MAST-OPTICREST project prototype measurements and physical model investigations are performed on the Petten Sea-defence ('Pettemer Zeewering'). Prototype measurements are performed and analysed within the MAST-OPTICREST project by Rijkswaterstaat, RIKZ. Two-dimensional physical model tests are performed by WL | Delft Hydraulics and three-dimensional physical model tests are performed by University College Cork. These three series of measurements on the Petten Sea-defence played a role in several studies within the MAST-OPTICREST project. In Annex II of the *'Annual Report (12 months)'*, Annex III of the *'Annual Report (To+12 till To+24)'* and Annex 3.4a of this report the three main research

reports produced within this project are given, each describing one of the three types of measurements. In this paragraph a brief summary is given of the main conclusions concerning these investigations, as well as conclusions based on a synthesis of the three types of measurements.

Objective of the synthesis of measurements

The objective of this synthesis of measurements on the Petten Sea defence is to provide an overview on the performed measurements and to study whether additional conclusions can be drawn based on a combination of knowledge from the three types of measurements.

Outline

Par. b.2) describes the main findings from the individual and combined measurements on the Petten Sea-defence. Par. b.3) provides an overview of the main conclusions and recommendations.

c.2) Petten measurements

(i) Prototype measurements

Prototype measurements were performed and analysed by Rijkswaterstaat-RIKZ. In Annex 2.3 and Annex II of the *'Annual Report (12 months)'* the description of the field site and measurement equipment is given. Figure 40 shows the foreshore perpendicular to the dike. The depth-contours in prototype are rather parallel to the coast while the mean angle of wave attack was nearly perpendicular. For the 2D model test the most relevant equipment concerns wave buoys/capacitance wires at locations MP3, MP5 and MP6, at respectively 635 m, 300 m and 130 m seaward of the crest of the dike. The dike itself consists of a 1:4.5 slope below the berm with a slope of 1:20 (between NAP + 5 m and NAP + 5.7 m) and a 1:3 slope above the berm. On this upper slope a wave run-up gauge is placed. Figure 41 shows that the measured wave run-up ($z_{2\%}$) correlates strongly with the measured water levels and wave heights.

The storms that were reproduced in both the 2D model tests are summarised in table 16.
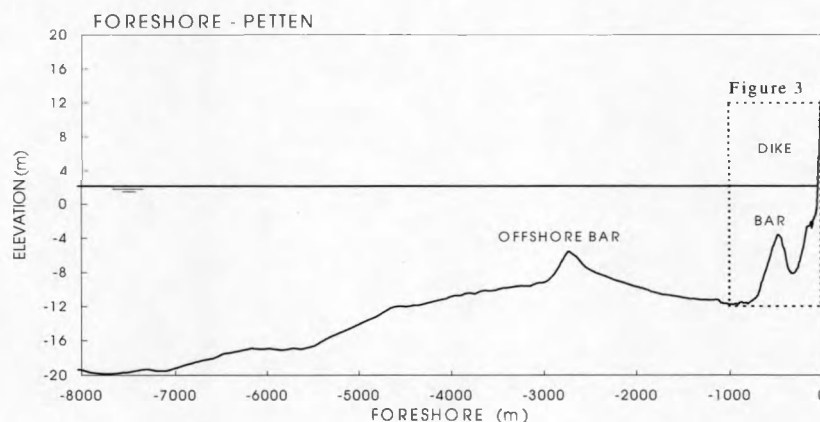
Figure 40: Measured foreshore perpendicular to the Petten Sea-defence.
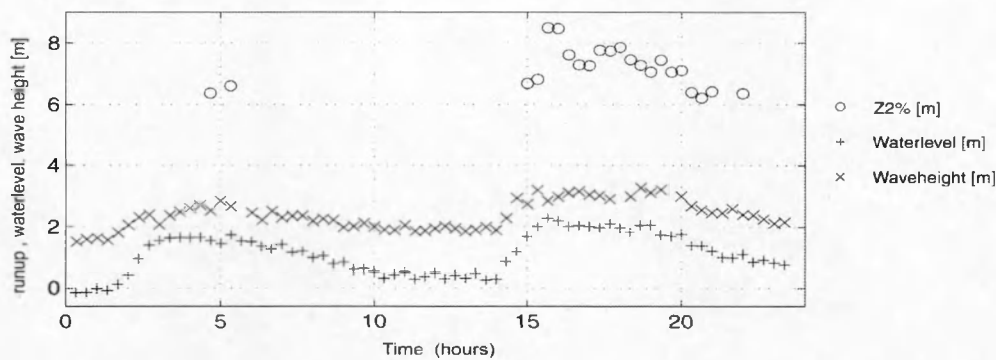
Figure 41: Example of wave run-up at run-up gauge; the water levels and wave heights are measured at 635 (MP3) and 130 m (MP6) from the toe of the dike, respectively.

Table 16: Measured storms and wave run-up levels in prototype.

Measured storms and wave run-up levels in prototype (data from Rijkswaterstaat-RIKZ).											
No	Date	MWL (NAP)	H_{s-T} (MP3)	$T_{-1.0}$ (MP3)	T_p (MP3)	H_{s-T} (MP5)	$T_{-1.0}$ (MP5)	T_p (MP5)	H_{s-T} (MP6)	$T_{-1.0}$ (MP6)	T_p (MP6)	$z_{2\%}$ (NAP)
1.01	1-1-1995	2.10	4.24	8.9	11.1	2.61	8.7	11.1	2.94	9.2	12.5	8.3
1.02	1-1-1995	2.01	4.24	8.6	11.1	2.65	8.7	11.1	2.81	9.1	12.5	7.6
1.03	2-1-1995	2.18	3.84	10.2	16.7	2.61	9.9	7.1	2.99	10.8	20.0	8.7
1.04	2-1-1995	1.64	4.24	10.4	16.7	2.39	10.1	16.7	2.64	10.8	12.5	6.9
1.05	2-1-1995	1.60	3.08	9.8	14.3	2.37	9.6	14.3	2.60	9.8	14.3	6.4
1.06	10-1-1995	2.00	3.70	8.8	10.0	2.66	9.0	11.1	2.78	9.4	9.1	7.7
These wave conditions are based on analysis of signals of total waves, including reflected waves, using the energy between the frequencies 0.03 and 0.3 Hz (Δf=0.01 Hz). NAP: Dutch vertical reference level											

(ii) 2D model tests

Two-dimensional physical model tests were performed and analysed by WL | Delft Hydraulics. Results of the 2D physical model tests on the Petten Sea-defence are given in Annex III of the *'Annual Report (To+12 till To+24)'*. Figure 4 shows the last kilometre of the foreshore as it was modelled in the flume (scale 1:40), while figure 5 shows the structure with the step gauge to measure wave run-up at the slope above the berm.

Since only the most landward bar could be modelled in the tests, the spectral shapes at the corresponding position of the wave board in the prototype situation were affected by wave breaking on the offshore bar. Therefore, for the tests where measured storms were modelled also the measured wave energy spectra were used, instead of standard spectral shapes such as Pierson-Moskowitz spectra or Jonswap-spectra. The waves, approximately 1000 waves per wave condition, were generated such that at the location MP3 the wave energy spectra were similar to those measured in prototype.

At several positions on the foreshore wave conditions were measured in the model tests; at deep water, at the crest of the bar, at the toe of the structure and at three positions where wave conditions have been measured in the prototype situation: MP3, MP5 and MP6. Figure 6 shows an example of the evolution of wave heights over the foreshore while figure 7 shows an example of the evolution of wave energy spectra over the foreshore.

Table 7 shows the comparison of the measured wave heights at three locations (MP3, MP5 and MP6). The average difference between the measured significant wave heights ($H_s = H_{1/3}$) in prototype and in the model tests is at MP3 (1.5 %), at MP5 (3.4%) and at MP6 (8.8%). These differences can be caused by many factors such as a slightly different foreshore during the actual storms than used in the model tests, 3D effects, effects of wind, schematisation-effects, slightly different data acquisition and data analysis procedures and scale effects. Nevertheless, the observed differences are considered acceptable to further investigate wave run-up.

In prototype thin water layers (between 0.02 m and 0.1 m) were also recorded as wave run-up while in the model tests the step gauge could not record water layers thinner than 0.1 m (prototype scale). Therefore, comparison between the wave run-up levels measured in prototype (indicated by 'P' in Table 7, including thin water layers, and the step gauge in the model tests (indicated by 'M1' in Table 7), not including thin water layers, is not straightforward. However, linear extrapolations based on the measured wave run-up levels with a minimum water layer of 0.1 m (step gauge) and the measured wave run-up levels with a minimum water layer of 0.2 m (wave gauge along the slope), yields estimates of wave run-up levels including thin water layers. These levels are indicated by 'M2' in Table 7. These 'M2'-levels are used for comparison with prototype measurements. The comparison is also made for the non-dimensional wave run-up level, where the wave run-up level is the height above the *mean* water level (MWL) and the wave heights are the total significant wave heights ($H_s = H_{1/3}$) measured at MP6. Although wave run-up levels are normally defined as the height above the *still* water level (SWL), the *mean* water level has been used for this comparison because for the prototype circumstances the *mean* water level is available, unlike the *still* water level. The differences in percentage are listed in the last column of table 7. The average of the differences (absolute values) is 3.9 %. Figure 8 shows the comparison between these wave run-up levels measured in prototype and in the model tests. Although these differences can also be caused by many factors such as schematisation and scale effects, related to for instance the roughness of the slope and the effects of wind on wave run-up, the differences are considered small.

In addition to the comparison with prototype storms a parameter analysis was performed where wave heights, wave periods, water levels and wave energy spectra were varied. For these results reference is made to Annex III of the *'Annual Report (To+12 till To+24)'*.

(iii) 3D model tests

Three-dimensional physical model tests were performed and analysed by University College Cork. In Annex 3.4a the description of the measurements (scale 1:40) and its analysis are given. The foreshore was similar to the one shown in figure 4, but now the seaward slope of the bar was 1:10 and not 1:30. This was done because of the limited length of the basin (25 m). The dike was

positioned over the full width (18 m) of the basin at about 24 m from the wave paddles. Perpendicular to the dike 4 groins were modelled. Wave run-up was measured using a step gauge at the slope above the berm (similar to figure 5).

Since only the most landward bar could be modelled in the tests, the spectral shapes at the corresponding position of the wave board in the prototype situation were affected by wave breaking on the offshore bar. Therefore, for the tests where measured storms were modelled also the measured wave energy spectra were used, instead of standard spectral shapes such as Pierson-Moskowitz spectra or JONSWAP-spectra. The waves, approximately 1000 waves per wave condition, were generated such that at the location MP3 the wave energy spectra were similar to those measured in prototype. Because the seaward slope of the bar was 1:10 in these tests, while in prototype a slope close to 1:30 was present, the depth at the position corresponding to MP3 was larger (approximately NAP-15 m compared to NAP-8.2 m). The spectra measured in prototype at MP3 were reproduced very accurately.

Table 17 shows the comparison of the measured wave heights at two locations (MP3 and MP6). The average difference between the measured significant wave heights ($H_s=H_{1/3}$) in prototype and in the model tests is at MP3 (1.6 %) and at MP6 (5.6 %). These differences can be caused by many factors such as a slightly different foreshore during the actual storms than used in the model tests, 3D effects, effects of wind, schematisation-effects, slightly different data acquisition and data analysis procedures and scale effects. Nevertheless, the observed differences are considered acceptable to further investigate wave run-up.

Table 17: Comparison between prototype measurements and 3D model tests.

Measured storms and wave run-up levels in prototype and physical model tests.									
	MWL (MP3)	H_{s-T}(MP3)		H_{s-T}(MP6)		$z_{2\%}$ (NAP)		$z_{2\%}/H_{s-T-MP6}$ differences		
Test	P	P	M	P	M	P	M	P	M	%
1.01	2.10	4.24	4.10	2.94	2.81	8.3	7.61	2.12	1.96	-7.5
1.02	2.01	4.24	4.32	2.81	2.85	7.6	7.33	1.99	1.88	-5.5
1.03	2.18	3.84	3.87	2.99	3.02	8.7	9.23	2.17	2.33	7.5
1.04	1.64	4.24	4.30	2.64	3.20	6.9	8.55	1.99	2.19	10.1
1.05	1.60	3.08	3.14	2.60	2.70	6.4	7.23	1.86	2.08	11.7
1.06	2.00	3.70	3.70	2.78	2.83	7.7	7.52	2.04	1.95	-4.4
P = 'Prototype'; M = 'Model tests'.										

Comparisons are also made between the non-dimensional wave run-up level, where the wave run-up level is the height above the *mean* water level (MWL) and the wave heights are the total significant wave heights ($H_s=H_{1/3}$) measured at MP6. Although wave run-up levels are normally defined as the height above the *still* water level (SWL), the *mean* water level has been used for this comparison because for the prototype circumstances the *mean* water level is available, unlike the *still* water level. The differences in percentage are listed in the last column of table 17. The average of the differences (absolute values) is 7.8 %. Figure 42 shows the comparison between these wave run-up levels measured in prototype and in the model tests. Although these differences can also be caused by many factors such as schematisation and scale effects, related to for instance the roughness of the slope and the effects of wind on wave run-up, the differences are considered small.
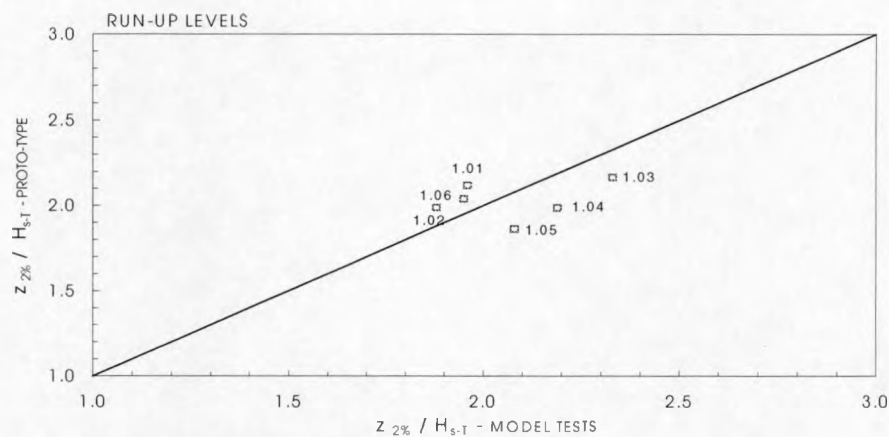
Figure 42: Comparison between wave run-up levels measured in 6 storms in prototype and those obtained from 3D model tests.

In addition to the comparison with prototype storms a parameter analysis was performed where wave heights, wave periods, water levels, wave direction and directional spreading were varied. For these results reference is made to Annex 3.4a.

(iv) Synthesis of measurements

Besides prototype measurements and physical model tests also numerical model computations have been performed. The results from the 2D physical model tests have been compared to results from a number of numerical models (van Gent and Doorn (2000); van Gent and Doorn (2001)); two for wave propagation over the foreshore (Swan and Triton) and two for wave interaction with the dike (Odiflocs and Skylla). Within this MAST-OPTICREST project results from the latter two numerical models have also been compared to wave overtopping tests (Oumeraci et al, 1999).

Combining results from the comparison between the prototype measurements, the 2D model tests on the Petten Sea defence, other 2D model tests, and numerical model computations led to the following conclusions (Van Gent, 2000):

• Comparisons between storms measured in prototype and storms modelled in the 2D physical model tests show good agreement. The non-dimensional wave run-up levels differ only 4% on average (absolute values of the differences); considering the observed differences between prototype measurements and physical model tests it can be concluded that the schematisation and scale effects in the physical model tests are small.

• Numerical model computations support the use of the wave period $T_{-1,0}$ at the toe of coastal structures to account for the effects of wave energy spectra on wave run-up. This is in conformance with the characteristic wave period by Battjes (1969) for wave energy transport.

- Physical model tests also support the use of the wave period $T_{-1,0}$ at the toe of coastal structures to account for the effects of wave energy spectra on wave run-up. In Van Gent (1999) it was shown that these conclusions are also valid for wave overtopping.

- Using the peak wave period in predictions on wave run-up may lead to large inaccuracies for situations with shallow foreshores.

- A smooth and simple formula for wave run-up on coastal structures was proposed with a gradual curve towards an upper limit of the non-dimensional wave run-up:

$$z_{2\%} / (\gamma H_s) = c_0 \, \xi_{s,-1} \qquad \text{for } \xi_{s,-1} \leq p$$
$$z_{2\%} / (\gamma H_s) = c_1 - c_2 / \xi_{s,-1} \quad \text{for } \xi_{s,-1} \geq p \tag{1}$$

where H_s is the significant wave height of the incident waves at the toe of the structure ($H_s = H_{1/3}$), the reduction factor γ ($\gamma = \gamma_f \, \gamma_\beta$) takes the effects of angular wave attack (γ_β) and friction (γ_f) into account, the surf-similarity parameter is defined as $\xi_{s,-1} = \tan\varphi / \sqrt{2\pi H_s / g T_{-1,0}^2}$, and continuity between both sections and their derivatives determine $c_2 = 0.25 \, c_1^2/c_0$ and $p = 0.5 \, c_1/c_0$. Equation 1 was calibrated based on physical model tests: $c_0 = 1.35$ and $c_1 = 4.7$ (with a standard deviation of 0.37). If for the significant wave height the spectral wave height $H_s = H_{m0}$ is used the coefficients become $c_0 = 1.45$ and $c_1 = 3.8$ (with a standard deviation of 0.24). Most data concerned situations in the range $1 < \xi_{s,-1} < 10$, in which $2.5 \leq \tan\varphi \leq 6$. To which extent application of Equation 1 outside these ranges is appropriate still needs to be investigated. This formula is rather generic because it can be used for situations with relatively deep water at the toe of coastal structures and also for situations with shallow foreshores. Important is that the influence of wave energy spectra on wave run-up is accounted for by using the spectral wave period $T_{-1,0}$ of the incident waves at the toe of coastal structures.

Besides further investigations to study the effects of surfbeat-phenomena, the propagation of wave groups and their associated long wave motions, their possible contribution to wave run-up more in detail, the influence of morphological changes during a storm on the wave attack, also the importance of 3D-effects need to be assessed. The 3D tests contributed to this by searching for information on the importance of directional spreading. Before analysing these aspects two important conclusions could be drawn (see Annex 3.4a):

- Comparisons between storms measured in prototype and storms modelled in the 3D physical model tests show good agreement (perpendicular wave attack and long-crested waves). The non-dimensional wave run-up levels differ only 8% on average (absolute values of the differences).

- For measuring wave run-up levels a step gauge can be considered to be the optimal type of instrument based on analyses of test results obtained with run-up probes and step gauges.

Figure 43 shows the comparison between tests results from the physical model tests in 2D (table 7 and figure 8) and in 3D (table 17 and figure 42). These non-dimensional wave run-up levels differ only 0% on average and 6% if the absolute values of the differences are used. Condition 1.05 contributes the most to these differences (15%). Nevertheless, there is a rather good match.
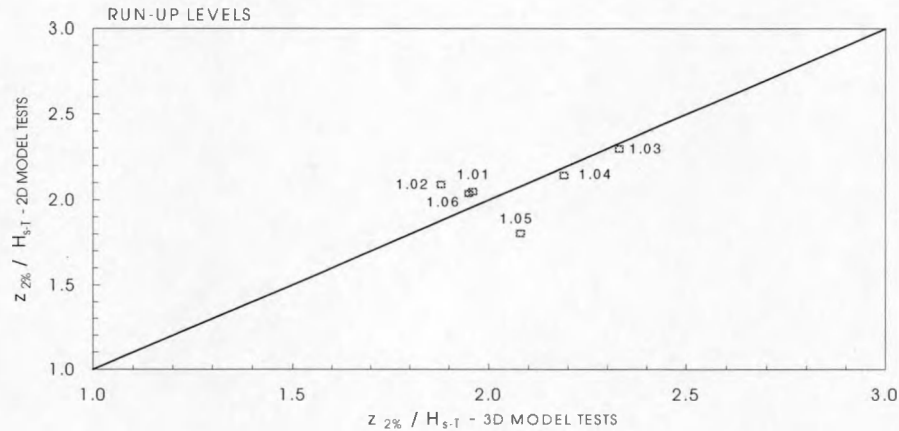
Figure 43: Comparison between wave run-up levels measured in 6 storms in 2D model tests and in 3D model tests.
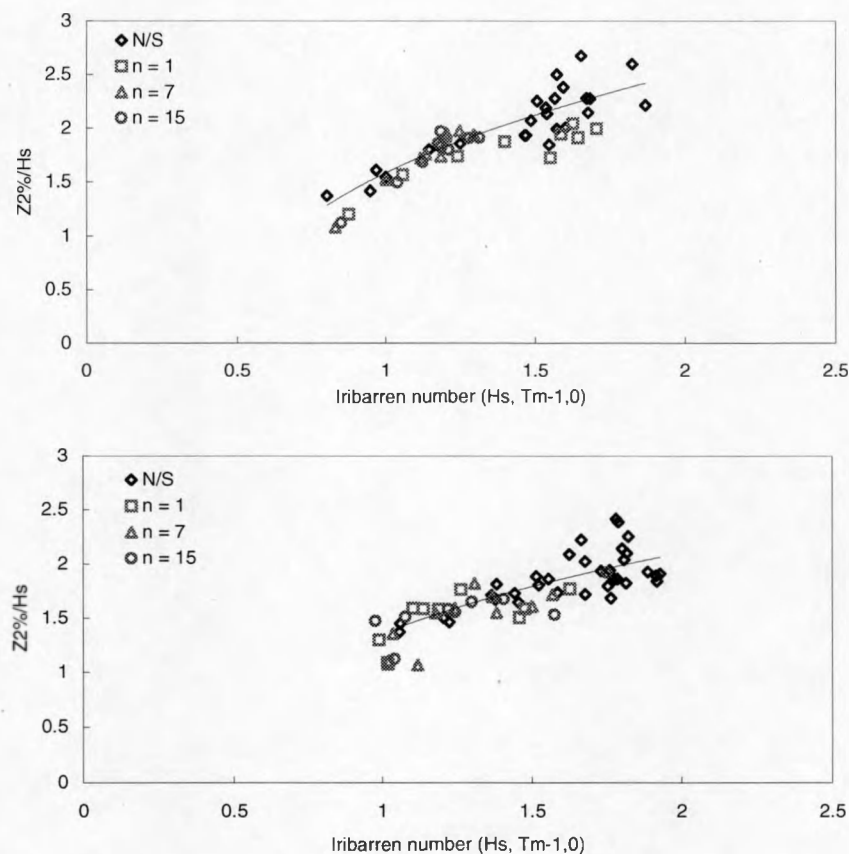
Figure 44: Measured wave run-up levels as function of the Iribarren number/surf-similarity parameter in 3D tests with different levels of generated directional spreading (N/S denotes no spreading); upper graph with higher water levels and lower graph with lower water levels; wave conditions (H_s and $T_{m-1,0}$) used in these graphs are those measured at MP6.

The 3D tests with directional spreading indicated that there is some influence of directional spreading but this influence appeared to be small compared to the common variations around the main trend. Figure 44 shows for tests with two different water levels the result of the wave run-up measurements with variations in directional spreading. These figures indeed indicate that the influence of directional spreading is relatively small and are dominated by other effects causing variations around the main trend.

Based on the synthesis of measurements and the individual measurements the main conclusions and recommendations for further research are summarised in the following paragraph. Recent research in different frameworks concern the analysis of low frequency waves at Petten and the possible influence of morphological changes on the required crest height.

c.3) Conclusions and recommendations

Based on the synthesis of measurements on the Petten Sea-defence the following conclusions and recommendations can be given:

Conclusions:

• Prototype measurements of waves and wave run-up have been performed at the Petten Sea-defence (Rijkswaterstaat-RIKZ). The wave field at this site is dominated by wind waves with severe wave breaking at the relatively shallow parts of the foreshore (two bars and shallow water at the toe of the dike). The reliability of the instruments under heavy storm conditions has been demonstrated and together with the use of data verification techniques, this measurement campaign resulted in a valuable data-set of wave dynamics and wave run-up. The use of a video-camera during storm conditions also provided important impressions of processes, such as the short-crested nature of the waves, the influence of the groins on waves, and variations in the wave run-up along the dike.

• Physical model tests (2D: WL IDelft Hydraulics and 3D: University College Cork) show a good agreement with storms measured in prototype. The non-dimensional wave run-up levels differ only 3.9% and 7.8% on average in the 2D and 3D model tests respectively. Considering the observed differences between prototype measurements and physical model tests it can be concluded that the schematisation and scale effects in the physical model tests were acceptably small.

• Differences in wave conditions and wave run-up levels in the three different measurement series could be subjected to further investigations. The effects of differences due to the amount of wave energy in the low frequencies and the short-crested nature of the waves are still topics for further analyses. The impression is that if a large amount of energy in low-frequencies is found, this may cause an increase in wave run-up levels. The short-crested nature of the waves affects the visual impression of the waves and wave run-up but the effects on the wave run-up statistics (e.g., $z_{2\%}$.) still need to be quantified. Physical model tests (3D) indicate that the actual wave run-up levels are not significantly affected by the short-crested nature of the waves. The

3D tests with directional spreading indicated that there is some influence of directional spreading but this influence appeared to be small compared to the common variations around the main trend.

- Other findings of the physical model tests are that for measuring wave run-up levels a step gauge can be considered to be the optimal type of instrument, that wave reflection by the Sea-defence affects the surface elevations considerably, and that low-frequency waves may contain a rather large percentage of the total wave energy.

Recommendations:

- Since the foreshore at the Petten Sea-defence causes significant wave breaking, the amount of wave energy present in low-frequencies is larger than for sites with a similar offshore wave climate but without severe wave breaking at the foreshore. Therefore, it is recommended to study the effects of surfbeat-phenomena, the propagation of wave groups and their associated long wave motions, and their possible contribution to wave run-up more in detail.

- Because the foreshore affects the wave conditions and the subsequent wave run-up, it is of importance to know the morphological changes during storms and their effects on the waves and wave run-up. Therefore, it is recommended to measure and analyse these morphological changes during storms.

- Besides wave run-up levels it is important to estimate overtopping discharges for conditions which are more severe than those which are likely to occur in prototype within a single storm season. Therefore, it is recommended to study layer-thicknesses (and possibly velocities), at the seaward slope during wave run-up. This information could then be used to estimate overtopping discharges during more severe conditions than those which can realistically be measured in prototype.

d) Link between prototype and laboratory results

The main objective of Task 4 was to link prototype and laboratory results in order to use the best methodology and to provide a reasonable estimation of the final discrepancies between prototype and laboratory observations. This link was defined creating a systematic procedure to feedback the prototype and laboratory experimental results. OPTICREST was ready to change concepts and methodologies during the project in a continuous feedback process. The preliminary goal was to improve methodology and the final goal was to know the reasons of the discrepancies of prototype and laboratory results and to discover the appropriate way to use them in providing adequate design guidelines for the crest level of coastal structures.

Annex 4a describes the systematic feedback process followed during the project OPTICREST to analyse methods and variables in Petten (prototype, 2D and 3D models). The discussions of concepts, ideas and comparisons made during OPTICREST guided the design and the deployment of new measurement systems in prototype (to measure the influence of low frequency components) and the positioning and type of run-up measurement system used in laboratory (step gauge).

Because a systematic evaluation of possible sources of discrepancy for run-up measurements were carried out during the project, and excellent agreement was found between prototype, 2D and 3D measurements of run-up for the analysed storms, the main conclusion of OPTICREST is that run-up on impermeable dikes can be correctly modelled at scale 1:40 without much distortions of results due to scale effects. The mean value of $Ru_{2\%}/H_{m0}$ was 2.03 and the differences found were 3.9% and 7.8% for resp.2D (DH) and 3D (UCC) models.

Although the measured discrepancy between run-up in prototype and scale models was small for the analysed storms, it became clear the influence of foreshore bathymetry (which may change during storms) which affects wave breaking and generation of infragravity waves. The importance of the low frequency component both in laboratory and prototype was considered relevant and was found during the laboratory experiments. The use of the parameter $T_{-1,0}$ instead $T_{0,1}$ or $T_{0,2}$ for characterising run-up results in Petten (see par. 4a.3) is a clear indicator that low frequency plays an important role in the run-up phenomenon.

Due to the large list of potential sources of discrepancy between prototype and model tests (time-domain characteristics of waves, wave generation techniques, resonance and long wave reflection in laboratory, surfbeat in prototype, measurement of long waves, run-up measurement systems, scale effects, wind effects, foreshore bathymetry, etc.), the small discrepancy between run-up measurements in prototype and scale models is a clear indicator that scale effects are nor relevant, most of the sources of discrepancy were less important than expected and some compensation of errors may have happen to obtain such a good agreement between measurements in prototype, 2D and 3D models (average errors lower than 4% and 8% respectively). Nevertheless, special attention must be paid to low frequency waves and changes in the foreshore because these two elements have been positively identified as important factors affecting wave run-up and wave overtopping in Petten. The measurement in prototype and the correct reproduction in scale models are crucial to obtain reliable results.

e) Overall conclusions and recommendations for Petten Sea-Defence i.e. impermeable smooth sea-dike

The most important final conclusions and recommendations of Task 4 in Petten can be summarised as follows:

1) Run-up on impermeable dikes can be correctly analysed using 2D and 3D models (scale 1:40). The scale effects found in OPTICREST are not relevant.

2) Step gauge run-up measurement systems must be used in scale models to avoid biased measurements of run-up.

3) Special attention should be paid in Petten to foreshore changes in time, because the foreshore has a significant influence on waves attacking the dike.

4) Surf beat phenomenon and low frequency wave components must be well described and measured in prototype because of the influence on wave run-up and wave overtopping.

5) Low frequency components must be analysed also in scale models of dikes because of the significant influence on run-up.

6) Wind may increase wave run-up and wave overtopping, but the results of OPTICREST (referred to breakwaters not dikes) only show a secondary influence.

4.2 Link between the Zeebrugge prototype and laboratory results

a) Introduction

This section describes task 4 corresponding to the Zeebrugge case.

Reference is made to following annexes:

- Annex 2.2 *'Prototype measurements Zeebrugge'*
- Annex 3.3a *'Laboratory investigations: two dimensional testing – the Zeebrugge breakwater'*
- Annex VIII of the *'Annual Report (To+12 till To+24)'*
- Annex 3.3b *'2D testing – the Zeebrugge model tests performed in UPV'*
- Annex 3.4c.1 *'Zeebrugge model: wave run-up under simulated prototype storms'*
- Annex 3.4c.2 *'Zeebrugge model: 3D wave run-up measurements and analysis'*
- Annex 3.4c.3 *'Zeebrugge model: (i) Wave run-up under simulated prototype storms (II) and (ii) The influence on wave run-up introducing a current'*
- Annex 4b *'Link between prototype and laboratory results: Zeebrugge case'*

The link between prototype and laboratory results is described in three paragraphs.

The first paragraph is the 'Methodology'. The methodology describes the procedures of task 4 defined in the Technical Annex of the OPTICREST project, the evolution of the methodology according to the results and the organisation of the final report of task 4 in which all the relevant work is described.

The second part ('Wave run-up measurements on a rubble mound breakwater: prototype versus scale model test results') is given in the second paragraph. Synthesis of wave run-up measurements on a rubble mound breakwater describes the measurements taken in prototype, 2D and 3D experiments and most important results of comparisons analysed during OPTICREST referred to Zeebrugge. The objective of the second paragraph is to provide an overview on the performed measurements corresponding to Zeebrugge breakwater in order to support the conclusions on rubble mound breakwaters.

The third paragraph gives the principal conclusions.

b) Methodology

Task 4 (link between prototype and laboratory results) was originally scheduled to start in month (To+24) and begin preliminary work in month (To+13). However, it was decided from the very beginning of OPTICREST that preliminary work should be done helping in the definition of the methodological aspects of OPTICREST (SubTask 3.1). Task 4 has been from the beginning of OPTICREST an assistant reflexive tool to improve the methodology applied both in prototype and laboratory observations of Zeebrugge. The continuous feed-back process of ideas and concepts, experimental methods and analysis of results was the main streamline of Task 4. At the end of the project, the analysis of laboratory and prototype results and the comparisons made reflect the sedimentation of ideas and concepts. This chapter includes both the synthesis of the prototype, 2D

and 3D measurements of runup, overtopping and wind effects in Zeebrugge and the link between prototype and laboratory results.

Past experience in running experiments in different laboratories recommended that a careful description of experiments was a necessary condition to avoid large discrepancies of measurements taken in different laboratories . In Zeebrugge, the difficulties were higher because the facilities, conditions and limitations were different for different partners (prototype, 3-D and 2-D). It was considered reasonable to be ready from the beginning of OPTICREST to face significant discrepancies between results obtained from similar experiments in different facilities. The basic elements to be considered, which were continuously defined and redefined during the project were: (1) anatomy of the sources of possible discrepancies between prototype and laboratory results, (2) "a priori" subjective estimation of the impact of each source of discrepancy on the results, (3) quantitative estimation of the effects of the resources of discrepancy and (4) recommendations.

Several causes of the observed discrepancies between prototype and laboratory experiments were indicated in the proposal (structural description, wave and runup measuring systems, wind, roughness, randomness of sea conditions, etc). During OPTICREST, a complete anatomy of those possible sources of discrepancies was constructed and re-constructed on the basis of the opinions (subjective) of the different experts in the group of partners (see Annex 4b). Because of different experts in the group had different points of view about the relative importance of some possible source of discrepancy, and because these views changed during the project, it was necessary to clarify what were the expectations (relative importance) of the different experts of the group on the discrepancies prototype-laboratory. Special attention was given to the most optimistic and pessimistic points of view in each aspect analysed.

The proposed first anatomy of sources of discrepancies corresponding to Zeebrugge was structured in four areas:
(1) SEA WAVES including the sources of discrepancies associated to the wave measurement, wave analysis and wave generation processes both in prototype and laboratory,
(2) LONG WAVES including the sources of discrepancies due to the generation of long waves in the field and laboratories and the corresponding resonance phenomena, as well as the different measurement techniques;
(3) RUNUP AND OVERTOPPING including the sources of discrepancies related to the measurement system selected in prototype and laboratory, as well as calibration, reliability of equipment, and the ones involved with wind effects; and
(4) WIND AND SPRAY including the measurement systems, calibration and influence of atmospheric variables.

A complete list of trouble-makers variables were analysed and re-analyzed during OPTICREST; the estimation of the impact on the results were not decreasing during the project because of the evidence of significant discrepancies between runup on 2D and 3D model tests and prototype. The differences found between prototype, 2D and 3D results forced a careful analysis of modelling and measuring techniques from which the step gauge was considered the appropriate method to measure runup both in prototype and laboratory and a common Runup Wave Measuring System (RWMS).

Commonly used capacitance wave gauges parallel to the slope significantly underestimated wave runup. Also the runup was identified to be very sensitive to the placement of the RWMS in the breakwater model so a detailed surveying of the prototype followed by a precise construction of the models is necessary.

The preliminary goal of task 4 was to improve methodology and the final goal was to know the reasons of the discrepancies of prototype and laboratory results and to discover the appropriate way to use them in providing adequate design guidelines for the crest level of coastal structures.

Annex 4b describes the systematic feedback process followed during the project OPTICREST to analyse methods and variables in Zeebrugge (prototype, 2D and 3D models). The discussions of concepts, ideas and comparisons made during OPTICEST guided the design and the installation of new measurement systems in prototype (runup step gauge added to spiderweb system, precise armour survey, etc.) and the fabrication and positioning of new runup measurement system in laboratory (step gauge instead of sensors parallel to the slope). Because a systematic evaluation of possible sources of discrepancy for runup measurements was carried out during the project, and no excellent agreement was found between prototype, 2D and 3D measurements of runup for the analysed storms, the analysis of the troublemaker variables listed in Task 4 was the central point of the design and re-design of experiments during OPTICREST

There are several conclusions obtained during of OPTICREST related to wave run-up and wave overtopping on mound breakwaters that may be very useful for engineers and researcher. Among the conclusions and recommendations, some may have significant methodological impact on past and future data and literature on runup and overtopping. Wave run-up has been found to be Rayleigh distributed both in prototype and scale models (1:30); this fact allows users to work with Rayleigh equivalent $Ru_{2\%}$ instead of $Ru_{2\%}$ which is quite difficult, if not impossible, to measure sometimes. Dimensionless runup in prototype (not in scale models) was significantly higher for low water levels; the lack of knowledge of the permeability of underlayers and the instability of sand core infiltration in models may be responsible of the discrepancies and different behaviour found in prototype for high and low water levels. Step gauge is the only reliable runup measurement system both in prototype and scale models.

Although the experiments were planned to be very similar in prototype and laboratories, the local limitations produced some small differences which should be considered in analysing the results. AAU used in the 3D tests a qualitatively different wave generation technique (with wave absorption) than FCFH and UPV (without wave absorption) and a different scale (1:40 instead 1:30). AAU needed several runs to fit each one of the target storm spectra while FCFH and UPV fitted the target spectra at the first or second trial. AAU and FCFH modelled the foreshore bar (550,-9.50) while UPV used a flat bottom at −13.30 and did not modelled the foreshore bar. UPV and AAU generate waves with big maximum strokes but maximun stroke was very limited in FCFH (30 cm). Although the step gauge was used by all laboratories and prototype, AAU and FCFH used a comb with bars perpendicular to the slope, UPV used a comb with vertical bars.

c) Wave run-up measurements on a rubble mound breakwater: prototype versus scale model test results.

c.1) Introduction

Prototype measurements are carried out on a rubble mound breakwater protecting the outer harbour of Zeebrugge (Belgium) by a joint effort of the Ministry of the Flemish Community - Coastal Division (FCCD) and Ghent University (UG). Two dimensional model test are performed at two locations: at Flanders Hydraulics (FCFH) and at Universidad Politécnica de Valencia (UPV). The same scale (1:30) has been used to model the Zeebrugge breakwater. At UPV a combined wave flume and wind tunnel facility was available to study the influence of wind on wave run-up. At Aalborg University (AAU), 3D tests are carried out on a scale model (1:40) of the Zeebrugge breakwater.

For the description and the conclusions of the prototype measurements and the laboratory investigations, reference is made to the respective final reports. In this report prototype measurement and laboratory test results are synthesised and compared. The main conclusions concerning these investigations are drawn.

c.2) Prototype measurements

Prototype measurements are carried out on a rubble mound breakwater armoured with 25 ton grooved cubes. Wave height and wave period(s) are measured by two wave rider buoys which are located at a distance of 150 m and 215 m respectively from the breakwater slope. The mean water level is measured by means of a pressure sensor or an infrared meter. Wave run-up is measured by two completely different measuring systems: a 'spiderweb system' and a run-up gauge.

Thirteen 'storm sessions' have been observed during the period 1995-2000. A detailed description is given in the final report on the Zeebrugge prototype measurements The storms that have been reproduced in the laboratories are summarised in table 18.

Table 18: Measured and reproduced storms in prototype.

Storm n°	Datum	Time	Δt	MWL [m]	H_s [m]	T_m [s]	H_{mo} [m]	T_p [s]	T_{01} [s]	$Ru_{2\%}$ [m]	$Ru_{2\%}/H_{mo}$ [-]	ξ_m [-]	ξ_p [-]
1	07/02/1999[RU]	16h00 - 18h00	2h	5.07	3.00	5.89	3.13	8.53	6.53	5.42	1.73	3.55	4.63
2	20/01/1998	04h15 - 06h15	2h	4.35	2.87	6.02	3.01	8.53	6.58	5.37	1.79	3.64	4.73
3	19/01/1998	15h45 - 18h15	2h30	4.80	2.83	5.94	2.95	8.53	6.61	5.09	1.73	3.70	4.77
4	28/08/1995	14h45 - 17h00	2h15	5.14	2.55	5.75	2.68	9.31	6.40	4.43	1.66	3.76	5.47
5	28/08/1995	03h30 - 04h45	1h15	5.46	2.74	5.68	2.87	7.31	6.18	4.27	1.49	3.51	4.15
8[*]	06/11/1999[RU]	11h30 - 13h30	2h	5.28	2.89	5.69	3.05	7.31	6.28	5.55	1.82	3.45	4.02
9[*]	06-07/11/1999[RU]	23h45 - 01h45	2h	5.11	2.44	5.36	2.59	7.31	6.09	4.76	1.84	3.64	4.37

[*]: due to the absence of waverider II (215 m in front of the breakwater), the data of wave rider I (150 m in front of the breakwater) is used in the analysis

c.3) Physical model tests

The scale models are built according the outline given in task 3.1 ('Methodology'). The core has been scaled in such way that the hydraulic gradients are reproduced properly. The armour units in the top layer of the model are placed according to the actual position in prototype. The first layer of

armour units is placed with a regular pattern. Various measuring devices have been employed to determine the wave run-up: several wire gauges placed at different heights above the surface of the breakwater slope and a novel step gauge developed by Ghent University. This step gauge is used to determine the final results. The step gauge is a comb of which the needles can be adjusted to the profile of the breakwater, so the distance between the armour units and the gauge is less than 2 mm. In case of a traditional run-up gauge the distance between the armour units and the gauge can reach much higher values because of the craggy slope surface.

FH and AAU reproduced seven measured storms (of which two cover half a tide cycle including 5 subsequent time series). UPV only reproduced two storms (each including 5 subsequent time series). All laboratories carried out parametric tests. For latter measurements, reference is made to the respective reports of the various laboratories.

2D Laboratory tests

Two 2D models have been built: one in the wave flume of Flanders Hydraulics (FH) and one in the combined wind tunnel and wave flume facility of Universidad Politécnica de Valencia (UPV) both on scale 1:30.

3D Laboratory tests

The 3D model is built in the wave tank of Aalborg University (AAU) on scale 1:40. For the simulation of prototype storms, longcrested waves which attack perpendicularly (i.e. 2D) are used.

c.4) Comparison of prototype measurements and laboratory testing

Table 19 gives an overview of the measured and reproduced storm sessions.

Table 20 summarises the $Ru_{2\%}/H_{mo}$ values obtained by reproduction of 7 prototype storms at high tide in the three laboratories as well as the prototype $Ru_{2\%}/H_{mo}$ values. Figure 45 shows the same results. On the horizontal axis, the Iribarren number $\xi_m = \dfrac{\tan\alpha}{\sqrt{\dfrac{2\pi H_{mo}}{gT_{0.1}^2}}}$ is plotted.

Task 2.2 ('Prototype measurements - Zeebrugge') revealed the overall mean prototype $Ru_{2\%}/H_{mo}$ value of 1.76 (based on much more storms than mentioned in table 2 and all measured with the more reliable run-up gauge).

The FH results show an underestimation of the prototype values. A mean $Ru_{2\%}/H_{mo}$ value is 1.46. The mean $Ru_{2\%}/H_{mo}$ value of UPV is 1.79.

Table 19: Overview of measured and reproduced 'storm sessions'.

	prototype	FH	UPV	AAU
Aug. 28, 1995 (03h30 - 04h45)	x[a]	x		x
Aug. 28, 1995 (14h45 - 17h00)	x[a]	x		x
Jan. 19, 1998 (15h45 - 18h15)	x[a]	x		x
Jan. 20, 1998 (04h15 - 06h15)	x[a]	x		x
Feb. 7, 1999 (16h00 - 18h00)	x[b]	x		x
Nov. 6, 1999 (09h30 - 10h30)	x	x	x	x
Nov. 6, 1999 (10h30 - 11h30)	x	x	x	x
Nov. 6, 1999 (11h30 - 13h30)	x	x	x	x
Nov. 6, 1999 (13h30 - 14h30)	x	x	x	x
Nov. 6, 1999 (14h30 - 15h30)	x	x	x	x
Nov. 6-7, 1999 (21h45 - 22h45)	x	x	x	x
Nov. 6-7, 1999 (22h45 - 23h45)	x	x	x	x
Nov. 6-7, 1999 (23h45 - 01h45)	x	x	x	x
Nov. 6-7, 1999 (01h45 - 02h45)	x	x	x	x
Nov. 6-7, 1999 (02h45 - 03h45)	x	x	x	x

[a]: wave run-up is measured only by the 'spiderweb system'
[b]: only three parts of the five-part run-up gauge was operational during the measurements

Table 20: Comparison of prototype measurement and laboratory test results

($Ru_{2\%}/H_{mo}$ values obtained by simulation of prototype storms).

storm n°	Datum	prototype	FCFH (2D, 1:30)	UPV (2D, 1:30)	AAU (3D, 1:40)
5	Aug. 28, 1995 am	1.49	1.48		1.52
4	Aug. 28, 1995 pm	1.66	1.42		1.91
3	Jan . 19, 1998	1.73	1.53		1.76
2	Jan. 20, 1998	1.79	1.40		1.89
1	Feb. 7, 1999	1.73	1.39		1.71
8	Nov. 6, 1999	1.82	1.44	1.81	1.41
9	Nov. 6-7, 1999	1.84	1.57	1.76	1.29

The results of AAU of storms 1 to 5 are close to the prototype results. However, one remark has to be made: the spectra obtained in the laboratory do not fit the prototype spectra very well. Although the significant wave height H_{mo} and the mean wave period $T_{0,1}$ have been adjusted well, the peak period of the produced laboratory spectra is shifted to a higher value, giving more energy to low frequency waves.

A mean $Ru_{2\%}/H_{mo}$ value for these 5 storms is 1.76. The reproduced spectra at AAU of storms 8 and 9 fit the prototype spectra very well (both H_{mo} and T_p), the $Ru_{2\%}/H_{mo}$ results are clearly lower. These two storms have a mean dimensionless 2% wave run-up value of 1.35. Taking all storms into account, the mean value $Ru_{2\%}/H_{mo}$ is 1.64.

Not only the $Ru_{2\%}/H_{mo}$ values, but also the $Ru_{5\%}/H_{mo}$ and the $Ru_{10\%}/H_{mo}$ values are calculated. The two storms (storm 8 & 9) of half a tide cycle are focussed. The results are summarised in table 21, 22, 23 and 24 for prototype, FH, UPV and AAU measurements respectively and these are plotted on a graph showing the $Ru_{x\%}/H_{mo}$ values vs. mean water level (MWL) (figure 46, 47 and 48).
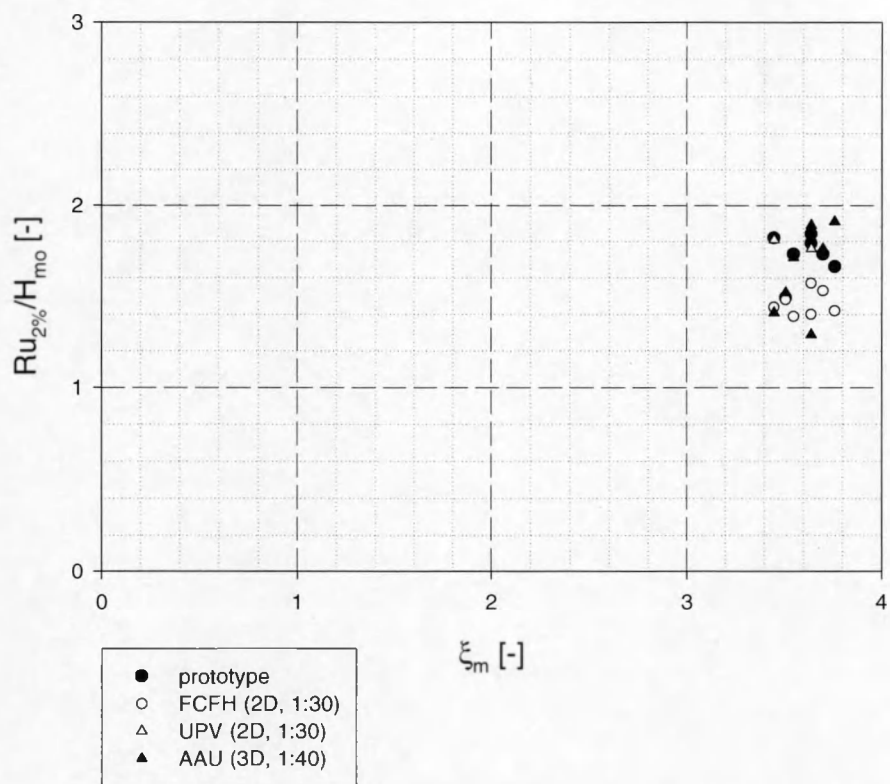
Figure 45: Comparison of prototype measurement and laboratory test results

(simulation of prototype storms)

Table 21: Prototype $Ru_{x\%}/H_{mo}$ values (x = 2, 5 and 10%)

(Nov. 6, 1999 & Nov. 6-7, 1999).

	MWL [m]	$\dfrac{Ru_{2\%}}{H_{mo}}$ [-]	$\dfrac{Ru_{5\%}}{H_{mo}}$ [-]	$\dfrac{Ru_{10\%}}{H_{mo}}$ [-]
Nov. 6, 199 (09h30 - 10h30)	3.45	2.56	1.96	1.58
Nov. 6, 1999 (10h30 - 11h30)	4.53	2.21	1.81	1.69
Nov. 6, 1999 (11h30 - 13h30)	5.28	1.82	1.54	1.33
Nov. 6, 1999 (13h30 - 14h30)	5.01	1.89	1.53	1.46
Nov. 6, 1999 (14h30 - 15h30)	4.28	2.34	1.94	1.51
Nov. 6-7, 1999 (21h45 - 22h45)	3.26	2.34	2.12	1.64
Nov. 6-7, 1999 (22h45 - 23h45)	4.16	2.24	2.00	1.61
Nov. 6-7, 1999 (23h45 - 01h45)	5.11	1.84	1.64	1.42
Nov. 6-7, 1999 (01h45 - 02h45)	4.71	2.11	1.81	1.49
Nov. 6-7, 1999 (02h45 - 03h45)	3.89	2.26	1.63	1.36

Table 22: FH laboratory $Ru_{x\%}/H_{mo}$ values ($x = 2$, 5 and 10%)

(Nov. 6, 1999 & Nov. 6-7, 1999).

	MWL [m]	$\dfrac{Ru_{2\%}}{H_{mo}}$ [-]	$\dfrac{Ru_{5\%}}{H_{mo}}$ [-]	$\dfrac{Ru_{10\%}}{H_{mo}}$ [-]
Nov. 6, 199 (09h30 - 10h30)	3.45	1.26	1.14	1.07
Nov. 6, 1999 (10h30 - 11h30)	4.53	1.46	1.37	1.27
Nov. 6, 1999 (11h30 - 13h30)	5.28	1.44	1.33	1.22
Nov. 6, 1999 (13h30 - 14h30)	5.01	1.47	1.41	1.30
Nov. 6, 1999 (14h30 - 15h30)	4.28	1.57	1.48	1.30
Nov. 6-7, 1999 (21h45 - 22h45)	3.26	1.37	1.17	1.08
Nov. 6-7, 1999 (22h45 - 23h45)	4.16	1.50	1.33	1.08
Nov. 6-7, 1999 (23h45 - 01h45)	5.11	1.57	1.44	1.35
Nov. 6-7, 1999 (01h45 - 02h45)	4.71	1.46	1.40	1.33
Nov. 6-7, 1999 (02h45 - 03h45)	3.89	1.34	1.07	0.97

Table 23: UPV laboratory $Ru_{x\%}/H_{mo}$ values ($x = 2$, 5 and 10%)

(Nov. 6, 1999 & Nov. 6-7, 1999).

	MWL [m]	$\dfrac{Ru_{2\%}}{H_{mo}}$ [-]	$\dfrac{Ru_{5\%}}{H_{mo}}$ [-]	$\dfrac{Ru_{10\%}}{H_{mo}}$ [-]
Nov. 6, 199 (09h30 - 10h30)	3.45	1.72	1.51	1.23
Nov. 6, 1999 (10h30 - 11h30)	4.53	1.97	1.56	1.33
Nov. 6, 1999 (11h30 - 13h30)	5.28	1.81	1.50	1.28
Nov. 6, 1999 (13h30 - 14h30)	5.01	1.91	1.55	1.36
Nov. 6, 1999 (14h30 - 15h30)	4.28	2.02	1.59	1.36
Nov. 6-7, 1999 (21h45 - 22h45)	3.26	2.13	1.62	1.26
Nov. 6-7, 1999 (22h45 - 23h45)	4.16	1.86	1.64	1.28
Nov. 6-7, 1999 (23h45 - 01h45)	5.11	1.76	1.48	1.35
Nov. 6-7, 1999 (01h45 - 02h45)	4.71	1.81	1.58	1.26
Nov. 6-7, 1999 (02h45 - 03h45)	3.89	1.53	1.35	1.02

Table 24: AAU laboratory $Ru_{x\%}/H_{mo}$ values ($x = 2$, 5 and 10%)

(Nov. 6, 1999 & Nov. 6-7, 1999).

	MWL [m]	$\dfrac{Ru_{2\%}}{H_{mo}}$ [-]	$\dfrac{Ru_{5\%}}{H_{mo}}$ [-]	$\dfrac{Ru_{10\%}}{H_{mo}}$ [-]
Nov. 6, 199 (09h30 - 10h30)	3.45	1.79	1.62	1.59
Nov. 6, 1999 (10h30 - 11h30)	4.53	1.51	1.36	1.28
Nov. 6, 1999 (11h30 - 13h30)	5.28	1.41	1.26	1.13
Nov. 6, 1999 (13h30 - 14h30)	5.01	1.43	1.30	1.21
Nov. 6, 1999 (14h30 - 15h30)	4.28	1.58	1.48	1.21
Nov. 6-7, 1999 (21h45 - 22h45)	3.26	1.65	1.57	1.42
Nov. 6-7, 1999 (22h45 - 23h45)	4.16	1.63	1.52	1.26
Nov. 6-7, 1999 (23h45 - 01h45)	5.11	1.29	1.22	1.15
Nov. 6-7, 1999 (01h45 - 02h45)	4.71	1.39	1.31	1.20
Nov. 6-7, 1999 (02h45 - 03h45)	3.89	1.63	1.57	1.52

<u>Figure 46:</u> Comparison of prototype and laboratory $Ru_{2\%}/H_{mo}$ values (simulation of prototype storms) *(Nov. 6, 1999 & Nov. 6-7, 1999).*
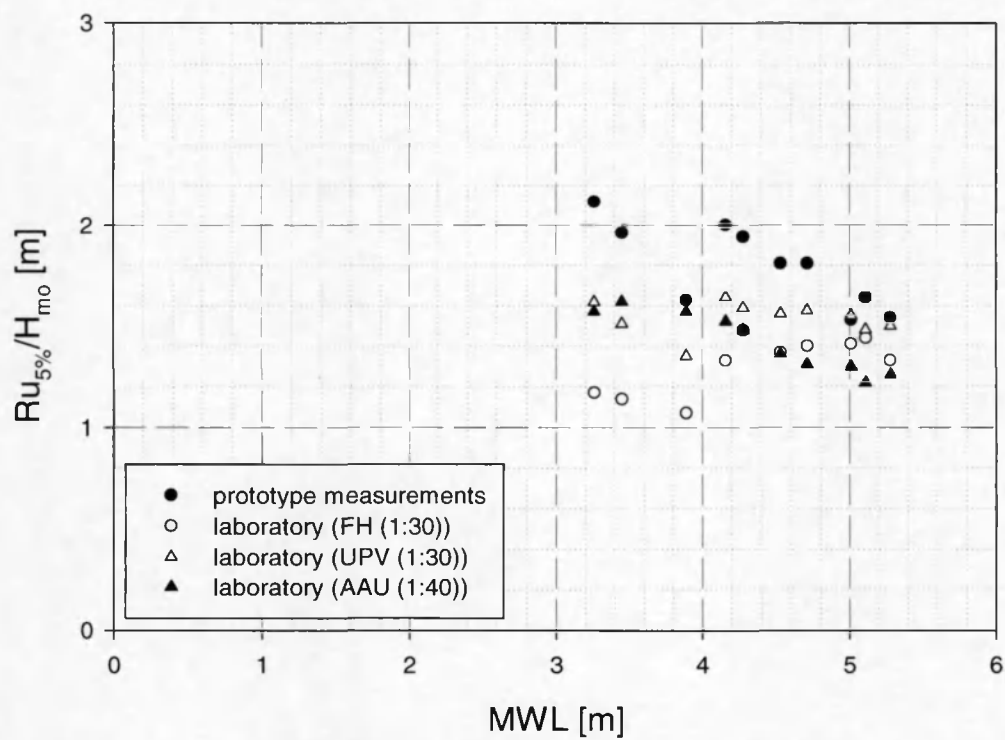
<u>Figure 47:</u> Comparison of prototype and laboratory $Ru_{2\%}/H_{mo}$ values (simulation of prototype storms) *(Nov. 6, 1999 & Nov. 6-7, 1999).*

From figure 46 it is seen that prototype results and AAU results have the same trend: dimensionless 2% wave run-up values increase with decreasing water depth. AAU results are lower than prototype results. UPV results equal prototype results at high water, but diverge from prototype results when the water level becomes lower. A slight increase in dimensionless 2% wave run-up is noticed in the UPV results when the water depth is decreasing. The results of FH are almost the same as the AAU results at high water, but remain almost constant when the water level changes. The dependency of wave run-up on the water level may also be influenced by the fact that at a lower water level, wave run-up occurs at a lower part of the breakwater which may have lower porosity, due to a settlement of the armour layer.

The difference between the results of all laboratories and prototype results become smaller and smaller when higher exceedence probabilities are considered. Figure 47 shows all $Ru_{5\%}/H_{mo}$ values. Similar to the previous graph, AAU results confirm the trend noticed in prototype (dimensionless wave run-up increases with decreasing water depth), but the laboratory results are smaller. At high tide UPV results have the same order of magnitude of prototype results, but remain constant when the water level changes. At high tide FH results are slightly higher than AAU results and decrease with decreasing water depth.
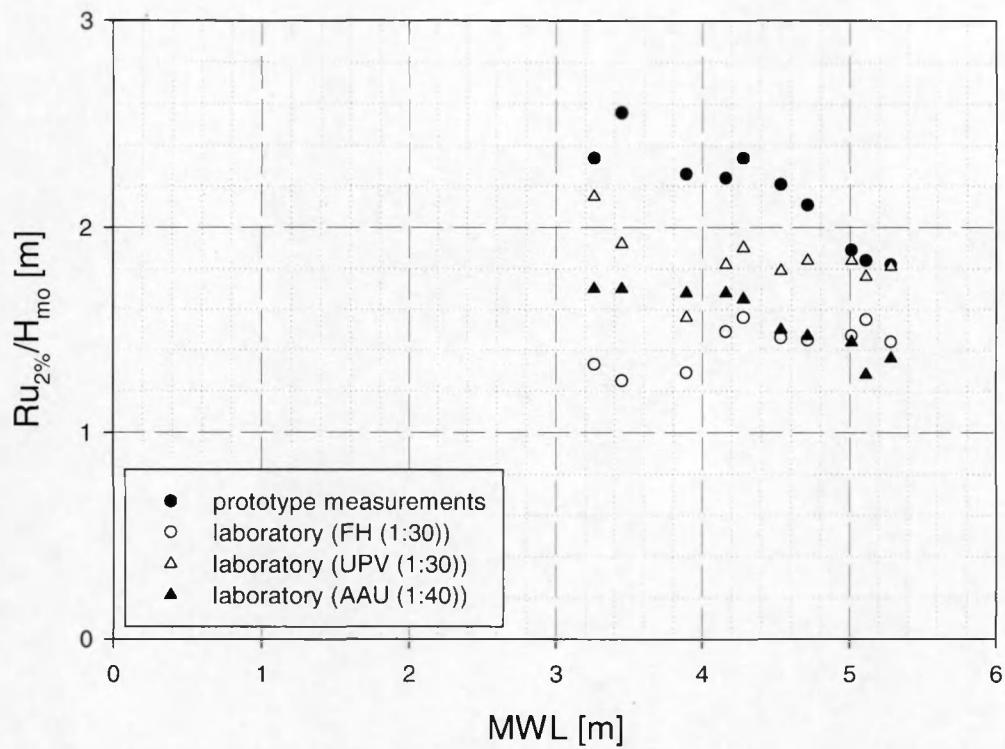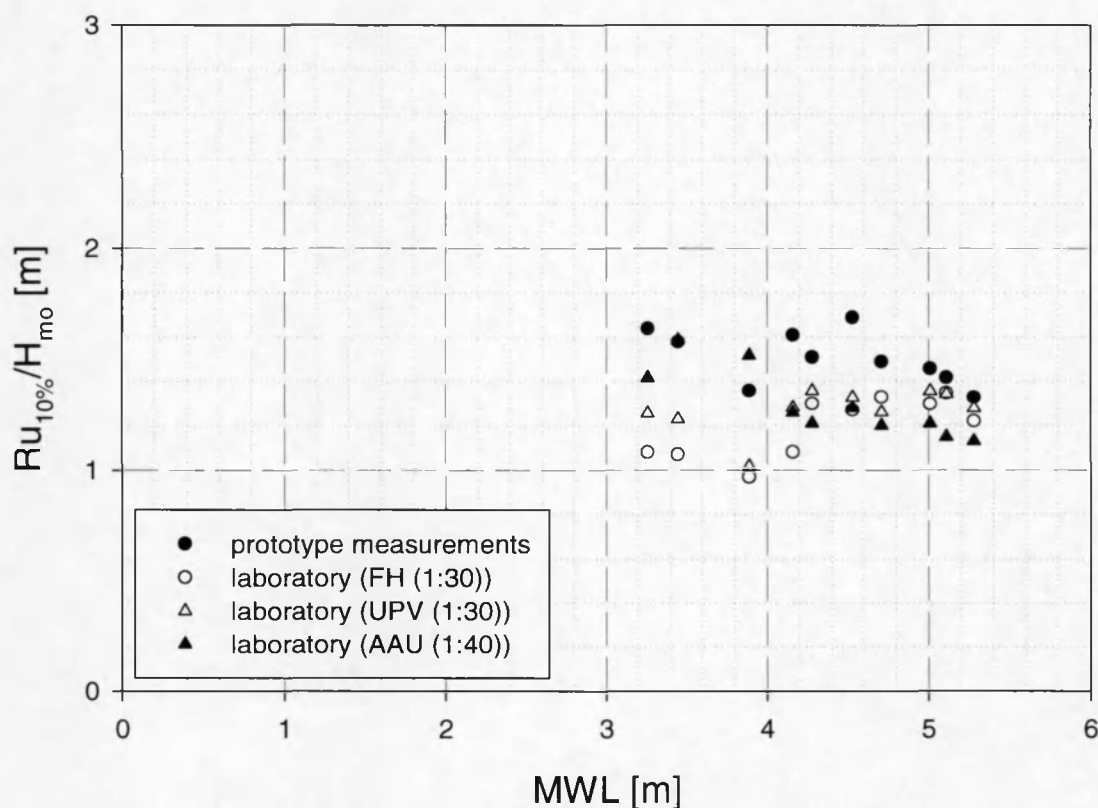

Figure 48: Comparison of prototype and laboratory $Ru_{10\%}/H_{mo}$ values (simulation of prototype storms) *(Nov. 6, 1999 & Nov. 6-7, 1999).*

All results become very similar when $Ru_{10\%}$ is taken into account (figure 48). At higher water all values have almost the same value.

In an attempt to search for the explanation for differences within the laboratory results and differences between laboratory results and prototype results, various points of thorough investigation are highlighted:

(a) the spectral width parameter ε, defined by $\varepsilon = \sqrt{\dfrac{m_0 m_2}{m_1^2} - 1}$, has an influence. There seems to be

an overall tendency: the dimensionless 2% wave run-up increases with increasing spectral width parameter value (figure 49). When wave spectra are reproduced in the laboratory, waves are only defined by their amplitude spectra (H_{mo} and T_p) which is not a complete representation of the kinematics of waves.

At AAU the same target spectrum has been reproduced several times. A quite large scatter is observed in the obtained $Ru_{2\%}/H_{mo}$ results. The spectral shape (and more specific the spectral width) seems to be of big importance: small variations of the ε parameter have a big effect on the $Ru_{2\%}/H_{mo}$ value.
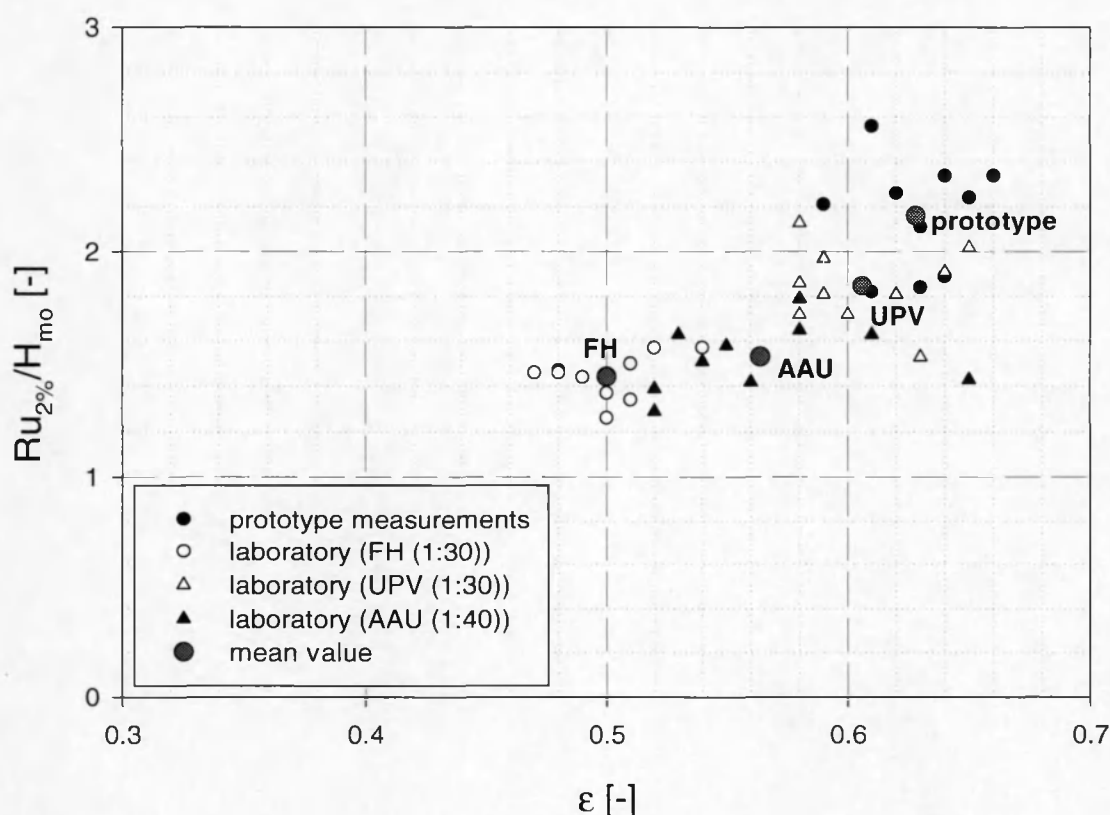
Figure 49: $Ru_{2\%}/H_{mo}$ versus spectral width parameter ε (Nov. 6, 1999 & Nov. 6-7, 1999).

(b) both prototype ánd laboratory tests have shown that wave run-up is Rayleigh distributed. Only the highest wave run-ups deviate from this distribution. However, the Rayleigh distribution of wave run-up shows that $Ru_{2\%}$ is a good parameter to describe wave run-up.

Figure 23 shows the 80% confidence bands of the Rayleigh equivalent $\dfrac{Ru_{2\%}}{H_{mo}}$ value (based on

the measured wave run-up distributions) corresponding to prototype, FH and UPV (for the Nov.

6, 1999 and the Nov. 6-7, 1999 storm) and the $\dfrac{Ru_{2\%}}{H_{mo}}$ values measured by AAU. The overlap of the 80% confidence bands of prototype, FH and UPV for the higher water levels ($MWL > z + 4.5$) indicate a reasonable modelling of both storms in laboratory. The overlapping of 80% confidence bands of FH and UPV in the full range of water levels seems to indicate a reasonable agreement of results obtained by FH and UPV.

(c) prototype wave spectra are reproduced in the laboratory. Only the parameters H_{mo} and a wave period parameter ($T_{0.1}$, T_p,...) are finetuned. It is noticed that the *wave height distributions* obtained by this way of working does not fit the prototype wave height distribution. Fine tuning only H_{mo} and e.g. $T_{0.1}$ is insufficient to reproduce the kinematics of the waves correctly.

(d) all laboratories used their own computer program to analyse the results. Cross checking of results have been carried out and no errors have been found.

(e) the armour units in the upper armour layer have been placed in exactly the same placement pattern as in prototype. The first layer is placed in a regular pattern. This is probably not the case in prototype. Further it has to be mentioned that the breakwater has been built in 1983, so some settlements of the armour units have occurred, by which the porosity in the lower part of the armour layer may be higher in the scale models. By filling up the gaps between the armour units (i.e. by changing the porosity), wave run-up increased remarkably (up to 30%). This was noticed both at AAU and FH.

(f) the effect of wind has been investigated at the combined wind tunnel and wave flume facility of UPV. Model wind speeds of 0 m/s and 5 m/s of 40 test cases were used with regular waves. Sixteen cases of the test matrix (irregular waves) were selected to be tested using model wind speeds of 0 m/s, 3 m/s, 5 m/s and 7 m/s. Figure 50 shows the observed overtopping dependency on wind speed ($RuH = 1.80.H_{mo}$). Only a slight increase in dimensionless wave overtopping for higher wind speed was observed. The observed increase of dimensionless wave overtopping at logarithmic scale was proportional to the square of the wind speed. A precise quantitative estimation of the influence of wind on wave run-up and wave overtopping was not possible (no overtopping events were measured in prototype), but in laboratory the influence is clear but not as important as crest freeboard and wave intensity. Therefore, only a slight increase in dimensionless wave run-up and wave overtopping should be considered for comparison of laboratory and prototype measurements of the Zeebrugge case.

(g) at AAU, in the wave tank tests an influence of currents is noticed. By creation of a long shore current, dimensionless wave run-up increased with increasing current velocity. In prototype, the maximum current velocity occurs at high tide. At mean tide, the current velocity is almost zero. Relying on the AAU results, the highest wave run-up should occur at high tide. This is in contradiction with the observed phenomenon at full scale: wave run-up increases with decreasing water level, so with decreasing current velocity.
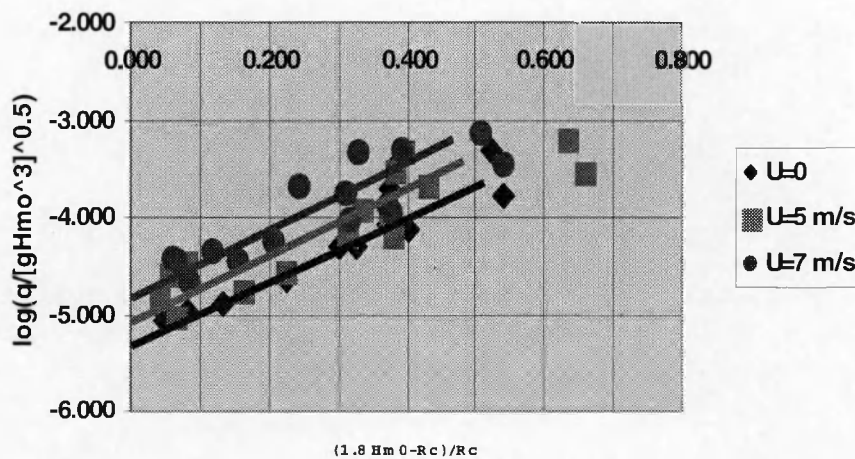
Figure 50: log($Q/(gH_{mo})$^1.5) as function of (RuH-Rc)/Rc and wind speed.

(h) the foreshores at FH and UPV are slightly different. FH modelled the Zeebrugge site up to 600 m in front of the breakwater to include the bar at approximately 550 m. UPV did not model the bar (crest elevation: -9.5 meters) and used a flat bottom at –13.3 depth to model the foreshore for distances larger than 210 meters from breakwater axis.

(i) in prototype, the core is partially filled with sand. Initially, this sand was present in the scale models but was washed out during the tests by which the core of the scale model became more permeable at lower levels than in prototype.

(j) a scale effect, which cannot be quantified, plays an important role in the small scale measurements.

c.5) Conclusion

1) For a rubble mound breakwater prototype measurements yield $Ru_{2\%}/H_{mo} \cong 1.76$ (valid for $H_{mo} \cong D_{n50}$) which is considerably higher than values found in literature for comparable structures. These published values are based on scale model tests.

2) Prototype results show significantly higher wave run-up than small scale modelling results. The difference is the largest at smaller water depths.

The reasons, which cannot be quantified one by one, are:
• model effects
  - imperfect modelling of porosity and permeability (armour units and core material)
  - no wind in models
  - no current in models
  - imperfect modelling of sea bed topography

- imperfect modelling of target spectra
- limitations of some wave generators (stroke)

• scale effects: viscous effect (one side bias). These effects are important for thin water tongues on a rough hard surface and for porous flow.

Although wave run-up can be measured very accurately by the novel step gauge, too much spreading is seen on the different results. Factors responsible for these differences have been highlighted. The 2% wave run-up level cannot be considered as the key parameter to design the crest level of a rubble mound breakwater. However, wave run-up levels can to some extent be linked to wave overtopping discharges in order to define a crest level height based on an agreed and allowable wave overtopping discharge. The overtopping discharge should be the criterion to determine the crest level of a rubble mound breakwater.

TASK 5: OPTIMISATION AND CALIBRATION OF NUMERICAL MODELS

5.1 Introduction

Preparative work on Task 5 has been reported in Annex XI of the *"Full Progress Report To+12→To+24 (MAS03/999)"*. This report contained a critical review of the state-of-the-art of numerical modelling of wave impact on coastal structures with emphasis on a description of the capabilities and limitations of the models operated by the partners involved in this task. The theoretical review included the following aspects:

a. Analysis of the equations governing fluid motion, together with some simplifications and specific treatments for dealing with arbitrary free surfaces (such as the Volume-Of-Fluid, abbreviated VOF technique);
b. Analysis of the existing formulations for porous media flow;
c. Turbulence modelling, particularly in the external flow;
d. Boundary conditions, particularly wave boundary conditions and boundary conditions for the turbulence-related variables.

The numerical models operated by the partners within the OPTICREST Numerical Work Group (NWG) are of two different types: 1D models and 2D models. The 1D models (ODIFLOCS by DH and FLOx by AAU) are based on adaptations of the shallow-water equations, together with treatments for the internal flow that were developed from porous media flow theory. The 2D models (2D-HYDROTUR/IH, NASA-VOF2/IH-version, SKYLLA/DH, VOFbreak^2/UG and a new refined code/UG) are more general but much more expensive. In this type of model, the position and time-evolution of the free surface is described by means of the VOF method, and the treatment of the internal flow is again based on developments based on the theory of flow through porous media. Some 2D models can treat both internal and external flow, whereas other models lack this capability. The 1D models have been used more as practical tools, whereas the 2D models have been regarded as research tools that require improvements in order to enhance their practical value.

Data from two prototype structures (the impermeable Petten sea dike and the permeable Zeebrugge breakwater) and from a physical scale model (the LWI dike) have been used for validation of the numerical simulation of wave interaction on and in the coastal structures that have been investigated in OPTICREST. The programme for the numerical simulations has been focussed on three different problems:

a. Simulation of the Petten sea dike;
b. Simulation of the Zeebrugge breakwater;
c. Simulation of the 1:6 LWI dike.

The study of the 1:6 dike is important because it provides a good test case for comparing the existing models in a situation involving only the external flow and a simple geometric layout. The

other two series of numerical computations have been application studies; one dedicated to the calculation of wave run-up on an impermeable structure (Petten) and the other to the coupled internal-external flow (Zeebrugge). The number of simulations to be performed, as well as the specifications for each simulation have been described in detail in Annex XI of the *Full Progress Report To+12→To+24 (MAS03/999)* on Task 5.

5.2 Results of the research topics

a) Implementation of turbulence models

The dissipation of wave energy due to turbulence generated by wave breaking and the friction with the solid or porous boundaries plays a key role in run-up and overtopping on coastal structures. In this perspective, the introduction of turbulence and friction effects is necessary to achieve a consistent calibration of the numerical models.

In the report *"Implementation of turbulence models"*, enclosed as Annex 5.1.a, practical guidelines on the implementation of turbulence models in VOF-based mathematical models for solving free surface flow problems have been presented. The information in the report extends the review presented in section 2.5 and 2.6 of Annex XI of the *Full Progress Report To+12→To+24 (MAS03/999)*, and includes more specific hints and items that are useful for code implementation in VOF-type models.

The methodology proposed is based on incremental step-by-step implementation of 0-equation (algebraic), 1-equation and 2-equation models. Boundary conditions for both the mean flow equations and the turbulence related variables have been discussed. This approach is used in the NASA-VOF2D model (IH version). The improvements in the physical description of the external flow have been tested on the VOF model operated by the IH, and applied to the calculation of overtopping and run-up in the 1:6 dike and Petten-problem.

The modelling of the internal flow, and the modelling of turbulence in connection with internal/external flow coupling have not been considered. This later issue is seldom discussed in the literature, and involves extra difficulties, e.g. the compatibility between the representations of turbulence transport phenomena in the internal and external flow regions.

b) An active wave generating-absorbing boundary condition for VOF type numerical model

Wave boundary conditions required for generation and absorption of the waves in the computational domain have been developed for the specific use in the numerical VOF models. In Annex 5.3, chapter 2 *"An active wave generating-absorbing boundary condition for VOF type numerical model"* describes the implementation of an active wave generating-absorbing boundary condition for a numerical model based on the Volume Of Fluid (VOF) method for tracking free surfaces. A new type of numerical boundary condition for combined wave generation and absorption in the numerical model VOFbreak[2] is presented (figure 51). It is based on an active wave absorption system that was first developed in the context of physical wave flume experiments using

a wave paddle. The method applies to regular and irregular waves. Velocities are measured at one location inside the computational domain. The reflected wave train is separated from the incident wave field in front of a structure by means of digital filtering and subsequent superposition of the measured velocity signals.

The incident wave signal is corrected, so that the reflected wave is effectively absorbed at the boundary. The theoretical derivation and practical design of the digital filters used in the active wave generating-absorbing boundary condition have been discussed. Compared to the performance of the system in physical wave flumes the numerical boundary condition has numerous specific properties which increase significantly the performance of the active wave absorption system in a numerical model. The effectiveness of the active wave generating-absorbing boundary condition has been proved using analytical tests and numerical simulations with VOFbreak^2.
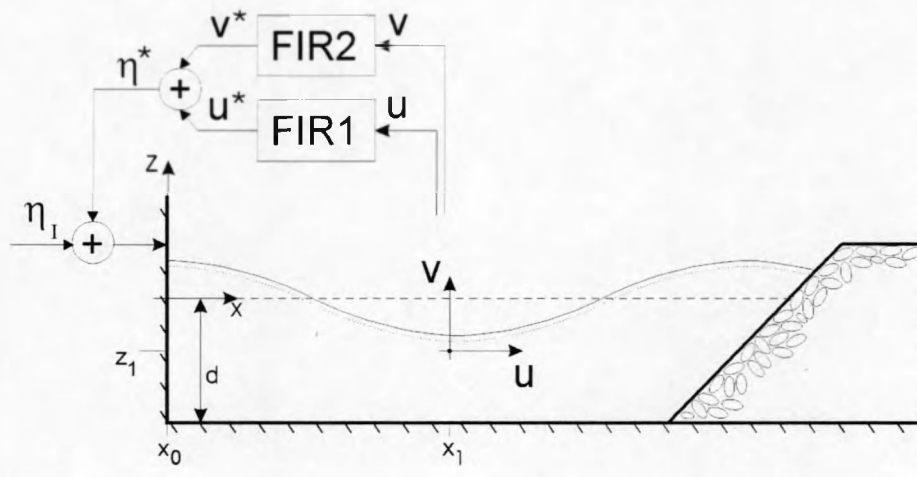
Figure 51: Definition sketch of the numerical wave flume set-up and the principle of the active wave generating-absorbing boundary condition.

5.3 Results of the numerical simulations

a) Results for the Petten sea dike

a.1) Numerical model investigations on coastal structures with shallow foreshores using SWAN, TRITON and ODIFLOCS

Annex 5.2 *"Numerical model simulations of wave propagation and wave run-up on dikes with shallow foreshores"*, describes comparisons between test results from the two-dimensional physical model tests of the Petten sea dike and numerical model computations. For the numerical computations use is made of the spectral wave model SWAN, the time-domain Boussinesq-type wave model TRITON, and the ODIFLOCS model, a time-domain model based on the non-linear shallow water wave equations.

These three numerical models have been applied and linked for the validation of wave interaction with the Petten dike, including the shallow foreshore and wave breaking in a situation with a berm. Applying the models together leads to accurate predictions of wave run-up levels for the present data set. The spectral wave model SWAN used for wave propagation of short waves over the foreshore yields small underestimation of the wave parameters at the toe of the dike (13% for H_{m0} and 21% for $T_{m-1,0}$). The time-domain model TRITON used for wave propagation over the foreshore shows accurate results for both H_{m0} and $T_{m-1,0}$ (deviation below 10%). Application of the ODIFLOCS model using measured surface elevations from incident waves, shows good agreement for wave run-up levels (on average 10% underestimation). Recommendations have been formulated for further improvements.

a.2) Numerical simulations using SKYLLA

The VOF-model SKYLLA has been applied to compare the computed wave breaking process with the measured one in the 2D tests on the Petten sea dike. The plunging waves were reproduced accurately in the computations, including the overturning wave tongue, the wave tongue hitting the impermeable smooth slope and the bouncing back from (upward motion) the slope. The numerically obtained wave run-up levels were systematically underestimated. Although the modelling of the wave breaking process is essential in the comparison with measurements to actually compare similar wave conditions, rather than comparing wave run-up levels belonging to different wave conditions, the dissipation in the thin wave run-up tongue apparently is too large in the computations.

For different dike-geometry also wave overtopping discharges were compared to results from physical model tests of the LWI dike. These wave overtopping discharges were overestimated, although differences are in the range where common scatter occurs in wave overtopping data from physical model tests. In general it is concluded that the model computes realistic wave breaking process, that reasonable wave overtopping discharges are computed but that dissipation in thin water layers is too large which causes underestimates of wave run-up levels.

a.3) Numerical simulations using the IH version of NASA-VOF2D

A numerical study of wave run-up/down and free surface configuration on the Petten sea dike using the IH version of NASA-VOF2D is presented in Annex 5.1.c *"Numerical simulation of wave run-up on Petten dike"*. The Petten dike is not overtopped except for very exceptional circumstances, and is impermeable. Four simulations involving regular waves only have been performed for different values of the wave period, namely T = 6 s, 8 s, 10 s and 12 s.

On the left boundary of the computational domain, the velocity and free surface elevation were specified using Fenton's approach. On the right boundary the free-outflow boundary condition was imposed. However, fluid is not expected to reach the right boundary. On the segments of the slope, a free-slip boundary condition was imposed. This can be considered a reasonable approximation, but some effort needs to be placed on the derivation of realistic wall friction models (in connection

with turbulence modelling) for this problem, in view of the key role played by wall friction on the run-up/down phenomenon.
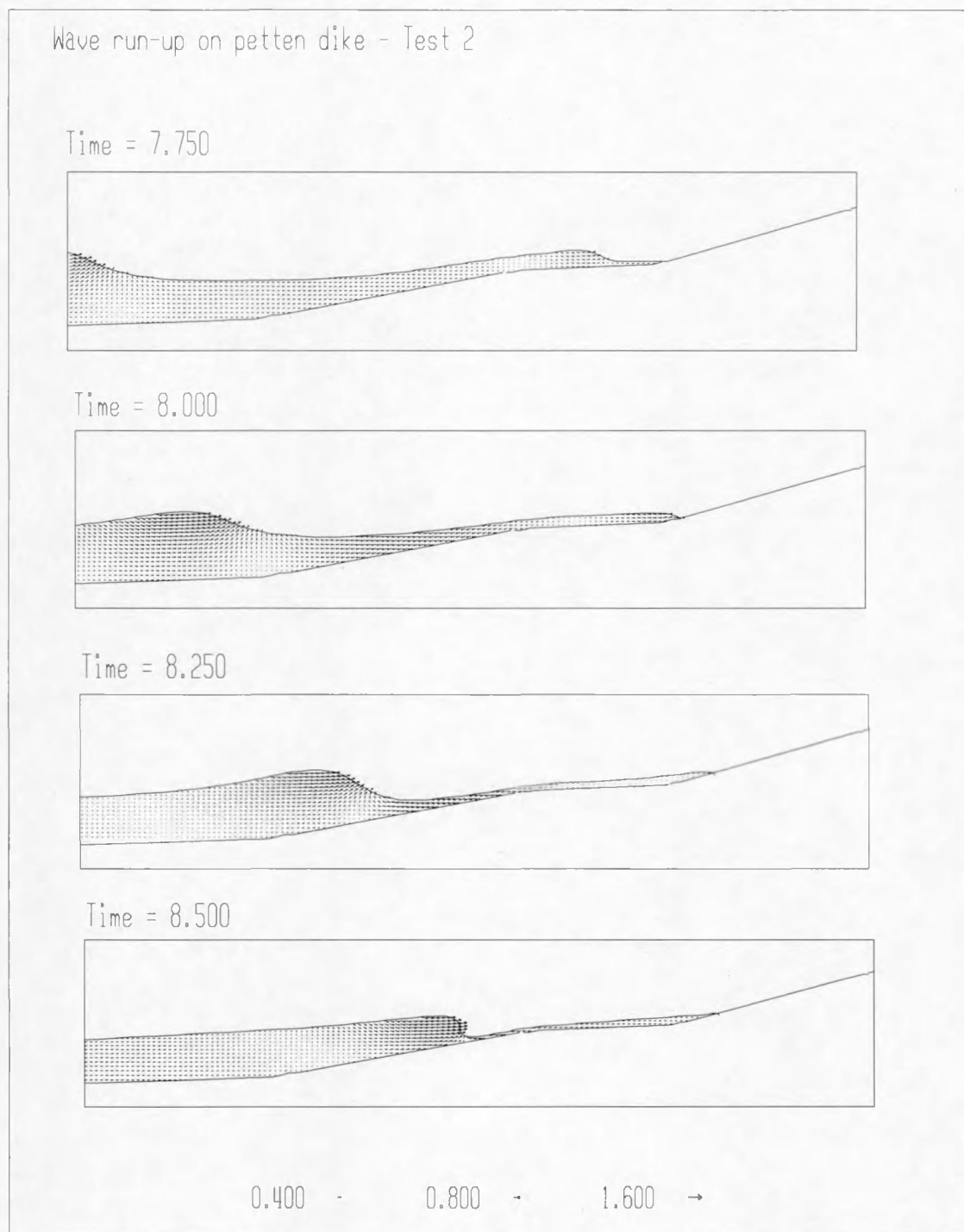
Figure 52: Results from numerical simulation of the Petten sea dike using NASA-VOF2D/IH-version: time sequence of the velocity field for test 2 using H = 4.0 m, T = 8.0 s.

Figure 52 illustrates a typical time sequence of the instantaneous velocity field and the free surface configuration, for four different stages of the wave interaction with the Petten sea dike (for test 2

with H = 4.0 m, T = 8.0 s). From figure 52 it is observed that breaking occurs close to the berm, affected by a strong return flow. A wave reformation takes place after the breaking point and over the berm (top graph in figure 52).

In Annex 5.1.c, the time histories of the maximum elevation attained by the water surface (=wave run-up levels) are shown. A strong and regular oscillation over the step gauge slope is observed. The interaction between the reflected waves and the inflow boundary is apparent in the pattern obtained. However, the interference effect is just a small and periodic variation in the amplitude of the run-up level oscillation.

It is concluded that the mathematical model provides a useful description of wave run-up/down, representing the details of wave breaking – breaking point, free surface configuration, wave overfolding, wave reformation and the interference between the breaking wave and the return flow. The time history of the frontwave vertical position shows that the run-up increases significantly when the wave period goes from 6 s to 10 s. For higher periods it is expected that this systematic increase should not be observed since there is a strong energy dissipation at the breaking point.

b) Numerical simulations of the Zeebrugge breakwater

b.1) Introduction

In Annex 5.3, chapter 3 *"Experimental study and numerical modelling of pore pressure attenuation inside a rubble mound breakwater"*, the wave interaction with the Zeebrugge breakwater is studied using experimental (prototype and physical model) data and using the numerical model VOFbreak^2. The main objective is to study the attenuation of the wave induced pore pressures inside the core of a rubble mound breakwater. The exact knowledge of the distribution and the attenuation of the pore pressures is very important for the design of a stable and safe breakwater. Until now no tools have been presented for the detailed determination of the pore pressures and the related porous flow field in the breakwater core.

b.2) Experimental study

Based on a theoretical background, an exponential damping model is derived for the attenuation of the pore pressure height inside the breakwater core. The attenuation is governed by a damping coefficient δ. The experimental study has been based on two data sets. The prototype data have been acquired at the Zeebrugge breakwater. From the analysis of the prototype data, it is concluded that the theoretical damping model fits well, and damping coefficients have been obtained. The large scale physical model data, taken from literature, have been re-analysed in detail. Again good agreement with the theoretical damping model has been found, and damping coefficients have been obtained. Based on the experimental study, a calculation method has been proposed for the determination of the attenuation of the pore pressure heights inside the breakwater core. The consecutive steps have been presented in detail. The calculation method will be very useful for applications where information about the pore pressure distribution or the porous flow velocities is required, such as slope stability analysis or a new scaling method for physical small scale models.

b.3) Numerical study

(1) Validation of numerical wave flume using physical model tests

Physical model test data have been acquired in a wave flume at Aalborg University (Denmark) for the validation of the wave interaction with a breakwater. The test set-up included a relatively simple breakwater lay-out with a vertical front wall and a core of homogeneous rock (porosity n = 0.426, mean grain size d_{50} = 0.0181 m), figure 53.
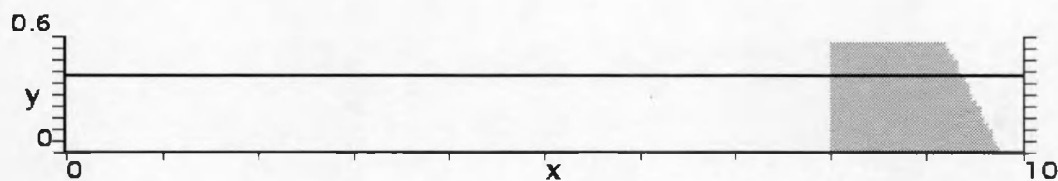
Figure 53: Geometry of the wave flume set-up, with wave generation and absorption at the left boundary (x = 0) and the breakwater near the right boundary.

The numerically calculated pore pressures inside the core are compared with the pore pressure measurements from the physical model at five positions on two horizontal levels. Figure 54 shows an example of the validation results for one test (reg10h), at two horizontal levels y' resp., for incident regular waves (H = 0.06 m, T = 1.80 s). In this case the viscous friction term is neglected and only turbulent friction losses are accounted for in the Forchheimer porous flow resistance model.

The solid and dashed lines in figure 54 indicate the fitted theoretical exponential damping model through the experimental and the numerical data resp., from where the damping coefficient δ is obtained and plotted in figure 54. It is clear from figure 54 that very good agreement is found between the physical model test data and the numerically calculated data. From these results it is concluded that the numerical model VOFbreak^2 is capable of simulating the wave interaction with a simple breakwater.
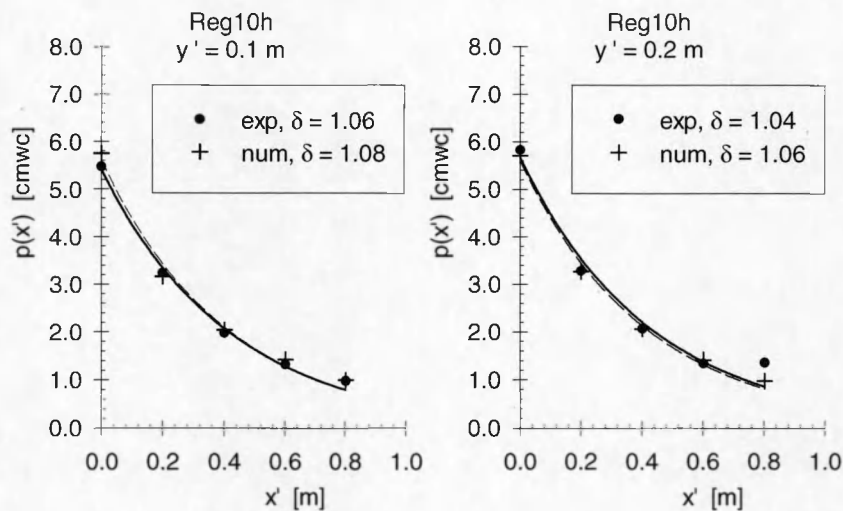
Figure 54: Distribution of pore pressure heights $p(x')$ versus position x', for two levels at resp. depth $y' = 0.10$ m and $y' = 0.20$ m, calculated from physical model tests (exp) and numerical simulations (num) resp., for test reg10h.

(2) Numerical modelling of wave interaction with Zeebrugge breakwater

The Zeebrugge prototype breakwater has been tested in the numerical wave flume VOFbreak[2]. A number of approximations have been used. The bathymetry in front of the breakwater is simplified by using a constant water depth d = 8.0 m. The incident waves are regular waves with wave height H = 3.0 m and wave period T = 8.0 s. The AWAVOF wave absorption system is switched on. The considerable energy dissipation in the armour and filter layers is modelled by using a layer on top of the breakwater core with higher permeability than the core material.

Figure 55 shows the numerical set-up with the wave generation/absorption system AWAVOF at the left boundary (x = 0 m) and the Zeebrugge breakwater with simplified geometry near the other boundary. At the right boundary (x = 160 m) a passive wave absorption system is installed. The simulation is started from still water conditions.
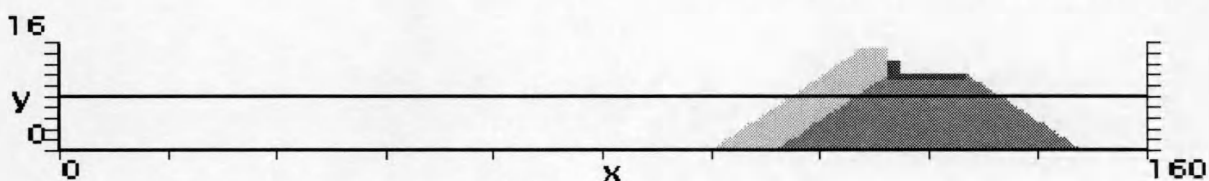
Figure 55: Geometry of the numerical wave flume set-up, with wave generation and absorption at the left boundary (x = 0) and the simplified Zeebrugge breakwater near the right boundary (non-distorted scales).

Figure 56 shows the resulting free surface position in front of the breakwater, in the armour layer and in the core from the simulation at t = 122 s (run-down) and t = 127 s(run-up). Inside the armour layer the energy dissipation of the wave action and the damped movements of the free surface are observed. The variation of the water level in the core is even more attenuated resembling the working principle of a breakwater.

Finally in figure 57 a snap-shot of the detailed calculated flow field in the zoomed area around the breakwater slope is given for the case of wave run-up at t = 127 s. Figure 57 shows the velocity vector field, the isobars and the position of the free surface. It is clearly perceptible that during wave run-up both infiltration (near the free surface) and seepage (near the bottom) occur at the same time along the slope. The wave interaction therefor cannot be reduced to one dimension.

The work presented in this section is a combination of theoretical, experimental and numerical work in order to study the wave induced pore pressures in the breakwater core. Hopefully it will be a clear contribution to the design tools related to rubble mound structures.

(a) wave run-up at t = 122 s

(b) wave run-down at t = 127 s
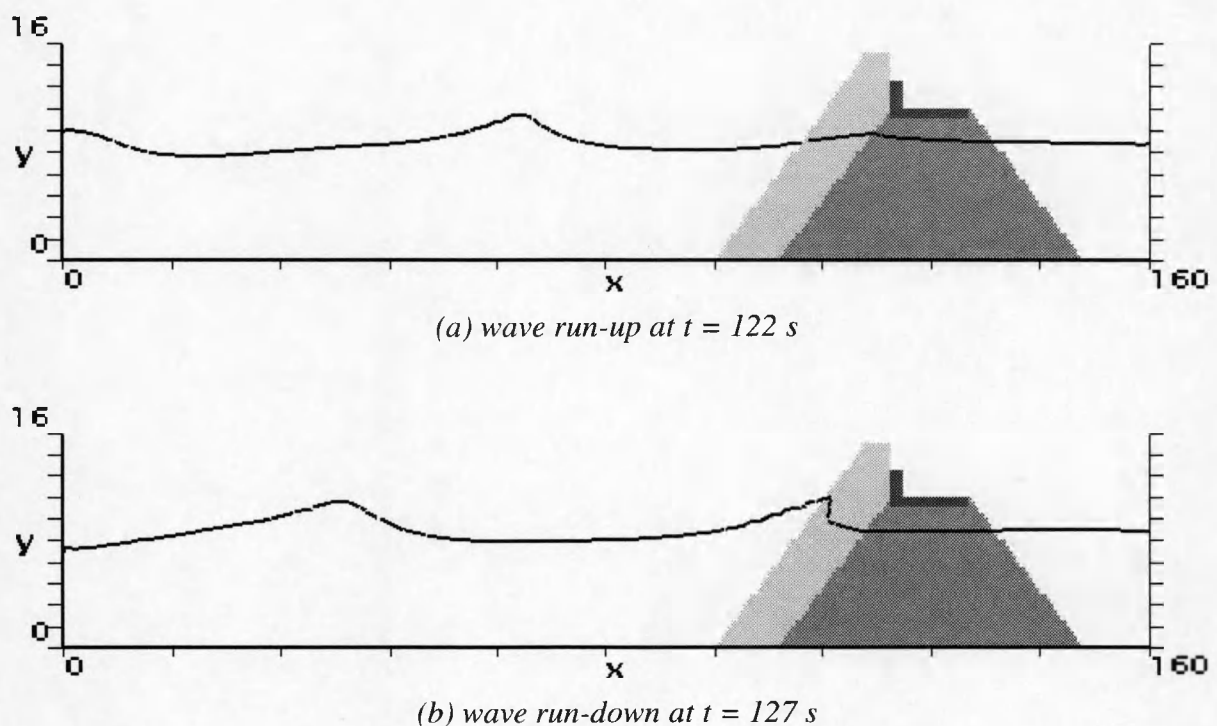
Figure 56: Results from numerical simulation with Zeebrugge breakwater at t = 122 s and t = 127 s, showing the free surface in front of the breakwater, in the armour layer and in the core (distorted scale in y direction using factor 2).
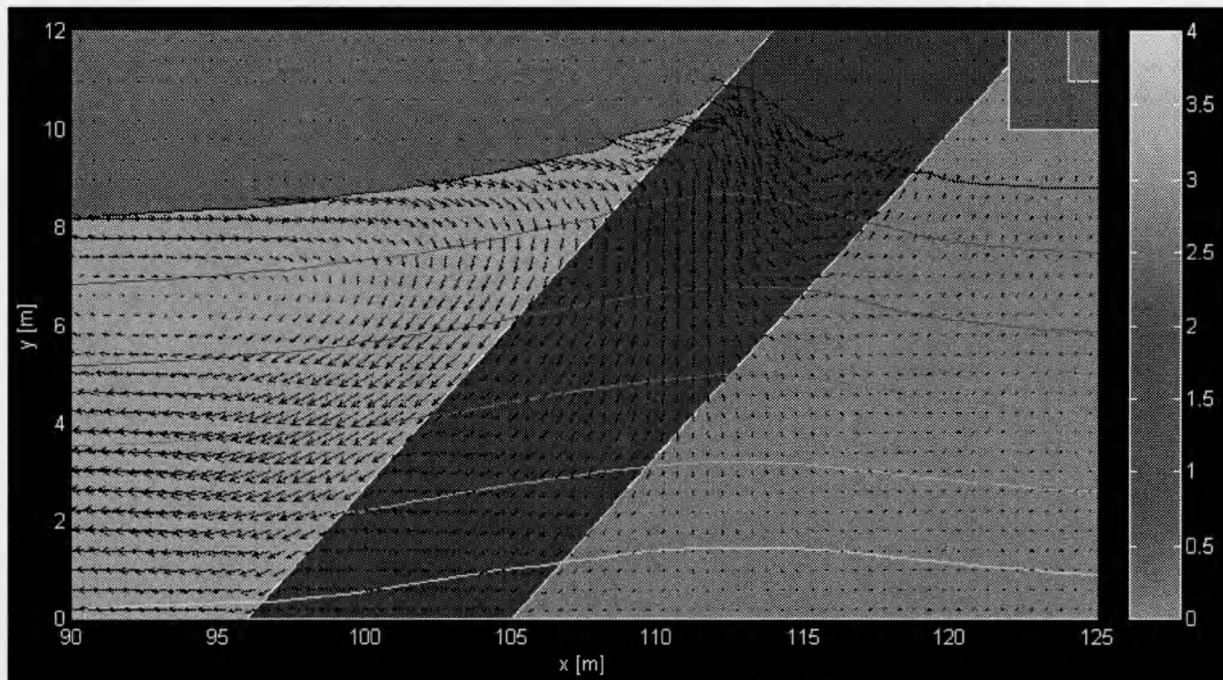
Figure 57: Zoom of calculated flow field near the breakwater slope during wave run-up at t = 127 s.

c) Numerical simulations of the LWI dike

c.1) Introduction

Physical model tests on a smooth impermeable sea dike have been performed in the small wave flume of LWI as part of Task 3.5 (Crest stability). The model tests have been executed using regular and irregular waves for a sea dike with varying seaward and landward slopes. Measurements from layer thickness, overtopping velocities, individual overtopping volumes and average overtopping rates are available for use in the numerical simulations.

The test case with a seaward slope of 1:6 and a landward slope of 1:3 has been selected within OPTICREST Task 5 for numerical simulations using all numerical models. The numerical study of the LWI dike is important because it provides a very good well-documented test case for comparing numerical models in a relatively simple situation involving only the external flow on the impermeable dike and a simple geometric lay-out.

The geometry for the numerical simulations is taken from the reports on Task 3.5 and Task 5 by LWI (Schüttrumpf and Bleck, 1998; Oumeraci et al., 1999). The selected test case of the sea dike is shown in figure 58. The seaward (or outer) slope is 1:6, the landward (or inner) slope is 1:3. The crest height is 0.80 m. The crest and both slopes are impermeable and smooth to the external fluid flow.

In the physical model tests the water depth d was varied from 0.60 m to 0.80 m. The wave height H was varied from 0.08 m to 0.20 m and the wave period T from 1.5 s to 6.0 s (for regular waves). For the numerical simulations, the default water depth d = 0.70 m has been selected.
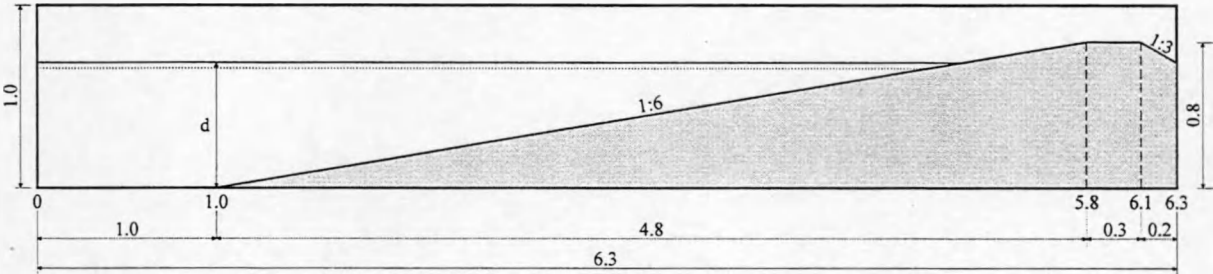
Figure 58: Cross section of the LWI dike cf. physical model tests at LWI (taken from Oumeraci et al., 1999).

The test programme for the numerical simulations is defined cf. the agreed test programme in the first progress report on Task 5 (Lemos and Troch, 1999) and cf. the test programme used for validation of the ODIFLOCS code by LWI (Oumeraci et al., 1999). Table 25 summarises the basic test programme that has been carried out for the numerical calculations of the LWI dike.

Table 25: Test programme for numerical simulations of the 1:6 LWI dike, including wave characteristics H, T, water depth d, surf similarity parameter ξ_0 and average overtopping rate q_{lab} (taken from Oumeraci et al., 1999).

	Test No.	H [m]	T [s]	d [m]	ξ_0 [-]	q_{lab} [l/sm]	LWI Test No.
1	1	0.155	1.959	0.70	1.0	**3.33**	A13
2	2	0.117	2.446	0.70	1.5	**2.32**	A09
3	3	0.119	3.154	0.70	1.9	**5.79**	A10
4	4	0.121	4.150	0.70	2.5	**8.59**	A11
5	2_75	0.117	2.446	0.75	1.5	**7.51**	C10
6	2_80	0.117	2.446	0.80	1.5	-	-
7	2*_80	0.082	2.503	0.80	1.8	**11.82**	B05

Table 25 includes, for each of the 7 tests, the wave characteristics (wave height H and wave period T for a regular wave), the water depth d, the surf similarity parameter $\xi_0 = 1/6\left/\left(2\pi H/gT^2\right)^{0.5}\right.$ and the average overtopping rate q_{lab} as measured in the physical model tests at LWI.

Tests 1, 2, 3 and 4 are four tests where the surf similarity parameter increases from 1.0 to 2.5 in steps of 0.5. These tests make up the test case that is simulated by all numerical models in OPTICREST. Additionally the water depth is increased in tests 2_75, 2_80 and 2*_80 (note that for test 2_80 no physical model results are available) in order to study the influence of water depth and induced variation of overtopping volumes on the calculation results of the new refined code.

<u>c.2) LWI simulations of the LWI dike using ODIFLOCS</u>

The results of an extensive numerical study of the wave interaction with the LWI dike using ODIFLOCS is presented in Annex IX *"Wave overtopping at seadikes, comparison of physical model tests and numerical computations"* of the *Full Progress Report To+12→To+24 (MAS03/999)*. A full calibration of the ODIFLOCS model was performed.

Although the model failed to reproduce realistic overtopping rates in some cases, it is concluded that ODIFLOCS is a useful engineering tool for predicting overtopping. The results of this study have been summarised in figures 59 till 61. Figure 59 shows no significant improvement was achieved by replacing the computed regular waves by measured waves. Figure 60 shows that in most tests the computed layer thickness is higher than the measured layer thickness. No significant difference can be seen between the application of an average friction coefficient f=0.015 and the exact values. For the overtopping velocity it makes a difference whether the average or the exact value for the friction coefficient is used for the computation (figure 61). In general the difference between computed and measured overtopping velocities is larger than the difference in computed and measured layer thicknesses. Also the standard deviation is higher for the overtopping velocities than for the layer thicknesses. The explanation for this has to be found in the time series of overtopping velocities.

The 1D model ODIFLOCS can only provide a crude representation of important physical phenomena, such as the dynamics of the wave breaking front, the formation of the up-/ and down-rushing laminas of fluid above the slope, and the pressure and shear stresses created by the overtopping waves. Therefore, the prospects of 1D models for the calculation of critical quantities that depend on the details of such phenomena is limited. The question remains if 2D (in the vertical x-z plane) VOF – type models are capable of a better representation of the physical phenomena that occur when the waves overtop the structure, and consequently of producing better predictions of the critical quantities.
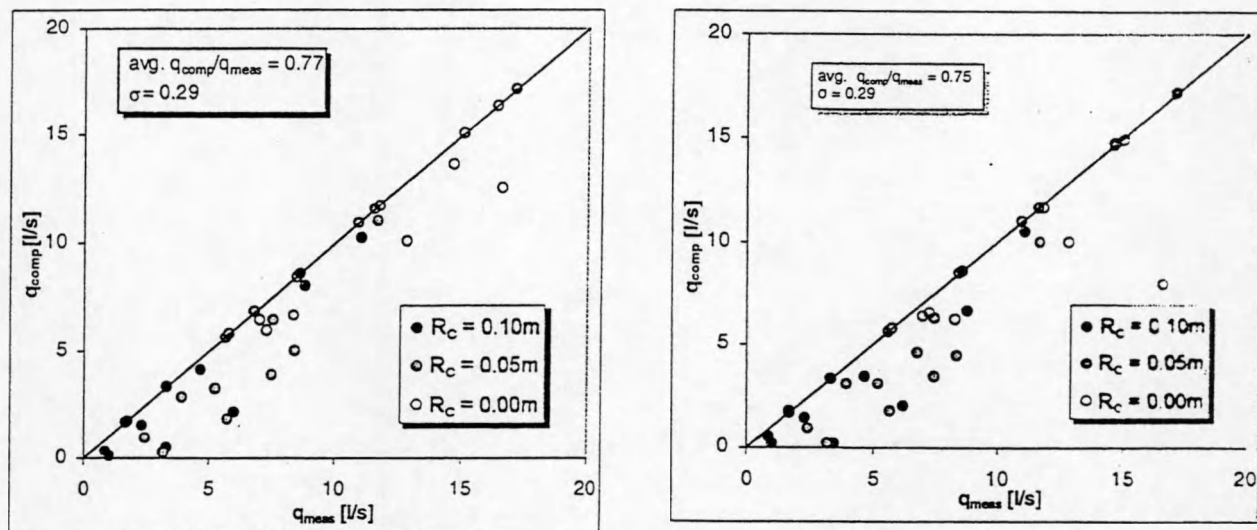
Figure 59: Ratio of measured to computed overtopping rates for (left) computed regular waves by ODIFLOCS and (right) measured regular waves at the toe of the dike in the physical model.
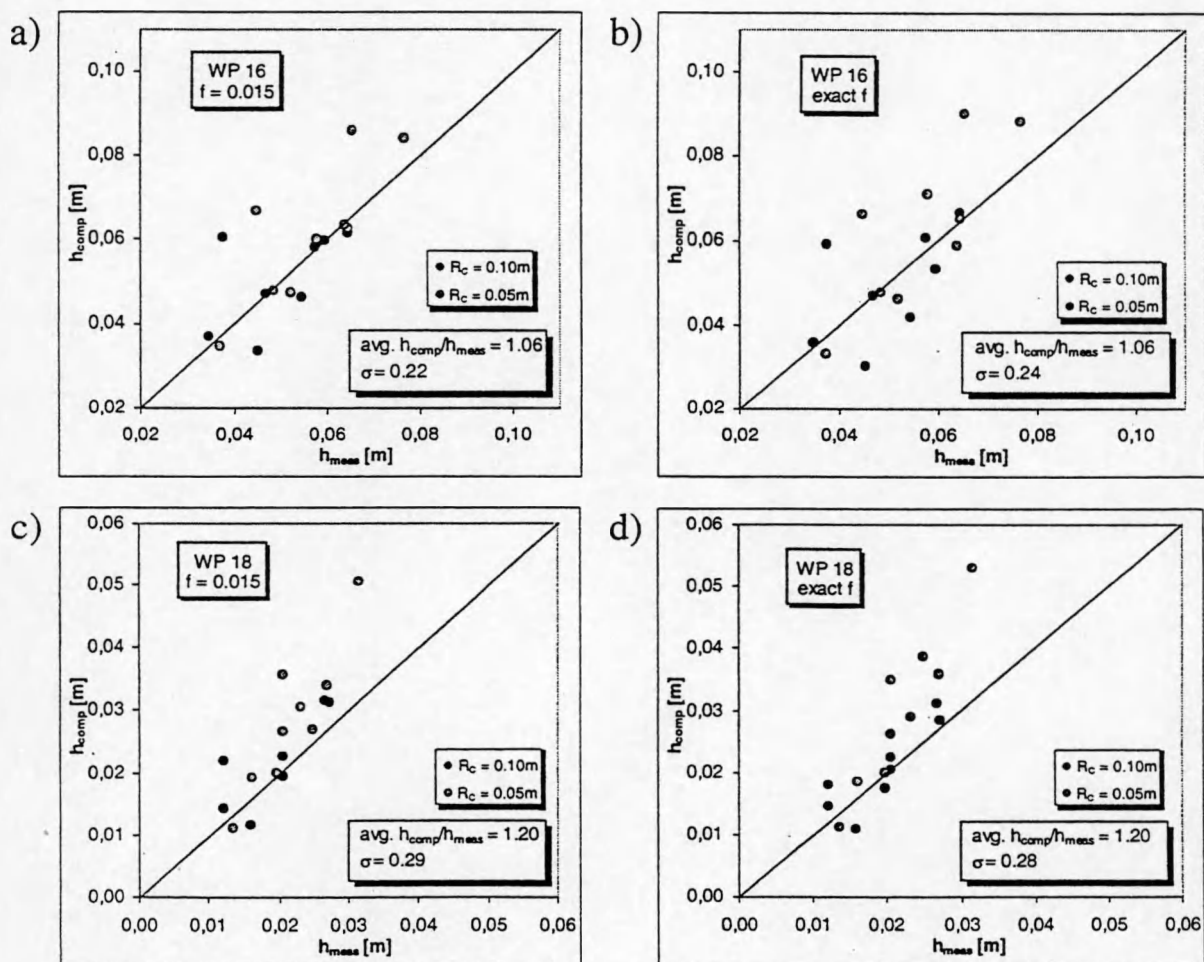
Figure 60: Comparison of computed and measured layer thicknesses.
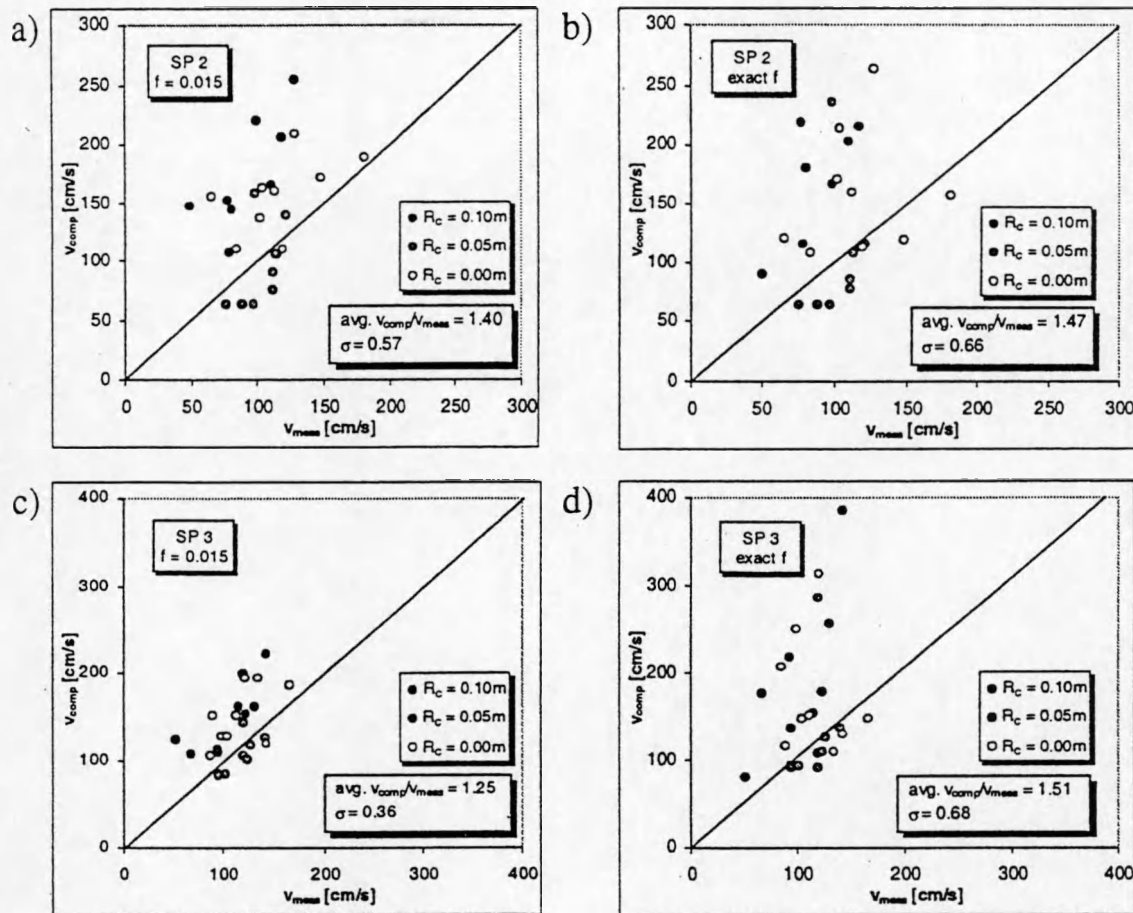
Figure 61: Comparison of computed and measured overtopping velocities.

c.3) IH simulations of the LWI dike using NASA-VOF2D/IH-version

In Annex 5.1.b *"Numerical simulation of overtopping on a 1:6 dike"*, a numerical study of wave overtopping on the 1:6 LWI dike is presented using the numerical model NASA-VOF2D/IH-version, for four different values of the surf similarity parameter, namely ξ = 1.0, 1.5, 1.9 and 2.5 (i.e. the first four tests of Table 25).

On the left boundary, the velocity and free surface elevation were specified using Fenton's numerical approach. On the right boundary, placed after the short section of the inner slope, the free-outflow boundary condition was imposed. On the bottom boundary, to the left of the dike's toe, free-slip boundary conditions were imposed. Free-slip boundary conditions were also imposed on the segments of the slope. This can be considered a reasonable approximation, but some effort needs to be placed on the derivation of realistic wall friction models (in connection with turbulence modelling) for this problem, in view of the key role played by wall friction on the overtopping phenomenon.

Figure 62 shows the instantaneous velocity field and free surface configuration at four different stages of the wave transformation along the outer slope, for test 2. The attacking wave breaks close to the dike's crest, and the wave overfolding is reinforced by a thin down-rushing lamina of fluid (top). The overtopping lamina is thick and massive, resulting in a large overtopping rate (second

and third images). A return flow is then formed, which interacts with the next approaching wave (bottom).
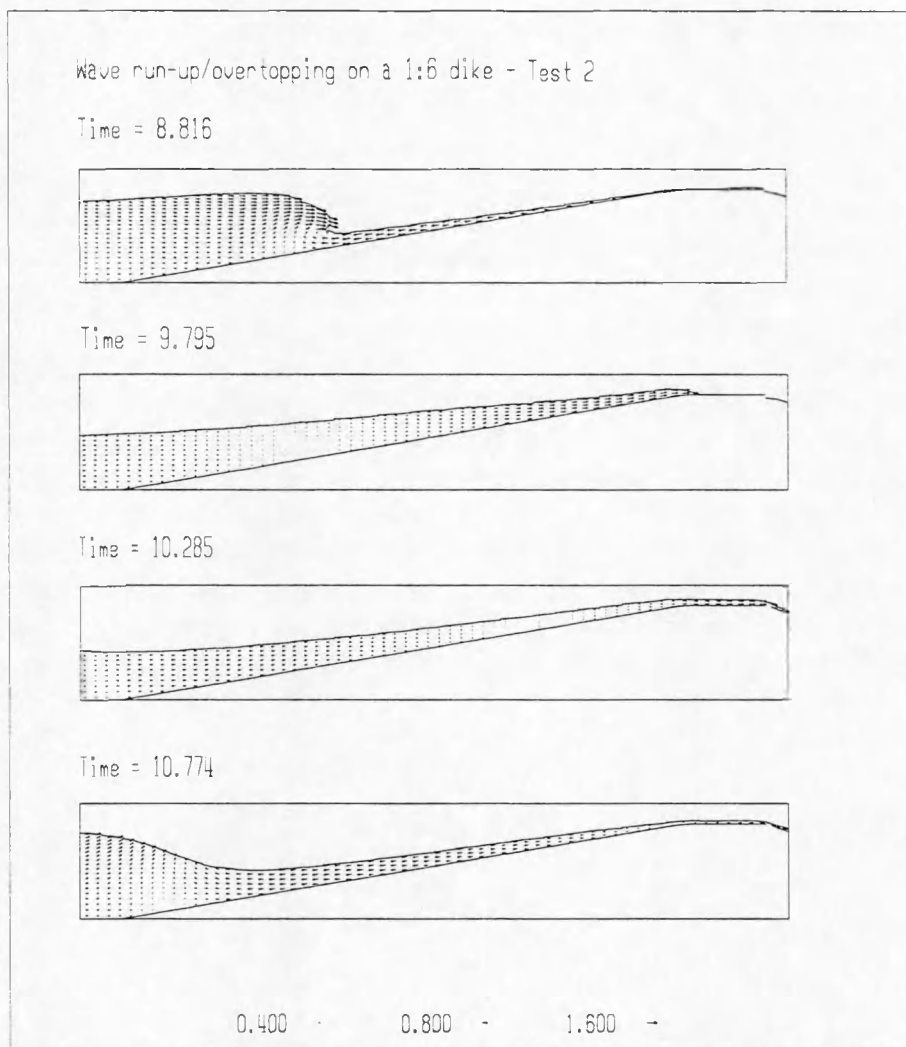
Figure 62: Results from numerical simulation of the 1:6 LWI dike using NASA-VOF2D/IH-version: time sequence of the velocity field for test 2 using H = 0.12 m, T = 2.45 s.

From the time histories of the overtopped volume, layer thickness and the maximum overtopping velocity at the seaward and landward edges of the dike's crest, obtained in the simulations with uniform grid in the z-direction, it is concluded that the model failed to provide a coherent representation of the physical phenomena involved in overtopping. The qualitative evolution of the relevant quantities does not correspond to the physical processes, and the overtopping rates are in great error with respect to the values measured in the laboratory experiments. Also, there is a complete lack of correspondence between the time evolution of the flow at the seaward and landward crests. This suggests that the model is strongly affected by numerical errors in the critical region of the flow (i.e. above the dike's crest). To overcome this faulty behaviour, the model was run with a non-uniform grid with smallest spacing at the level of the dike's crest. The model provided a realistic time-history of the overtopping velocity at the seaward crest, and it can be observed that the peak values of the velocity at the landward crest follow closely those at the

seaward crest. The residual minimum velocities are due either to numerical errors or to some influence of the artificial outflow boundary. The quantitative values of the relevant variables are much closer to those obtained in laboratory experiments.

The computed overtopping rates were larger than those obtained in the laboratory experiments, in the four tests. The discrepancy was larger for test cases 1 and 2 (58% and 100% respectively) than for test cases 3 and 4 (26% and 35% respectively). These discrepances are attributed mainly to the approximate nature of the free surface boundary conditions, which affect the critical region of the flow (thin up- and down-rushing laminas and the overtopping laminas over the dike's crest), and to the use of free-slip conditions instead of a well-calibrated wall friction law.

It is concluded that the mathematical model provided a useful description of the physical phenomena involved in wave overtopping on the dike's crest. The specific details of each test case were well captured, particularly the relationship between the critical quantities – overtopping rate, maximum velocity and layer thickness – and the breaking point, free surface configuration at breaking conditions and interference between the breaking wave and the return flow down the slope.

c.4) UG simulation of the LWI dike using VOFbreak^2 and a new refined code

(1) VOFbreak^2 results

Annex 5.3, chapter 4 *"Numerical simulation of laboratory tests of the LWI dike"* reports the results from numerical calculations of the LWI dike carried out by UG using the VOFbreak^2 model and a new refined code.

From the numerical simulations using VOFbreak^2 (on a uniform grid), e.g. for test 2 in figure 63, it is concluded that the physical process of wave overtopping is not simulated in a realistic way. No regular wave overtopping pattern at the crest is obtained, and there is no correlation between fluid flows in the two sections at the crest. The resulting overtopping rates underestimate considerably the overtopping rates measured in laboratory. The numerical model results are strongly affected by numerical errors in the critical regions of the flow, i.e. on the outer slope (slope friction induced by staircase modelling seems too high) and on the crest (flow in thin lamina not well discretised).

$t = 10.2\ s$ $t = 10.8\ s$
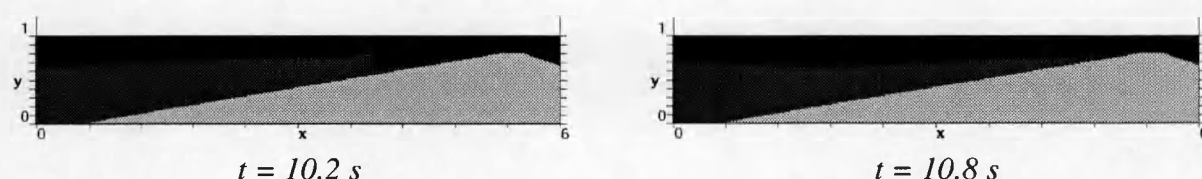
Figure 63: Typical results from test 2 using VOFbreak^2, **high** resolution grid, wave characteristics $H = 0.117$ m, $T = 2.446$ s, water depth $d = 0.70$ m. Free surface configuration and velocity field at 2 time intervals within one wave period

It is clear that VOFbreak^2, originally developed and calibrated for wave interaction with porous structures, requires modifications for the correct simulation of wave interaction with impermeable structures. These modifications concern the implementation of a technique for modelling slope boundaries through cells, the generation of non-uniform grids that allow high grid resolution in critical flow areas, and higher order upwind discretisation schemes for momentum convention.

However it is concluded to use a new state-of-the-art basic hydrodynamic VOF code that already includes these improvements and that has many more interesting features. This way no useless efforts are needed, but new developments can be concentrated on important and attractive coastal engineering modelling issues. This new refined code is presented in the next section.

(2) A new refined code

The new refined code that has been developed in the framework of the OPTICREST project is based on Ripple (Kothe et al., 1991), a 2D successor VOF code that incorporates the latest advances in numerical algorithms and parallel processing. It is straightforward to transplant the wave boundary conditions and the porous flow resistance model into this code without any tedious operations. As a result the new refined code is easily transformed into a numerical wave flume that has state-of-the-art features beyond the possibilities of the existing codes within OPTICREST.

The new refined code has been used for the 9 simulations of the test programme of Table 25. The test set-up shown in figure 58 is used, and is discretised using a non-uniform grid with highest resolution near the SWL (y-direction) and near the dike crest (x-direction). At the left boundary ($x = 0$) the incident regular waves are generated. The wave generation routines that are available from VOFbreak^2 have been used and transplanted into the new code. The bottom and top boundaries are modelled as free slip boundaries. The right boundary ($x = 6.3$) is modelled as free outflow boundary allowing the fluid to leave the computational domain without interaction with the wave run-up and overtopping processes.

Figure 64 shows a comparison of wave overtopping on the dike crest for test 2, 2_75 and 2_80 respectively, at $t = 9.0$ s (zoomed in order to see the details). For higher water depths (from $d = 0.75$ till 0.80) the layer thickness on the crest and the volume of overtopping water increases clearly.

The numerically obtained average overtopping rates q_{num} are compared to the average overtopping rates q_{lab} obtained from the physical model tests, for all tests. Comparing both q_{lab} and q_{num}, it is clear that there is an underestimation of the discharges in the numerical model. The underestimation ranges from $q_{num}/q_{lab} = 0.30$ for small overtopping volumes, till $q_{num}/q_{lab} = 0.71$ for large overtopping volumes. The deviation is largest for small q values and decreases for larger q values. However the relative magnitude of the discharges remains the same for all tests. The same ranking is found for the numerically obtained q_{num} - values, proving that the numerical results contain the logical physical behaviour and that the deviations are consistent, and not random. Taking into account the scatter present in obtaining the measurements of the overtopping volumes in the

physical model, it is concluded that this underestimation is not too bad, and that there is a reasonable agreement between physical model tests and numerical simulations.

Zoom   **LWI dike: Test 2, t = 9.0 s, d = 0.70 m, F variable**

LWI dike: Test 2_75, t = 9.0 s, d = 0.75 m, F variable

LWI dike: Test 2_80, t = 9.0 s, d = 0.80 m, F variable
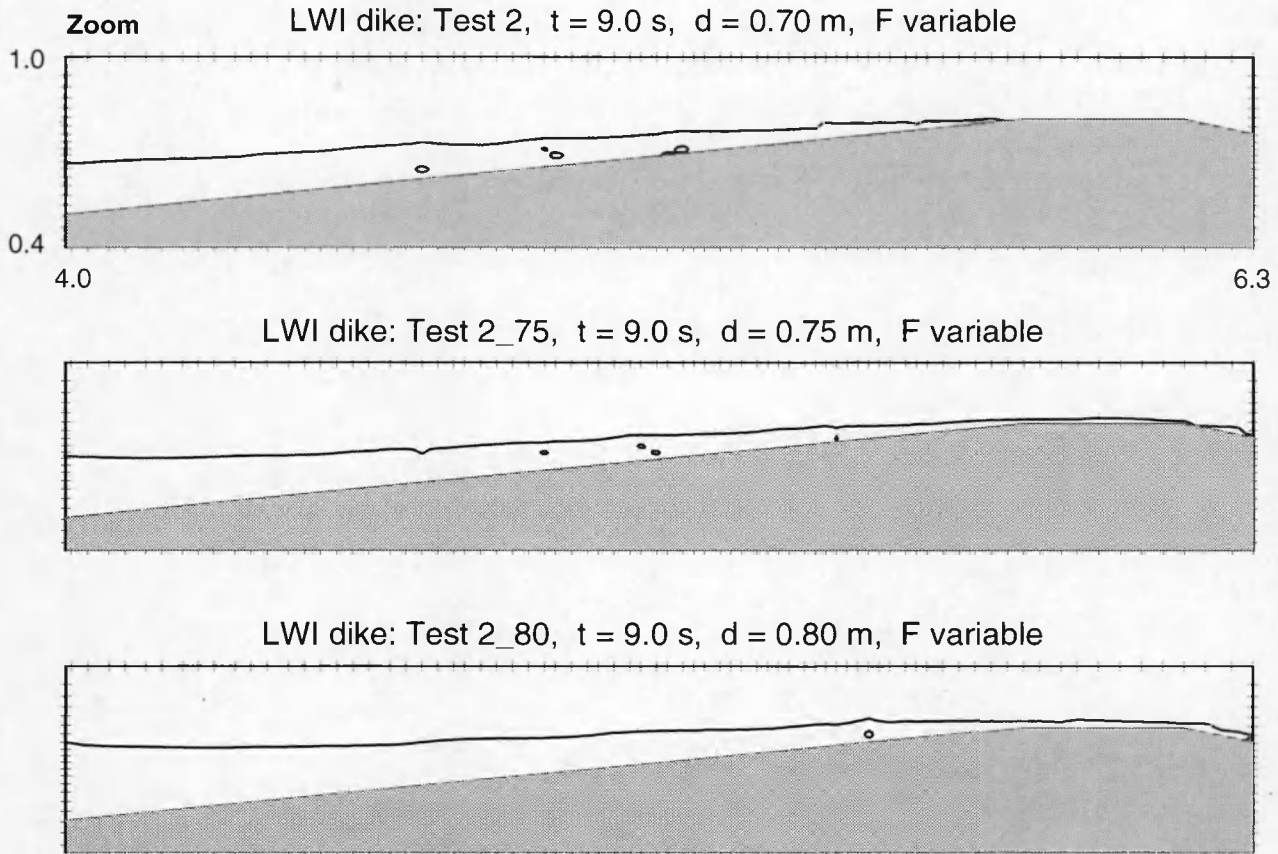
Figure 64: Free surface configurations (derived from volume fraction F) at time step $t = 9.0$ s, for a zoomed area near the dike crest, for test 2, test 2_75 and test 2_80 (i.e. for increasing water depth).

In order to test the sensitivity of the numerical results, the grid has been modified slightly. The same number of cells is used, but the discretisation in y-direction was modified in such a way that the SWL now coincides with the cell boundary. The numerically obtained value q_{num} increases considerably, from $q_{num} = 0.7$ to 1.82 for test 2 and from $q_{num} = 4.3$ to 6.34 for test 2_75. The underestimation observed in the previous results reduces considerably, with an even better agreement of $q_{num}/q_{lab} = 0.81$ on average.

From these simulations it is concluded that the choice of the computational grid is critical in obtaining good agreement with physical measurements, and that a lot of attention has to be paid to the definition of the grid.

TASK 6: EXPLOITATION AND DISSEMINATION OF RESULTS

The objective of this task was to work out into more detail the plan to exploit and disseminate results of the project starting from the exploitation and dissemination plan as described in the Technical Annex.

Project results have already been and will be presented at a number of international conferences. The papers cover all relevant project results. Results also have been and will be published in international journals. Project results are disseminated through posters, by the project website and the elaboration of data and results in PhD studies,... The project results will be made public through the 'coastal list' in early 2001.

A complete list of EC reports, publications in (peer reviewed) literature and specialist journals, publications in proceedings of international conferences,... is found in Annex 6.

A market analysis has been carried out and the end-users of the project results are defined. Two main groups are defined: the scientific world and the 'practical' world. They are and will be made aware of the project results by both soft and active promotion.

The two exploitation managers (J. De Rouck (Ghent University) and M. van Gent (Delft Hydraulics)) will supervise the execution of further exploitation plans during the first year after the end date.

Further research on both measuring sites will be continued. Various proposals have been submitted for national and international funded research.

A detailed overview of all results is given in the full scientific report (MAS03/1031). The project results have been checked if these meet the project objectives (MAS03/1178 *'Abstract of project objectives and results'*).

TASK 7: SYNTHESIS AND CONCLUSIONS

The subject, c.q. the objectives, of the OPTICREST-project are summarised to one statement in the full title. Indeed, in view of the crest level design, wave run-up is studied in detail on an impermeable sea dike and a rubble mound breakwater. For both structures prototype measurements, scale model tests and numerical modelling were carried out. Sea dike failures often are initiated by wave overtopping and following erosion of the inner slope. So, a clear attention was also paid to the hydraulic phenomena related to wave overtopping of sea dikes hereafter named "crest stability".
In this paragraph the main results obtained within OPTICREST are summarised.

7.1 Impermeable sea dike

Prototype measurements of incident waves and wave run-up have been performed at the Petten Sea-Defence which is a smooth sloping dike with a berm. 2D and 3D physical model tests have been carried out on scale 1:40.

a) Prototype measurements

The Petten sea dike is smooth and impermeable: it consits of a lower slope 1:4 (protected by basalt blocks), an almost horizontal berm of ca. 20 m and an upper slope 1:3.5 (protected by asphalt and asphaltic concrete).
The wave field at the Petten site is characterised by wind waves with severe wave breaking at the relatively shallow parts (bars) of the foreshore. The reliability of the instruments under heavy storm conditions has been demonstrated and together with the use of data verification techniques, this measurement campaign resulted in a valuable data set of wave dynamics and wave run-up. The use of a video camera during storm conditions also provided important information on processes, such as the short-crested nature of the waves, the influence of the groins on waves, and spatial variations in the wave run-up along the dike.

b) Physical modelling

Physical model tests show good agreement with storms measured in prototype. The non-dimensional wave run-up levels differ only 3.9% and 7.8% on average in respectively the 2D and 3D model tests compared to prototype measurements. Considering these observed differences it is concluded that the model effects and scale effects in the physical model tests were acceptably small and that wave run-up on an impermeable sea dike can be modelled correctly. The nature of the foreshore in Petten reduces the level of wave variability that can occur and so leads to the relatively good agreement between various results.

Differences in wave conditions and wave run-up levels in the three different measurement series were subject to further investigations. A large amount of energy was found within low frequency waves and this may cause an increase in wave run-up levels with respect to situations without heavy wave breaking (deeper water). Physical model tests (3D) indicated that the actual wave run-up

levels are not significantly affected by the short-crested nature of the waves. One reason for this is the fact that the nearshore bathymetry reduces the level of directional spreading near the dike. Therefore, short-crested waves became 2D waves at the structure. The 3D tests with directional spreading indicated that there is some influence of directional spreading but this influence appeared to be small compared to the common variations around the main trend.

Other findings of the physical model tests were that for measuring wave run-up levels a step gauge should be considered to be the optimal type of instrument, that wave reflection from the Sea-Defence affects the surface elevations considerably, and that low frequency waves contain a rather large percentage of the total wave energy.

Since the foreshore at the Petten Sea-Defence causes significant wave breaking, the amount of wave energy present at low frequencies is larger than for sites with a similar offshore wave climate, but without severe wave breaking at the foreshore. Therefore, it is recommended to study the effects of surf beat phenomena, the propagation of wave groups and their associated long wave motions, and their possible contribution to wave run-up more in detail.

Because the foreshore affects the wave conditions (e.g. height and kinematics of the incoming waves) and the subsequent wave run-up, it is of importance to know the topographical changes during storms and their effect on the waves and wave run-up. Consequently, the envelope of the sea bed level variations should be estimated as a basis for estimation of the incident waves. Therefore, it is recommended to measure and analyse the topographical changes of the foreshore during storms.

Besides wave run-up levels it is important to estimate wave overtopping for conditions which are more severe than those which are likely to occur in prototype within a single storm season. Therefore, it is recommended to study layer thicknesses (and possibly velocities), at the seaward slope during wave run-up. This information could then be used to estimate overtopping discharges during more severe conditions than those already measured in prototype.

Next to the Petten Sea-Defence investigation, also an extended series of tests were performed on a smooth 1:6 dike. Latter tests highlighted the influence of the foreshore and showed that care is needed when reduction factors for wave directionality and spreading are applied to wave run-up values as these parameters are highly influenced by local site conditions. Whereas the Petten site has a shallow foreshore which reduces the level of directional spreading in front of the structure such that wave run-up was is greatly influenced, the 1:6 dike had no foreshore and large reductions in wave run-up were observed. Wave obliqueness and directional spreading have the effect of reducing the magnitude of wave run-up from the equivalent longcrested direct wave approach situation. The combined effect of wave obliqueness and directional spreading on wave run-up was determined by considering the influence of each individually and multiplying the relevant reduction factors.

c) Crest stability

Maximum layer thicknesses and maximum velocities on the seaward slope, the dike crest and the inner slope were estimated on the basis of small scale and large scale model tests with smooth and semi-smooth (concrete) surfaces respectively.
No wind effect and no 3D effects have been included

For the estimation of maximum layer thickness and wave run-up velocity, a theoretical model has been developed on the basis of simplifications of the two dimensional Navier-Stokes equations and the continuity equation. The theoretical model was calibrated for wave run-up velocities for the moment when the water tongue at the top of the seaward slope has reached its maximum thickness.

Calculations and subsequent verification of overtopping discharge with irregular waves have been performed.
The results were limited to crest levels lower than the 2% wave run-up level because of limitations in the small scale model.

7.2 Rubble mound breakwater

The instrumented Zeebrugge breakwater is a conventional rubble mound breakwater consisting of a core (2-300 kg), an underlayer (1-3 ton) and a 25 ton grooved cubes armour layer. The seaward slope is approximately 1:1.5. The inner slope is covered by a sandfill. Prototype measurements were carried out on the Zeebrugge breakwater. Two 2D models (1:30) and one 3D model (1:40) were built. In the scale models the core has been scaled such that the hydraulic gradients were reproduced properly. The armour units in the top layer were placed according to the actual position in prototype.

a) **Prototype measurements**

Wave run-up was measured with a run-up gauge (RU) and with a so-called spiderweb system (SP). The following main conclusions are drawn:

(1) Mean dimensionless **wave run-up** values of respectively $\dfrac{Ru_{2\%}}{H_{mo}}$ = 1.76 (RU data) and 1.75 (SP data) were obtained when time series of 2 hours at high tide were considered. When the same high tide data were analysed in time series of 30 minutes, one finds $\dfrac{Ru_{2\%}}{H_{mo}}$ = 1.77 (RU) and 1.78 (SP), respectively. The value is almost independent of the measuring device and the length of the considered time series. This value is clearly higher than the published value, which was generally accepted and used for rubble mound breakwaters.

It has to be mentioned that this value is found for H_{mo} which is of the same order of magnitude as D_{n50} of the armour units. For the design storm of the Zeebrugge breakwater H_{mo} is almost two times D_{n50}.

The dimensionless wave run-up $\dfrac{Ru_{2\%}}{H_{mo}}$ increases to 2.24 (RU) at mean tide: so the dimensionless wave run-up increases with decreasing water level (i.e. decreasing water depth). This may also be influenced by the fact that at a lower water level, wave run-up occurs at a lower part of the breakwater armour layer which may have lower porosity, due to a settlement of the armour units.

For higher exceedence probabilities (5%, 10%,...) the $\dfrac{Ru_{x\%}}{H_{mo}}$ is less dependent on the water level.

The highest wave run-up occurs at rising tide (i.e. higher than at receding tide) for the same water level. This indicates some influence of the tidal current and/or the asymmetric tide.

Finally, prototype wave run-up results are Rayleigh distributed.

(2) **Wave run-down**, characterised by $\dfrac{Rd_{2\%}}{H_{mo}}$, equals -0.86 (SP data, 2 hours time series at high tide). This means that wave run-down $Rd_{2\%}$ is approximately 50% of wave run-up $Ru_{2\%}$.

b) Physical modelling

Initiated by the fact that in prototype high wave run-up values were measured which were clearly higher than published and generally accepted values and also clearly higher than values measured in laboratories in the start of the project, big efforts were made to measure wave run-up in laboratory as accurate as possible. This was mainly achieved by the development and construction of a novel step gauge which makes it possible to measure wave run-up very accurately even on a rough slope.

By simulating prototype storms only a limited range of wave parameters could be investigated as all available prototype storms have similar H_{mo}, T_p, Iribarren number ξ and spectral width ε. Within this small range it was shown that the dimensionless parameter $Ru_{2\%}/H_{mo}$ gave a consistent estimate of wave run-up. Also $Ru_{x\%}/H_{mo}$ values with $x > 2$ were considered. Two types of tests have been carried out: (1) simulation of prototype storms and (2) parametric investigation. Seven prototype storms were considered: the average prototype value is $Ru_{2\%}/H_{mo} = 1.72$. Simulation of these prototype storms gave an average value for $Ru_{2\%}/H_{mo}$ of 1.46 (FH, 7 storms), 1.79 (UPV, 2 storms) and 1.64 (AAU, 7 storms). For AAU the scatter is large: the minimum value is 1.29 and the maximum value 1.91. For all AAU tests H_{mo} was reproduced rather accurately. However, for the first group of 5 storms, the spectrum was slightly shifted to the low frequency waves yielding an average of 1.76. The second group of storms with an almost perfect reproduction of the spectrum yielded 1.35.

Numerous AAU model tests, performed with the same target spectrum, showed that $Ru_{2\%}/H_{mo}$ is very dependent on the spectral width ε (figure 29).

c) Comparison prototype - scale model

a) For a rubble mound breakwater armoured with grooved cubes, the prototype value $Ru_{2\%}/H_{mo} = 1.76$ (high tide) is clearly higher than known and generally accepted before the OPTICREST project.

b) In general, wave run-up in prototype is clearly higher than found in scale model tests.

c) For two consecutive storms (Nov. 6, 1999 and Nov. 6-7, 1999) half a tide cycle is reproduced in three laboratories. The variations of $Ru_{2\%}/H_{mo}$ with the mean water level (MWL) is determined (figure 46) :
- AAU test results yield lower $Ru_{2\%}/H_{mo}$ values than prototype but show a similar dependency on the MWL as noticed in prototype.
- for UPV: at high tide $Ru_{2\%}/H_{mo}$ is equal to prototype but only little dependency on MWL is noticed.
- for FH: the $Ru_{2\%}/H_{mo}$ value at high tide is lower than the prototype value and almost no influence of MWL is noticed.

In general $Ru_{2\%}/H_{mo}$ is 36% higher in prototype than found in scale model tests.

d) Analysis of all data (prototype and all scale model tests) of the Nov. 6, 1999 and the Nov. 6-7, 1999 storm shows a clear relationship between $Ru_{2\%}/H_{mo}$ and ε (figure 49).

e) In AAU tests it is found that $Ru_{2\%}/H_{mo}$ increases slightly with increasing tidal current. On site the tidal current is maximum at high tide. So this phenomenon has to be taken into account when comparing prototype with laboratory tests: especially at the top of high tide. At mean tide tidal currents are negligible.

f) Waves are only defined by their amplitude spectra (H_{mo} and T_p) which is not a complete representation of the kinematics of waves.

g) The difference between prototype and laboratory results is larger when lower exceedence probabilities x are considered. When $Ru_{5\%}/H_{mo}$ and $Ru_{10\%}/H_{mo}$ values of prototype and laboratory are compared over half a tide cycle, it is noticed that results become very similar at high water for an exceedence probability $x \geq 10$. The same trends (increasing wave run-up for decreasing water levels) remain but become less pronounced for higher exceedence probabilities (figure 47 and 48).

h) The parametric study has shown that wind has only a limited influence on wave run-up.

i) Parametric tests also showed the influence of wave obliqueness: dimensionless 2% wave run-up decreases from about 1.80 to about 1.25 when the mean incident wave angle θ increases from perpendicular wave attack to $\theta = 45°$ (figure 34).

d) Conclusions on rubble mound breakwater

1) For a rubble mound breakwater prototype measurements yield $Ru_{2\%}/H_{mo} \cong 1.76$ which is considerably higher than values found in literature for comparable structures. These published values are based on scale model tests. The value 1.76 is only slightly lower than values found for rip-rap (van der Meer and Stam (1992), Ahrens and Heimbaugh (1988),...). So, the OPTICREST project has learned that for a conventional rubble mound breakwater with heavy armour units the $Ru_{2\%}/H_{mo} \cong 1.76$, valid for $H_{mo} \cong D_{n50}$.

2) Prototype results show significantly higher wave run-up than small scale modelling results. The difference is the largest at lower water levels.

   The reasons, which cannot be quantified, are:
   • model effects
       - imperfect modelling of porosity and permeability (armour units and core material)
       - no wind in models
       - no current in models
       - imperfect modelling of sea bed topography
       - imperfect modelling of target spectra
       - limitations of some wave generators (stroke)
   • scale effects: viscous effect (one side bias). These effects are important for thin water tongues on a rough hard surface and for porous flow.

3) Wave run-up is Rayleigh distributed both in prototype and scale models. Therefore it may be convenient to use Rayleigh equivalent $Ru_{e2\%}$ instead of $Ru_{2\%}$ when $Ru_{2\%}$ is difficult if not impossible (overtopping) to measure.

4) Step gauge run-up measurement systems must be used in prototype and scale models to avoid underestimation of wave run-up. Most existing data on wave run-up and formulae in literature must be taken with caution because the most common technique to measure wave run-up in laboratory is to place wave gauges parallel to the slope and assume linearity; this technique has been proved to underestimate wave run-up.

5) Wind was found to increase wave run-up and wave overtopping (2D model in the wind and wave facility of UPV). Although no prototype confirmation was possible and scale laws on wave and wind experiments are not known yet, it is possible to affirm (based on 2D experiments) that wave run-up is roughly proportional to the square of the wind speed but that the influence is not very important (order of 5% for moderate winds).

6) Wave overtopping can be measured in scale models (1:30) with excellent repeatability. Measurements of wave overtopping in laboratory is more reliable than wave run-up and more important to define breakwater crest elevation.

7.3 Optimisation and calibration of numerical models

Several numerical models (both engineering tools cf. ODIFLOCS, SWAN and research tools cf. SKYLLA, VOFbreak[2], 2D-HYDROTUR, TRITON) have been used for simulation of wave action on and in the coastal structures that have been investigated in OPTICREST. A new refined VOF type code has been developed and applied. It is based on a state-of-the-art VOF model and includes wave boundaries. Data from two prototype structures have been used for validation: the impermeable Petten sea dike and the permeable Zeebrugge breakwater, and data from a physical scale model: the LWI dike.

Results for the Petten sea dike

Three numerical models have been applied and linked for the validation of wave interaction with the Petten dike, including the shallow foreshore and wave breaking in a situation with a berm. Applying the models together leads to accurate predictions of wave run-up levels for the present data set. The spectral wave model SWAN used for wave propagation of short waves over the foreshore yields small underestimation of the wave parameters at the toe of the dike (13% for H_{mo} and 21% for $T_{-1,0}$). The time-domain model TRITON used for wave propagation over the foreshore shows accurate results for both H_{mo} and $T_{-1,0}$ (deviation below 10%). Application of the ODIFLOCS model using measured surface elevations from incident waves, shows good agreement for wave run-up levels (on average 10% underestimation). Recommendations have been formulated for further improvements.

The VOF-model SKYLLA has been applied to compare the computed wave breaking process with the measured one in the 2D tests on the Petten sea dike. The plunging waves were reproduced accurately in the computations, including the overturning wave tongue, the wave tongue hitting the impermeable smooth slope and the bouncing back from (upward motion) the slope. The numerically obtained wave run-up levels were systematically underestimated. Although the modelling of the wave breaking process is essential in the comparison with measurements to actually compare similar wave conditions, rather than comparing wave run-up levels belonging to different wave conditions, the dissipation in the thin wave run-up tongue apparently is too large in the computations. For different dike-geometry also overtopping discharges were compared to results from physical model tests of the LWI dike. These overtopping discharges were overestimated, although differences are in the range where common scatter occurs in wave overtopping data from physical model tests. In general it is concluded that the model computes realistic wave breaking process, that reasonable overtopping discharges are computed but that dissipation in thin water layers is too large which causes underestimates of wave run-up levels.

Result for the Zeebrugge breakwater

The wave induced pore pressure attenuation inside the permeable Zeebrugge prototype breakwater has been simulated using the VOF-model VOFbreak[2]. From analysis of the numerically obtained pore pressures and comparing to the experimentally obtained conclusions (from prototype), the

same conclusions on the pore pressure distribution have been found, and a reasonable agreement is obtained.

Results for the LWI dike

Physical model tests on the LWI dike with a 1:6 seaward slope provide a comprehensive data set for validation of the numerical models for wave overtopping and mutual comparison.

Simulations using the ODIFLOCS model showed that the ratio between computed (q_{comp}) and measured (q_{meas}) average overtopping rates is quite good for regular waves: $\dfrac{q_{comp}}{q_{meas}} \approx 0.88$. This agreement is very good compared to the scattering of experimental and also numerical data especially for high crest freeboards and resulting low overtopping rates. For wave spectra the agreement between measured and computed overtopping rates using ODIFLOCS is less good: $\dfrac{q_{comp}}{q_{meas}} \approx 0.45$. A comparison for measured and computed layer thickness shows a good agreement for the seaward and landward slope.

The 2D-HYDROTUR code provides a useful description of wave run-up/down and wave overtopping on sloping coastal structures such as the Petten dike and the LWI dike. The numerical solution gives reasonable results of the relevant variables - overtopping rate, maximum velocity and layer thickness - fairly representing the details of the free surface configuration at the breaking point. Wave overtopping at the LWI dike is slightly overestimated: $\dfrac{q_{comp}}{q_{meas}} \approx 1.56$. However, only with a formulation of a wall friction law and the implementation of a turbulence model it will be possible to set-up a better calibration of this model.

Simulations of wave overtopping at the LWI dike using the refined code (which is based on the VOFbreak^2 code) show reasonable agreement between computed and measured average overtopping rates: $\dfrac{q_{comp}}{q_{meas}} \approx 0.81$. It was found that the choice of the computational mesh is critical in obtaining good simulation results.

7.4 Project objectives and results

Four main objectives have been put forward:

1. Provide improved design rules for the crest level design of sloping coastal structures, mainly based on prototype data and supported by physical scale model results.

2. Verify and calibrate physical scale models with prototype data for wave run-up.

3. Calibrate numerical models with prototype data and physical scale model results for wave run-up.

4. Improve existing wave run-up monitoring devices plus ancillary software and install on two prototype coastal structures.

Two types of coastal structures are investigated: a smooth impermeable sea dike and a conventional rubble mound breakwater. Prototype measurements have been carried out on the Petten sea dike (the Netherlands) and the Zeebrugge rubble mound breakwater (Belgium). Small scale models have been built and tested in six laboratories all over Europe. Numerical calculations have been performed. The influence of wave run-up and wave overtopping on the crest stability has been investigated theoretically and by laboratory testing.

The *first* objective is met by the formulation of <u>improved design rules</u>.

For an **impermeable dike**, laboratory tests confirm prototype measurement results. So, conventional scales and methodologies may be used if use is made of a step gauge.

An important aspect is the foreshore. The Petten site is complex because of the presence of a shallow foreshore with two sand bars which needs to be modelled very accurately because the bars in front of the structure have an important influence on wave breaking and on low frequency waves. Therefore, the modelling of the nearshore sea bed topography is essential.

Based on the analysis of the Petten Sea-defence measurements and other investigations of wave run-up on dikes, the following formula has been derived (with wave breaking in front of the dike due to depth limitations, so mainly valid for shallow foreshores):

$$\frac{Ru_{2\%}}{\gamma H_{mo}} = c_0 \xi \qquad \text{for } \xi \le p$$

$$\frac{Ru_{2\%}}{\gamma H_{mo}} = c_1 - \frac{c_2}{\xi} \qquad \text{for } \xi \ge p$$

If the Iribarren number ξ is defined as $\xi = \dfrac{tan\,\varphi}{\sqrt{\dfrac{2\pi H_{mo}}{gT_{-1.0}^{2}}}}$, where H_{mo} is the wave height of the incident

waves at the toe of the structure, the coefficients become $c_0 = 1.45$, $c_1 = 3.8$ while continuity

between both sections and their derivatives determine $c_2 = 0.25\dfrac{c_1^2}{c_0}$ and $p = 0.5\dfrac{c_1}{c_0}$. The reduction

factor γ takes the reduction due to roughness into account which is not required for the Petten dike $(\gamma = 1)$.

The influence of various different parameters (such as the influence of wave directionality and directional spreading) on the design should be investigated thoroughly because these parameters are highly dependent on the location (e.g. foreshore).

For the estimation of maximum layer thickness and wave run-up velocity, a theoretical model has been developed on the basis of simplifications of the two dimensional Navier-Stokes equations and the continuity equation. The theoretical model was calibrated for wave run-up velocities for the moment when the water tongue at the top of the seaward slope has reached its maximum thickness. These results agree very well the laboratory experiment results.

The project clearly has demonstrated that wave run-up on a prototype **rubble mound breakwater** armoured with conventional armour units (e.g. grooved cubes) is clearly higher than accepted before OPTICREST. Prototype results are very consistent: the scatter of 13 measured storms was low. Following values at high tide are found: $Ru_{1\%}/H_{mo} = 1.89$, $Ru_{2\%}/H_{mo} = 1.76$, $Ru_{5\%}/H_{mo} = 1.55$ and $Ru_{10\%}/H_{mo} = 1.34$. $Ru_{2\%}/H_{mo}$ is slightly lower but of the same order of magnitude as found for rip rap slopes.

Much scatter was seen on the results of the different laboratories and the prototype results. Several factors (on the one hand scale effects and on the other hand model effects such as tidal currents, wind, imperfect modelling of porosity and permeability, sea bed topography and target spectra,...), all contributing to these differences have been identified.

Although suitable for dikes, the 2% wave run-up level (which is accepted to be almost equivalent to an overtopping discharge of 1 l/m/s) cannot be considered as the key parameter to design the crest level of a rubble mound breakwater. However, wave run-up levels can to some extent be linked to overtopping discharges in order to define a crest level height based on an agreed and allowable overtopping discharge. The overtopping discharge should be the criterion to determine the crest level of a rubble mound breakwater.

The mean water level had an important influence on wave run-up at the Zeebrugge breakwater.

For *design purposes* it is advised
• to take into account an extra safety when relying on wave run-up levels on permeable slopes in small scale model test results.

- to repeat model tests to study the repeatability of the results.

- to use a step gauge for detection of wave run-up.

- to determine the allowable wave overtopping (which depends on the crest stability, the use of the area behind the crest, measures take in view of the wave overtopping,…) and to use this allowable wave overtopping as design criterion.

The *second* and *third* objectives are also fulfilled.

Data from two prototype structures (the impermeable Petten sea dike and the permeable Zeebrugge breakwater) and data from a physical scale model (the LWI dike) have been used for validation of numerical models.

Verification of scale model tests with prototype data has indicated that an impermeable sea dike (Petten Sea-Defence) is modelled correctly. One of the main conclusions of the rubble mound breakwater (Zeebrugge breakwater) investigation is that scale model tests in general clearly underestimate wave run-up.

The *fourth* objective is met (i) by the development of a novel digital step gauge for laboratory investigation (similar to the one used in the tests on the Petten Sea-Defence) and (ii) the design, construction and installation of the run-up gauge and wave overtopping measuring devices (overtopping tank and wave detectors) on the Zeebrugge breakwater for respectively wave run-up and wave overtopping measurements. These devices can be used for every breakwater independent of the type of armour unit, crest,…

REFERENCES

Ahrens J.P., Heimbaugh M.S., *Irregular wave run-up on rip rap revetments,* Journal of Waterway, Port, Coastal, and Ocean Engineering, Vol. 114, No. 4, July 1988.

Battjes J.A., 1969, *Discussion of paper by J.N. Svašek: "Statistical evaluation of wave conditions in a deltaic area".* Proc. Symp. "Research on wave action" at Delft Hydraulics, Vol. 1, Paper 1.

Burcharth H. F., Liu Z. and Troch P., 1999, *Scaling of core material in rubble mound breakwater model tests.* Proceedings of the 5th International Conference on Coastal and Port Engineering in Developing Countries (COPEDEC V), Cape Town, South African, April 1999.

de Waal J.P., van der Meer J.W., 1992, *Wave run-up and overtopping on coastal structures.* Proceedings 23rd ICCE, Venice, p. 1758-1771, 1992.

Kingston K. and Murphy J., 1994, *Wave run-up / run-down.* Thematic report in the MASTII project 'Full Scale Dynamic Load Monitoring of Rubble Mound Breakwaters' (MAS2-CT92-0023).

Losada M.A. and Giménez-Curto L.A., 1982, *Mound breakwaters under oblique wave attack; a working hypothesis.* Coastal engineering 6, pp. 83-92.

National Institute for Coastal and Marine Management/RIKZ, 1999, *Verification set Case Study Petten (CD-ROM).* National Institute for Coastal and Marine Management/RIKZ, The Netherlands.

Oumeraci H., Schüttrumpf H., Bleck M., 1999, *Wave overtopping at seadikes; comparison of physical model tests and numerical computations.* MAST-OPTICREST report Leichtweiss-Institute für Wasserbau, October 1999, Braunschweig.

Schüttrumpf, H., 2001, *Wellenüberlaufströmung an Seedeichen – Experimentelle und theoretische Untersuchungen.* Dissertation. Leichtweiss-Institut, TU Braunschweig. pp. 1-127 (in German).

van der Meer J.W., Stam J.C., *Wave run-up on smooth and rock slopes of coastal structures,* Journal of Waterway, Port, Coastal and Ocean Engineering, Vol. 118, No. 5, pp. 534-550, 1992.

van Gent M.R.A., 1999, *Physical model investigations on coastal structures with shallow foreshores; 2D model tests with single and double-peaked wave energy spectra.* Delft Hydraulics Report H3608, December 1999, Delft.

van Gent M.R.A., 2000, *Wave run-up on dikes with shallow foreshores.* Paper at 27th Int. Conf. on Coastal Engineering, Sydney, Australia.

van Gent M.R.A., Doorn N., 2000, *Numerical model investigations on coastal structures with shallow foreshores; Validation of numerical models based on physical model tests on the Petten Sea-defence.* MAST-OPTICREST report and Delft Hydraulics Report H3351, May 2000, Delft.

van Gent M.R.A., Doorn N., 2001, *Numerical model simulations of wave propagation and wave run-up on dikes with shallow foreshores.* Paper at Coastal Dynamics 2001, Lund, Sweden.

van Gent M.R.A., Wolf F.C.J., Murphy J., 2001, *Synthesis of Petten measurements.* MAST-OPTICREST report, RIKZ-WL/DH-UCC Report, March 2001.

Versluys T., 1999, *Data for calculation of slope in Zeebrugge.* OPTICREST document MAS03/790, Ghent, April 1999.

Reference has also been made to following Annexes which can be found in the first annual report (*'Annual Report (12 months)'*), the second annual report (*'Annual Report (To+12 till To+24)'*) or this final report.

First annual report (*'Annual Report (12 months)'*):

Annex I: **Verdonck R., Troch P., De Rouck J., Burcharth H.,** June 1998, *Review of available information.* OPTICREST research report on Task 1.

Annex II: **Wolf F.C.J., Troch P., De Rouck J., Van Damme L.,** November 1998, *Description of field sites for the measurement of wave run-up.* OPTICREST Research Report on Subtask 2.1.

Annex IV: **Murphy J.,** March 1999, *Wave run-up measurement techniques.* OPTICREST Research Report on Subtask 3.2.

Second annual report (*'Annual Report (To+12 till To+24)'*)

Annex II: **Frigaard P., Schlütter F.,** June 1999, *Laboratory investigations – Methodology.* OPTICREST Research Report on Subtask 3.1

Annex III: **van Gent M.R.A.,** July 1999, *Physical model investigations on coastal structures with shallow foreshores – 2D model tests on the Petten sea-defence.* OPTICREST Research Report on Subtask 3.3.

Annex VIII: **Schlütter F., Frigaard P.,** September 1999, *Zeebrugge models: laboratory investigation.* OPTICREST Research Report on Subtask 3.4.

Annex IX: **Oumeraci H., Schüttrumpf H., Bleck M.,** October 1999, *Wave Overtopping at Seadikes - Comparsion of Physical Model Tests and Numerical Computations.* OPTICREST Research Report on tasks 3.5 & 5.

Final report

Annex 2.2:   **Van de Walle B., Bal J.,** April 2001, *Prototype measurements Zeebrugge.* OPTICREST Research Report on Subtask 2.2.

Annex 2.3:   **de Kruif A.C.,** September 2000, *Stormdata of the Petten field site 1995-2000.* OPTICREST Research Report on Subtask 2.3.

Annex 3.3a: **Willems M., Kofoed J.P.,** April 2001, *Laboratory investigations: Two dimensional testing – the Zeebrugge breakwater.* OPTICREST Research Report on Subtask 3.3.

Annex 3.3b: **Medina J.R., González-Escrivá J.A., Garrido J.,** April 2001, *2D testing – Zeebrugge model tests performed in UPV.* OPTICREST Research Report on Subtask 3.3.

Annex 3.4a: **Murphy J.,** August 2000, *3D physical model tests of wave run-up on coastal structures.* OPTICREST Research Report on Subtask 3.4.

Annex 3.4b: **Schüttrumpf H., Murphy J.,** September 2000, *3D model tests on wave overtopping for 1:6 dike.* OPTICREST Research Report on Subtask 3.4.

Annex 3.4c.1: **Schlütter F., Frigaard P., Liu Z.,** May 2000, *Zeebrugge model: wave run-up under simulated prototype storms.* OPTICREST Research Report on Subtask 3.4.

Annex 3.4c.2: **Liu Z., Frigaard P.,** May 2000, *Zeebrugge model: 3D wave run-up measurements and analysis.* OPTICREST Research Report on Subtask 3.4.

Annex 3.4c.3: **Jensen M.S., Frigaard P.,** September 2000, *Zeebrugge model: (i) Wave runup under simulated prototype storms (II) and (ii) The influence on wave run-up introducing a current.* OPTICREST Research Report on Subtask 3.4.

Annex 3.5:   **Schüttrumpf H., Oumeraci H.,** April 2001, *Prediction of wave overtopping flow parameters on the crest and landward slope of sea dikes.* OPTICREST Research Report on Subtask 3.5.

Annex 4a: **Medina J.R., González-Escrivá J.A.,** March 2001, *Link between prototype and laboratory results: Petten case.* OPTICREST Research Report on Task 4.

Annex 4b: **Medina J.R., González-Escrivá J.A.,** April 2001, *Link between prototype and laboratory results: Zeebrugge case.* OPTICREST Research Report on Task 4.

Annex 5.1.a: **Lemos C.M., Pinto J.P.,** January 2001, *Implementation of turbulence models.* OPTICREST Research Report on Task 5.

Annex 5.1.b: **Lemos C.M., Pinto J.P.,** November 2000, *Numerical simulation of overtopping on a 1:6 dike.* OPTICREST Research Report on Task 5.

Annex 5.1.c: **Lemos C.M., Pinto J.P.,** March 2001, *Numerical simulation of wave run-up on Petten dike.* OPTICREST Research Report on Task 5.

Annex 5.2:   **van Gent M.R.A., Doorn N.,** 2001, *Numerical model simulations of wave propgation and wave run-up on dikes with shallow foreshores.* Proceedings Coastal Dynamics 2001, 11pp.

Annex 5.3:   **Troch P.,** April 2001, Numerical simulation of wave interaction with coastal structures. OPTICREST Research Report on Task 5, MAS03/1151/pth.

Annex 6:   **De Rouck J., Van de Walle B.,** April 2001, *Exploitation and dissemination of results.* OPTICREST Research Report on Task 6.